SENSOR LOCATION PROBLEMS FOR ESTIMATION OF ORIGIN-DESTINATION DEMANDS AND TRAVEL TIMES UNDER UNCERTAINTY

FU HAO

PhD

The Hong Kong Polytechnic University

2022

The Hong Kong Polytechnic University

Department of Civil and Environmental Engineering

Sensor Location Problems for Estimation of Origin-Destination Demands and Travel Times under Uncertainty

Hao FU

A thesis submitted in partial fulfilment of the requirements

for the degree of Doctor of Philosophy

March 2022

Certificate of Originality

I hereby declare that this thesis is my own work and that, to the best of my knowledge and belief, it reproduces no material previously published or written, nor material that has been accepted for the award of any other degree or diploma, except where due acknowledgement has been made in the text.

Signature:
Name of student: Hao FU

Abstract

To monitor traffic congestion and improve road network performance, various types of traffic sensors have become available and affordable with the rapid development of advanced sensing technologies. Smartly determining the locations of the multi-type sensors is crucial to collect multi-source data for the development of strategic transport models. In view of this, this thesis proposes a new modeling approach to optimize the number and locations of multi-type traffic sensors by taking into account the traffic demand variation and/or travel time uncertainty. The optimum deployment of multi-type traffic sensors is proficient in the separate and simultaneous estimation of day-to-day vehicular traffic demand by origin-destination (OD) pair and travel time on links with covariance effects on a daily scale. The novelty of the research presented in this thesis mainly resides in the incorporation of covariance of OD demands and/or link travel times when deploying single-type or multi-type traffic sensors onto a road network for updating strategic transport models.

In literature, most of the existing methods estimate only the mean (average) OD demands using the observed data from a single-type sensor system. However, vehicular traffic demands between different OD pairs in a typical hourly period (e.g., morning peak hour) are statistically correlated from day to day because of daily variation in activity patterns. Traffic demands during different hourly periods within a day are also highly interrelated, owing to the hourly variation of travel patterns. Moreover, travel times on road links during the peak hour period are stochastic and correlated, especially the travel times of adjacent links under congested conditions.

To overcome the limitation of the existing methods, both the mean and covariance of OD demand and of link/path travel time will be estimated separately and simultaneously with making use of the various data from different sensor systems. In

summary, the following key contributions of the thesis are highlighted.

First, spatial covariance of peak-hour OD demand between different OD pairs is explicitly considered in traffic sensor (i.e., traffic count) location problems. The vehicular traffic demands between different OD pairs in a typical hourly period (e.g., the morning peak hour) can be statistically correlated from day to day because of joint travel behaviors and daily variation in activity patterns over a year. A new criterion based on the weighted maximum possible relative error is employed to measure the estimation accuracy of OD demand covariance (i.e., the maximum estimation error of the worst case) without the need for the ground truth of OD demand covariance. A new model is then developed to optimize traffic sensor (i.e., traffic count) locations and thereby minimize the new criterion. The conventional traffic sensor location model is therefore a special case of this new model.

Second, this traffic sensor location model is extended to optimize the location of multi-type traffic sensors by incorporating the spatiotemporal covariance of vehicular traffic demands between different OD pairs in multiple periods. Due to hourly variation of travel patterns by time of day and day of the year, the traffic demands of OD pairs are highly interrelated during different periods (e.g., morning peak and evening peak hours). Thus, a Kalman filter method based on principal component analysis is developed to estimate multi-period OD demands and their covariances. In addition, a novel model is devised for optimizing the locations of multi-type traffic sensors by minimizing the uncertainty of multi-period OD demand estimates. Overall, both the number and locations of multi-type traffic sensors, including point sensors and automatic vehicle identification (AVI) sensors, are optimized under a constraint on the total available budget. The mathematical properties of the new model are studied to determine the effect of multi-period OD flow covariance on the model results.

Thirdly, to develop consistent strategic transport models, an integrated traffic sensor location model is formulated for simultaneous estimation of OD demands and link travel times with consideration of two sources of spatial covariance. The two sources of spatial covariance include the traffic demand covariance between different OD pairs and the travel time covariance between different links during the peak hour period. Coherent estimations of these stochastic link travel times and OD demands are facilitated by multi-source data from multi-type sensors. With these simultaneous estimations, a multi-type sensor location model is developed to efficiently use or fuse these multi-source data. Based on the data observed from the installed multi-type traffic sensors such as link speed/flow and path travel time information, a novel Kullback–Leibler divergence-based model is proposed to achieve the simultaneous estimation. The proposed model can accommodate different probability distributions of OD demands and link travel times under different traffic conditions.

An improved firefly algorithm is developed for efficiently searching for the near-to-global solution, which enables the efficient solution of multi-type sensor location problems that belong to integer programming and are NP-hard. In this improved algorithm, the search strategy is enhanced by taking into account the mean and covariance of OD demand and link travel time. Numerical examples of synthetic and real-world road networks are conducted to illustrate the applications and merits of the proposed sensor location models for separate and simultaneous estimation of OD demands and link travel times with covariance effects. Consequently, the optimal multi-type sensor location schemes can be determined for estimation of day-to-day peak hour vehicular traffic demands by OD pair and/or link travel times. Based on these results, transportation planners and traffic engineers can easily deploy efficient sensor systems to monitor traffic conditions and assess the congestion levels in road networks with uncertainty.

Publications arising from the thesis

Journal papers:

1. **Fu, H.**, Lam W.H.K., Shao, H., Xu, XP, Lo, HP, Chen BY, Sze NN, Sumalee A., 2019. Optimization of traffic count locations for estimation of travel demands with covariance between origin-destination flows. *Transportation Research Part C* 108, 49–73. (Chapter 3 in the thesis)

2. **Fu, H.**, Lam, W.H.K., Shao, H., Kattan, L., Salari, M., 2022. Optimization of multi-type traffic sensor locations for estimation of multi-period origin-destination demands with covariance effects. *Transportation Research Part E* 157, 102555. (Chapter 4 in the thesis)

3. **Fu, H.**, Lam, W.H.K., Shao, H., Ma, W., Chen BY, 2022. Optimization of multi-type sensor locations for simultaneous estimation of link travel times and origin-destination demands with covariance effects. *Transportation Research Part B.* (Accepted) (Chapter 5 in the thesis)

4. **Fu H.**, Lam W.H.K., Ho H.W., Ma W., 2022. Optimization of multi-type traffic sensor locations for network-wide link travel time estimation with consideration of their covariance. *Transportmetrica B.* (Revised and resubmitted)

5. Mostafa S., Lina K., Lam, W.H.K., Mohammad A. E., **Fu H.**, 2021. Modeling the effect of sensor failure on the location of counting sensors for origin-destination (OD) estimation. Transportation Research Part C 132, 103367.

Conference paper:

6. **Fu H.**, Lam W.H.K., Shao H., Sumalee A., 2019. Optimization of traffic count locations for estimation of stochastic origin-destination demands under uncertainty with sensor failure. In: *Proceedings of the 24th International Conference of Hong Kong Society for Transportation Studies*, 447-453

Acknowledgements

I would like to convey my deepest gratitude to my chief supervisor, Prof. William H. K. Lam, for his insightful guidance, dedication, and suggestion throughout my study in Hong Kong. He guided me to the suitable mentality of a researcher to keep exploring new things based on the range of my knowledge. It is impossible to complete this thesis without his encouragement and sagacious input. Additionally, sincere thanks to my ex-co-supervisor, Prof. Agachai Sumalee for his helpful advice on technical paper writing.

Special thanks should be given to Prof. Lina Kattan for supporting me as an exchange student at the University of Calgary, Canada. The exchange program became the starting point for our further research collaboration. My deepest gratitude to Dr. H.P. Lo, who I also worked with at the early stage of my research. May him be in peace and mercy. I also appreciate Prof. Francesco Viti and Prof. W.Y. Szeto for serving in my thesis committee, and for their valuable suggestions and encouragement.

I would like to thank Prof. Hu Shao for his kind advice on not only technical issues but also his attitude towards research. I also gratefully appreciate Prof. Anthony Chen for his valuable lectures leading me to the network modeling studies and for his suggestions on the extension of my knowledge apart from my research area. I would like to show my thankfulness to Dr. Tony Sze, who taught me how to organize the paper presentation logically. My appreciation should also be given to Dr. Wei Ma for his productive suggestions and constant help.

I would like to declare that the research presented in this thesis is partly funded by the Research Grants Council of the Hong Kong Special Administrative Region (Project No. PolyU 152628/16E) and the Smart Traffic Fund from the Transport Department of the Government of the Hong Kong Special Administrative Region, China (Ref. No.:

PSRI/06/2108/PR).

My past and present colleagues and friends in The Hong Kong Polytechnic University deserve my appreciation, including but not limited to Dr. Karen Tam, Prof. Bi Yu Chen, Dr. Xiao Fu, Dr. Julio Ho, Dr. Yongsheng Zhang, Dr. Kai Liu, Dr. Junbiao Su, Dr. Xiaomeng Shi, Dr. Chaoyang Shi, Dr. Mostafa Salari, Dr. Yuyang Zhou, Haodong Xiang, Yepeng Yao, Ang Li, Vo Dang Khoa, Yunping Huang, Can Chen, Dr. Dianchen Zhu, Guoyuan Li.

Above all, mere words, in any of the languages that I know, are inadequate to express my thanks to my parents, my lovely sister, and my fiancée, Xin Du for their unconditional love, care, and support.

Table of Contents

List of Figures

List of Tables

List of Notations

The notations used throughout the thesis unless otherwise specified are listed below.

Abbreviations

ALPR	Automatic license plate recognition
ATC	Annual traffic census
AVI	Automatic vehicle identification
BPR	Bureau of Public Roads
CPR	Castle Peak Road
EM	Entropy maximization
FA	Firefly algorithm
GA	Genetic algorithm
GLS	Generalized least square
ITS	Intelligent transportation systems
JS	Jensen–Shannon
JTIS	Journey time indication system
KL	Kullback–Leibler
MAPE	Mean absolute percentage error
MLE	Maximum likelihood estimator
MPRE	Maximum possible relative error
OD	Origin-destination
PCA	Principal component analysis
pdf	Probability density function
RFID	Radio-frequency identification
SHA	Sequential heuristic algorithm
SLP	Sensor location problem
SMP	Speed map panels
SUE	Stochastic user equilibrium

TMR	Tuen Mun Road
US$	United States dollars with exchange rate at US$ 1.0 = HK$ 7.8
Var-cov	Variance-covariance
WMPRE	Weighted maximum possible relative error
WMPREC	Weighted maximum possible relative error for covariance of OD demand
WMPREM	Weighted maximum possible relative error for mean OD demand

Variables used in model formulation

$cc_{w,w'}$	Coefficient of correlation between OD demands in OD pair w and w' $(w, w' \in \mathbf{W})$
$cc^{l}_{t_a,t_{a'}}$	Coefficient of correlation between travel times on links a and a' $(a, a' \in \mathbf{A})$
$cv^{l}_{t_a}$	Coefficient of variation for travel time on link a
cv_w	Coefficient of variation for OD demand in OD pair w
q_w	Estimated mean traffic demand in OD pair w $(w \in \mathbf{W})$ (veh/hour)
$q_{w(h)}$	Estimated traffic demand in OD pair w during period h
q^{*}_{w}	"True" mean traffic demand in OD pair w
q^{prior}_{w}	Prior mean traffic demand in OD pair w
Q_w	Random OD demand in OD pair w
t^{l}_{a}	Estimated mean travel time on link a $(a \in \mathbf{A})$ (hour)
$\tilde{t}^{l}_{a}$	Sample mean of travel time on observed link a $(a \in \widetilde{\mathbf{A}})$ (hour)
$\tilde{t}^{l}_{a(d)}$	Mean travel time on observed link a $(a \in \widetilde{\mathbf{A}})$ during observational window on day d for all detected vehicles (hour)
t^{p}_{k}	Mean travel time on path k (hour)
t_{w_r}	Mean travel time between a node pair w_r $(w_r \in \mathbf{W}_r)$ (hour)
V_a	Random traffic flow on link a

$\tilde{v}_a^l$	Sample mean of hourly traffic flow on observed link a ($a \in \widetilde{\mathbf{A}}$) (veh/hour)
v_a^l	Mean value of link flow on link a ($a \in \mathbf{A}$) (veh/hour)
$v_{a(h)}$	Mean of hourly traffic flow on link a observed by point sensors in period h
$v'_{a(h)}$	Mean of partial traffic flow on link a observed by AVI sensors in period h
$\tilde{v}_{a(d)}^l$	Traffic flow on observed link a ($a \in \widetilde{\mathbf{A}}$) during observational window on day d (veh/hour)
$v'_{r(h)}$	Mean of partial traffic flow on path or path segment r observed by AVI sensors in period h
z_a	Binary variable representing point sensor location, $z_a = 1$ if a point sensor is installed on link a; $z_a = 0$ otherwise
$z_n{}'$	Binary variable representing AVI sensor location, $z_n{}' = 1$ if an AVI sensor is installed on node n; $z_n{}' = 0$ otherwise
λ_w^{mean}	Relative deviation of the estimated mean OD demands from the "true" one for OD pair w
$\lambda_{w,w'}^{cov}$	Relative deviation of the estimated covariance variable of OD demands from the "true" one for different OD pairs w and w'
$\sigma_{t_a,t_{a'}}^l$	Estimated var-cov of travel time between links a and a' ($a, a' \in \mathbf{A}$) $(\text{hour})^2$
$\tilde{\sigma}_{t_a,t_{a'}}^l$	Sample var-cov between observed travel times on the links a and a' ($a, a' \in \widetilde{\mathbf{A}}$) $(\text{hour})^2$
$\sigma_{t_a}^l$	Standard deviation of travel time on link a (hour)
$\sigma_{t_k,t_{k'}}^p$	Var-cov between travel time on the paths k and k' $(\text{hour})^2$
$\sigma_{t_{w_r},t_{w_{r'}}}$	Var-cov between observed travel times for node pairs w_r and $w_{r'}$ ($w_r \in \widetilde{\mathbf{W}}_r$) $(\text{hour})^2$

$\tilde{\sigma}^{l}_{v_a,v_{a\prime}}$ Sample var-cov between observed traffic flows on the links a and a' $(a, a' \in \widetilde{\mathbf{A}})$ $(\text{veh/hour})^2$

$\sigma^{l}_{v_a,v_{a\prime}}$ Var-cov between traffic flows on links a and a' $(a, a' \in \mathbf{A})$ $(\text{veh/hour})^2$

$\sigma_{v_{a(h)},v_{a\prime(h\prime)}}$ Covariance of point sensor observation between link flows v_a during period h and $v_{a\prime}$ during period h'

$\sigma_{v'_{a(h)},v'_{a\prime(h\prime)}}$ Covariance of AVI sensor observation between partial link flows v'_a during period h and $v'_{a\prime}$ during period h'

$\sigma_{v'_{r(h)},v'_{r\prime(h\prime)}}$ Covariance of AVI sensor observation between partial path flows v'_r during period h and $v'_{r\prime}$ during period h'

$\sigma_{w,w'}$ Estimated covariance of OD demand between OD pairs w and w' $(w, w' \in \mathbf{W})$ $(\text{veh/hour})^2$

σ_w Standard deviation of OD demand on OD pair w (veh/hour)

Parameters

B Total budget (US$)

p^{l}_{aw} Link choice proportion that means the proportion of OD pair w passing through link a

$p^{p}_{kw_r}$ Path choice proportion that means the proportion of node pair w_r passing through path k

α Weighting parameter of WMPREC

β Installation and maintenance cost of a point sensor (US$)

β' Installation and maintenance cost of an AVI sensor (US$)

δ_{ak} Link-path incidence, $\delta_{ak} = 1$ if the path k going through link a; $\delta_{ak} = 0$, otherwise

$\delta_{w,a}$ OD-link indicende, $\delta_{w,a} = 1$ if the trips on OD pair w pass through link a; $\delta_{w,a} = 0$, otherwise.

ρ_w Weight of traffic flows in OD pair w

$\rho_{w,w'}$	Weight of covariance between traffic flows in OD pairs *w* and *w'*
ψ	Upper bound of the KL divergence constraint
ω^l	Weighting parameter that represents the importance of observations from point sensors for link travel time estimation
ω_q	Weighting parameter that represents the importance OD demand estimates
ω_z	Weighting parameter of OD demand estimation variation in sensor location model

Sets

$\widetilde{\mathbf{A}}$	Observed link set in which traffic flows and travel times can be observed by sensors on these links
$\mathbf{D}$	Set of days of interest
$\mathbf{G} = (\mathbf{N}, \mathbf{A})$	A road network, with $\mathbf{N}$ ($n \in \mathbf{N}$) being the set of nodes and $\mathbf{A}$ ($a \in \mathbf{A}$) being the set of links
$\mathbf{H}$	Set of hourly periods of interest
$\mathbf{W}$	Set of OD pairs in a road network ($w \in \mathbf{W}$)
$\mathbf{W}_r$	Set of node pairs ($w_r \in \mathbf{W}_r$)
$\widetilde{\mathbf{W}}_r$	Set of observed node pairs where the AVI sensors are installed on both end nodes

Vectors and matrices

$\mathbf{c}$	Vector of estimated principal OD demand components in multiple periods
$\mathbf{c}_0$	Vector of prior principal OD demand components in multiple periods
$\mathbf{CC}_t$	Matrix of the coefficient of correlation for link travel time
$\mathbf{CC}_w$	Matrix of the coefficient of correlation for OD demand
$\mathbf{CV}_t$	Vector of coefficient of variation for link travel times, $\mathbf{CV}_t =$

	$[\dots, cv_{t_a}^l, \dots]^T$
$\mathbf{CV}_w$	Vector of coefficient of variation for OD demand, $\mathbf{CV}_w = [\dots, cv_w, \dots]^T$
$\mathbf{I_w}, \mathbf{I_t}$	Row vectors with size $1 \times \lvert\mathbf{W}\rvert$ and size $1 \times \lvert\mathbf{A}\rvert$, respectively whose elements are all ones
$\mathbf{P}$	Matrix of link choice proportion
$\widetilde{\mathbf{P}}$	Sub-matrix of link choice proportion matrix whose links are equipped with traffic sensors
$\mathbf{P}_{0(h)}$	Matrix of prior link choice proportion in period *h*
$\mathbf{P'}_{0(h)}$	Matrix of prior path or path segment choice proportion in period *h*
$\mathbf{P}_{(h)}$	Matrix of updated link choice proportion in period *h*
$\mathbf{P'}_{(h)}$	Matrix of updated path or path segment choice proportion in period *h*
$\mathbf{q}$	Vector of estimated mean OD demands
$\mathbf{q}*$	Vector of "true" mean OD demands
$\mathbf{q}^-, \mathbf{q}^+$	Vector of Lower bound and upper bound of mean OD demand estimates
$\mathbf{q}_{(h)}$	Vector of estimated OD demands in period *h*
$\mathbf{q}^{prior}$	Vector of prior mean OD demands
$\tilde{\mathbf{t}}^l$	Vector of sample mean travel time on observed links, $\tilde{\mathbf{t}}^l = (\dots, \tilde{t}_a^l, \dots)^T$
$\mathbf{t}^l$	Vector of estimated mean travel time, $\mathbf{t}^l = [\mathbf{t}_o^l; \mathbf{t}_u^l]$
$\tilde{\mathbf{t}}_{(d)}^l$	Vector of travel time on observed links on day *d*, $\tilde{\mathbf{t}}_{(d)}^l = (\dots, \tilde{t}_{a(d)}^l, \dots)^T$
$\mathbf{t}^{l-}, \mathbf{t}^{l+}$	Vector of lower bound and upper bound of mean link travel time estimates
$\mathbf{t}_o^l$	Vector of estimated mean travel time on observed links

$\mathbf{t}_{oprior}^{l}$	Vector of prior travel time on observed links
$\mathbf{t}_{u}^{l}$	Vector of estimated mean travel time on unobserved links
$\mathbf{t}_{uprior}^{l}$	Vector of prior travel time on unobserved links
$\tilde{\mathbf{t}}_{w_r}$	Vector of sample mean travel time between observed node pairs
$\tilde{\mathbf{t}}_{w_r(d)}$	Vector of travel time between observed node pairs on day *d*
$\mathbf{t}_{w_r}$	Vector of estimated mean travel time between node pair w_r
$\tilde{\mathbf{v}}^{l}$	Vector of sample mean link flow on observed links, $\tilde{\mathbf{v}}^{l} = (\dots, \tilde{v}_{a}^{l}, \dots)^{T}$
$\mathbf{v}^{l}$	Vector of estimated mean link flow on links
$\mathbf{v}_{a(h)}$	Vector of mean link flows observed by point sensors in period *h*
$\mathbf{v}'_{a(h)}$	Vector of mean partial link flows observed by AVI sensors in period *h*
$\tilde{\mathbf{v}}_{(d)}^{l}$	Vector of traffic flow on observed links on day *d*, $\tilde{\mathbf{v}}_{(d)}^{l} = (\dots, \tilde{v}_{a(d)}^{l}, \dots)^{T}$
$\mathbf{v}'_{r(h)}$	Vector of mean partial path flow observed by AVI sensors in period *h*
$\mathbf{z}$	Vector of point sensor location variables
$\mathbf{z}'$	Vector of AVI sensor location variables
$\mathbf{\Theta}_0$	Transformed prior link choice proportion matrix in multiple periods, that is, the transform of the original link choice proportions to the orthonormal basis matrix of eigenvectors $\mathbf{E}$ for OD demand covariance matrix
$\mathbf{\Theta'}_0$	Transformed prior path or path segment choice proportion matrix in multiple periods, that is, the transform of the original path or path segment choice proportions to the orthonormal basis matrix of eigenvectors $\mathbf{E}$ for OD demand covariance matrix

$\boldsymbol{\Theta}_{(h)}$	Transformed updated link choice proportion matrix
$\boldsymbol{\Theta}'_{(h)}$	Transformed updated path or path segment choice proportion matrix
$\boldsymbol{\Sigma}_c$	Var-cov matrix of estimated principal OD demand components in multiple periods
$\boldsymbol{\Sigma}_{c0}$	Var-cov matrix of prior principal OD demand components in multiple periods
$\boldsymbol{\Sigma}_e$	Var-cov matrix of measurement error from point sensors
$\boldsymbol{\Sigma}'_e$	Var-cov matrix of measurement error from AVI sensors
$\boldsymbol{\Sigma}_q$	Var-cov matrix of estimated OD demands
$\boldsymbol{\Sigma}_{q*}$	Var-cov matrix of "true" OD demands
$\widetilde{\boldsymbol{\Sigma}}_t^l$	Sample var-cov matrix of observed link travel times among different links
$\boldsymbol{\Sigma}_{\mathbf{t}}^l$	Var-cov matrix of travel time among all links in the road network
$\boldsymbol{\Sigma}_{t_u,t_o}^l$,$\boldsymbol{\Sigma}_{t_o,t_u}^l$	Matrix whose elements are the covariance of travel time between observed and unobserved links
$\boldsymbol{\Sigma}_{t_u}^l$, $\boldsymbol{\Sigma}_{t_o}^l$	Var-cov matrix of travel time among unobserved links, and among observed links, respectively
$\widetilde{\boldsymbol{\Sigma}}_t^{w_r}$	Sample var-cov matrix of observed travel time among different node pairs
$\boldsymbol{\Sigma}_t^{w_r}$	Var-cov matrix of estimated travel time among different node pairs
$\widetilde{\boldsymbol{\Sigma}}_v^l$	Sample var-cov matrix of traffic flow among different observed links
$\boldsymbol{\Sigma}_v^l$	Var-cov matrix of estimated traffic flow among different links
$\boldsymbol{\lambda}^{\mathbf{cov}}$	Matix of relative deviations of the estimated covariance of OD demands
$\boldsymbol{\lambda}^{\mathrm{mean}}$	Vector of relative deviations of the estimated mean OD demands

1. Introduction and objectives

1.1 Problem statement

The sensor location problem (SLP) presents a fundamental issue that directly affects the development of strategic transport models. The solution of the SLP reveals the minimum number and optimal locations of traffic sensors that should be installed to enable the estimation of traffic flow or travel time on links or paths in the network without installed sensors. To monitor traffic congestion and improve road network performance, various types of sensors have become available and affordable with the rapid development of advanced sensing technologies. For instance, to comprehensively monitor traffic conditions in Hong Kong, Transport Department has recently installed about 1,210 traffic detectors along the strategic routes and major roads by the end of 2020 for intelligent transportation system (ITS) development (Transport Department, 2020). Smartly determining the number and locations of the multi-type sensors and efficiently using or fusing these multi-source data with different characteristics are significant.

Different types of traffic sensors, such as point sensors and automatic vehicle identification (AVI) sensors, are deployed to provide multi-source data. The previous related studies on SLPs in road networks have focused mainly on the installation of point sensors, although some of these point sensors may provide only limited information on the observed links in practice.

To obtain more reliable and comprehensive information, emerging technologies such as AVI sensors have recently been deployed in road networks. Different types of traffic sensors provide various traffic data of travel time and traffic flow by link and/or path.

For example, path travel time information provided by AVI sensor pairs could supplement the link-level information obtained from point sensors. The integration of data obtained from differently sited sensors has the potential to lay a solid foundation to enhance the effectiveness of data collection for the development of ITS and strategic transport models.

Estimation of origin-destination (OD) demands by traffic sensors has been commonly used for transport planning and traffic management purposes in the past decades. The OD demand estimation problem focuses on the inference of vehicular traffic flows for OD pairs in a road network based on observational data (e.g., observed link flows or path flows) collected by installed traffic sensors. The vehicular traffic demand by OD pair is a fundamental input for traffic assignment or traffic simulation models to estimate the link flows onto the road networks (Caggiani et al., 2013; Antoniou et al., 2016). Traditionally, the deployment of traffic sensors deserved serious consideration for accurate estimates of the mean (or expected value) of the OD demands. Attributed to the daily variations in travel activity patterns, OD demands for a typical hourly period are not deterministic but actually fluctuate from day to day (Clark and Watling, 2005; Yin et al., 2009; Zhang et al., 2010; Fei et al., 2013). Shao et al. (2014) revealed that there are day-to-day variations in hourly OD demand and traffic flow on links, especially during morning peak hourly periods over the year.

The day-to-day fluctuations in vehicular traffic demand, especially during the morning peak hour period, are remarkable (Tian et al., 2014; Bian et al., 2015). Apart from the promotion of daily variation of travel patterns and network topology, trip chaining is also one of the possible factors that can lead to the covariance between different OD pairs, especially in peak periods.

Similarly, carpooling and ridesharing are two emerging contributors to the OD demand

covariance. For instance, the Uber ridesharing service was introduced in the United States in 2010 ("How Uber Works: Insights into the Business and Revenue Model," 2018). Uber is a burgeoning transport industry. In the United States, the user penetration of online ridesharing services was increased from 12.6% to 17.8%, while the number of ridesharing users was increased from 40.6 to 58.5 million respectively, in the two years from 2016 to 2018. As a result, the revenue in ridesharing has been increased by 87.8% within the period concerned ("Ride-Hailing - United States | Statista Market Forecast," 2018). Indeed, ridesharing could generate considerable covariance between traffic demands by OD pairs. With the use of a ridesharing service, the user could even share the same car with a stranger.

Knowledge of the travel times on the road network to be expected is a well-perceived priority of travelers. Estimated or predicted travel time enables travelers to make more accurate and appropriate decisions regarding their travel choices, thus avoiding unnecessary delays, particularly under non-recurrent conditions (Taylor, 2013). Travel time on a road link over the peak hour period is also stochastic as a result of network uncertainties due to recurrent and non-recurrent traffic congestions. In particular, there exist covariance effects on travel times, particularly between adjacent links, because of the propagation of traffic congestion.

Estimations of both link travel time and OD demands are the most efficient when based on the observed data obtained from different types of advanced traffic sensors such as point sensors and AVI detectors. For instance, observed data from point sensors (e.g., loop detectors) enables OD demands to be estimated daily during a selected typical period. Additionally, the acquisition of data from AVI sensors (e.g., Bluetooth or Wi-Fi) enables the estimation and prediction of travel time of a territory-wide road network. Thus, using different types of sensors based on a specific sensor location scheme can enable simultaneous estimation of link travel times and OD demands. The

economic potential of simultaneous estimation has excited significant interest recently.

1.2 Research objectives

This thesis is devoted to proposing new models to optimize the number and locations of multi-type traffic sensors for separate and/or simultaneous estimation of day-to-day vehicular traffic demand by OD pair and travel time on links with covariance effects.

In this research, the proposed modeling approach aims to optimize the locations of different types of traffic sensors, such as point sensors and AVI sensors in the road network. These optimally located sensors in the road network can offer sundry information that can be organized and used to estimate valuable traffic information such as OD demands and link travel times. However, link-level data collected by point sensors are inconsistent with path-level data collected by AVI sensors due to measurement errors and travel demand variation. This inconsistency between multi-source data should be solved. The variations of the OD demands and link travel times are considered in this research to make the proposed model more robust under different traffic conditions.

The following objectives of this research are described:

1. To propose effective rules for determining the locations of traffic sensors and estimating both mean and covariance of day-to-day peak hour vehicular traffic demands by OD pairs in road networks with uncertainty.
2. To formulate and solve the multi-type sensor location and OD demand estimation problems considering spatial covariance between different OD pairs and/or temporal covariance between multiple hourly periods.
3. To develop an integrated model that optimizes multi-type sensor locations for simultaneously estimating day-to-day OD demands and link/path travel times with

uncertainty and solves the inconsistency of multi-source data from different types of sensors.

Firstly, a traffic sensor (i.e., traffic count) location optimization model is developed for day-to-day OD demand estimation considering spatial covariance between different OD pairs during the peak hour period (objective 1). Secondly, the proposed model is then extended to a multi-type sensor location model for travel demand estimation incorporating spatial-temporal covariances of OD demand between different OD pairs during different time periods (objective 2). Thirdly, based on these models achieved by objectives 1 and 2, an integrated model is proposed to install multi-type traffic sensors for simultaneously estimating mean and covariance of OD demand and mean and covariance of link travel time with uncertainty (objective 3).

1.3 Structure of the thesis

This thesis consists of six chapters. The relationships among these chapters are illustrated in Figure 1.1. Chapter 1 briefly introduces the research problems and the objectives of the thesis. In Chapter 2, the state-of-the-art on SLPs for estimation of OD demand estimation and link/path travel time is extensively reviewed. The core of this thesis is composed of the following three chapters. Chapters 3 and 4 focus on the covariance effects of OD demand between different OD pairs and/or between different time periods on the SLPs. Chapter 5 explores the covariance effects of OD demand and of link travel time for the multi-type SLPs. Chapter 6 summarizes the key findings of the research and suggests further studies.

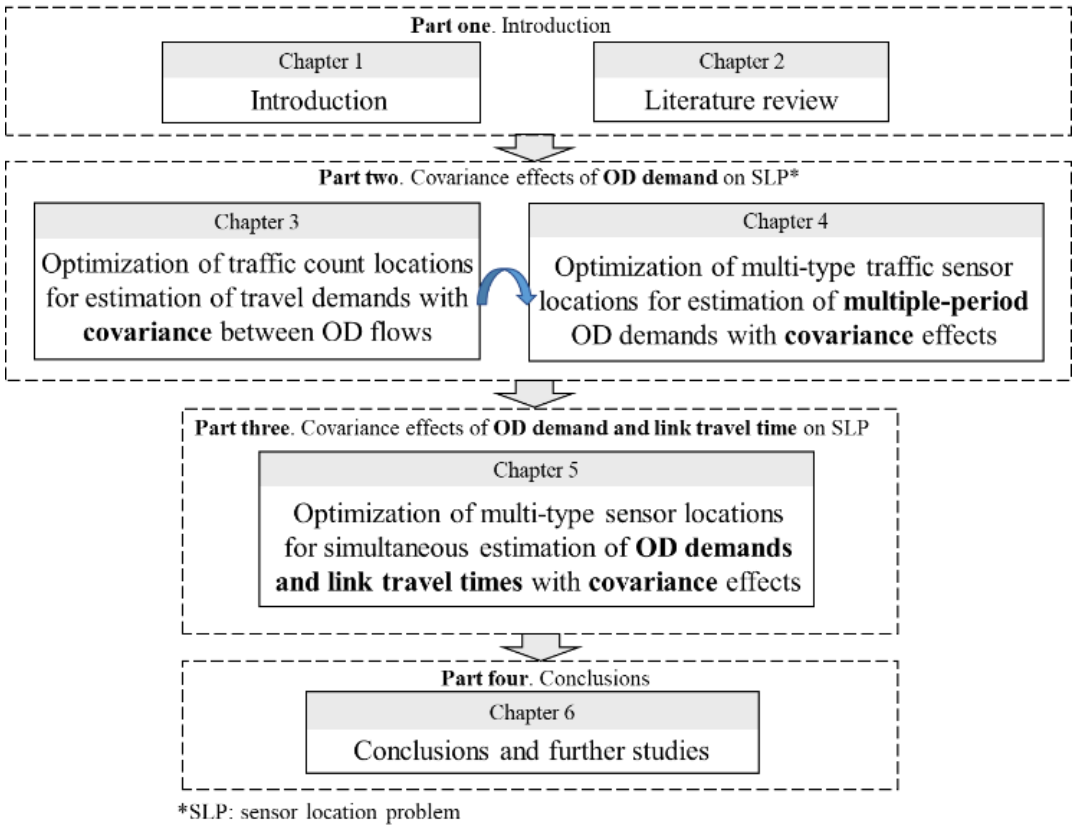

Figure 1.1 Structure of the thesis

In Chapter 3, to explicitly consider the covariance effects of vehicular traffic demand between different OD pairs, the traffic sensor (i.e., traffic count) locations are optimized for stochastic OD demand estimation. The research presented in Chapter 3 proposes a new traffic sensor location model that considers the mean, variance, and covariance of OD demand. With an extension of the maximum possible relative error (MPRE) concept, the proposed model intends to minimizing the weighted sum of two MPRE related to the mean and covariance of OD demand estimates with a given budget constraint.

For fully utilizing the information obtained from different types of sensors, some critical issues are explicitly considered in the research presented in Chapter 4. How to optimize the multi-type sensor locations is investigated in accounting for both spatial

and temporal covariance of stochastic OD demand during different time periods. The mathematical properties of the proposed model and empirical experiments are studied to examine the trade-off between point sensors and AVI sensors.

Even though significant progress has been made in formulating and solving the traffic SLPs, the determination of traffic sensor locations for different objectives (e.g., traffic flow estimation, travel time estimation) is valuable to be studied. Constrained by the financial budget, a limited number of traffic sensors can be allocated in a road network. However, traffic planners and managers prefer to make comprehensive use of each traffic sensor for various traffic management and control purposes. Therefore, in Chapter 5, an integrated model is developed to deploy multi-type traffic sensors, importantly for simultaneously estimating OD demand and link travel time with covariance effects. Finally, Chapter 6 concludes this research with key findings and suggestions for further studies.

2. Literature review

Traffic sensor technologies have been rapidly developed to provide abundant data in this new era. This research, as also mentioned in Chapter 1, aims to comprehensively study the traffic SLPs by explicitly considering covariance effects of OD demand and/or vehicular travel time for ITS applications.

This chapter is structured as below. Section 2.1 introduces different types of traffic sensors that provide multi-source traffic data. Section 2.2 shows the OD demand estimation models with and without consideration of OD demand covariance. In addition, Section 2.3 focuses on the stochastic travel time estimation problems under uncertainty. By combining OD demand estimation and travel time estimation, the fundamental traffic sensor location models are reviewed in Section 2.4. Various criteria to determine sensor locations proposed in the literature are summarized.

2.1 Types of traffic sensors

Sundry traffic sensors serve as productive data sources in ITS for providing sufficient observations to monitor traffic conditions. Based on the type of the collected data, traffic sensor systems can be categorized into two groups (Table 2.1): (i) point sensor system and (ii) AVI (also referred to as point to point) sensor system.

Point sensors detect the vehicular traffic flows traversing the road links, together with the average vehicle speeds captured within the detection range of each point sensor. Taking the microwave radar sensor as an example, smart microwave sensors can count all the vehicles passing by these point sensors and detect their vehicular speeds within a road segment up to a 300-meter range (Smartmicro, 2020). Inductive-loop vehicle detectors can detect all vehicles passing a certain point using a moving magnet to

induce an electric current in a nearby wire. It is rational to assume that the link travel times can be approximated by the observations from point sensors, particularly for urban road links with a length less than 300 m (Li et al., 2006a; Xing et al., 2013; Gentili and Mirchandani, 2018).

For the group of point sensors, the loop detector is one of the most commonly used sensors with low cost but high measurement errors (Coifman, 2004). On the contrary, microwave radar sensors can provide more reliable and accurate observations of travel time (or speed) information with 1% to 5% measurement errors (Schubert et al., 1995).

In addition to point sensors, the AVI sensor system can record the locations and timestamp the vehicles equipped with AVI tags. By matching the records from AVI sensors installed at both ends of a selected path, the path travel time of tagged vehicles can be reported by the AVI sensor system. According to Antoniou et al. (2004), AVI sensors can be classified into three groups: (i) area-wide tracking sensors (e.g., Global Positioning Systems and cell phone tracking systems), (ii) location-based entire vehicle identification sensors (e.g., automatic license plate recognition (ALPR) detectors), and (iii) location-based partial vehicle identification sensors (e.g., radio-frequency identification (RFID) readers, Bluetooth detectors, and Wi-Fi systems).

Sensors in Group (i) can track vehicles throughout the entire road network. Sensors in Group (ii) can identify all vehicles in a short-range area, as all vehicles should, by law, have a license plate in a visible position. Sensors in Group (iii) can recognize only a portion of vehicles equipped with specific tags in a short-range area. The AVI sensors considered in this research belong to Group (iii), which are location-based partial vehicle identification sensors. These AVI sensors normally have two main functions: counting the number of tagged vehicles passing a specific sensor location and matching the tagged vehicles at different locations for recording partial path flows.

In practice, different types of AVI technology have various detection zones and matching accuracy. For instance, Bluetooth (or Wi-Fi) sensors can detect vehicles equipped with Bluetooth devices within a short-range area around the sensors. These sensors are capable of capturing traffic from different directions but with higher detection errors. On the other hand, the RFID reader and ALPR camera can only detect one-direction traffic with higher accuracy in matching the same vehicle. However, due to privacy issues, only commercial vehicle data captured by RFID and ALPR sensors are allowed to be used in Hong Kong. In this research, it is assumed that point sensors with lower costs can observe both the link flows and link travel times at the installed locations. AVI technologies such as ALPR can detect relatively accurate path travel time data between the locations installed with AVI sensors.

Table 2.1 Different types of traffic sensors

Type of sensors	Example	Traffic data collection	Application
Point sensor	Loop detector, Video detector, Magnetic sensor	Link flow/speed	OD estimation; link travel time estimation
AVI sensor	Bluetooth sensor, Wi-Fi sensor, RFID reader, ALPR system	Partial link/path flow; Path (segment) travel time	OD estimation; Path travel time estimation; Link or path choice proportion estimation;

It is believed that under the financial budget constraint, more point sensors than AVI sensors should be installed because AVI sensors are normally more expensive and can provide only the partial path flow/travel time information between node pairs with AVI sensors installed at both ends. Nevertheless, due to the limited budget and physical constraints, it is impossible to install point sensors on each link for the entire road network with over a thousand links. Furthermore, point sensors can only provide traffic

information on a point (e.g., flow, speed, and/or travel time on a link), while AVI sensors are able to cover a spatial area by matching the timestamp information between the node pair with AVI sensors (i.e., the path travel time between the node pair). In reality, AVI sensors are also valuable as a complementary data source, particularly for each path with many links but a limited number of point sensors.

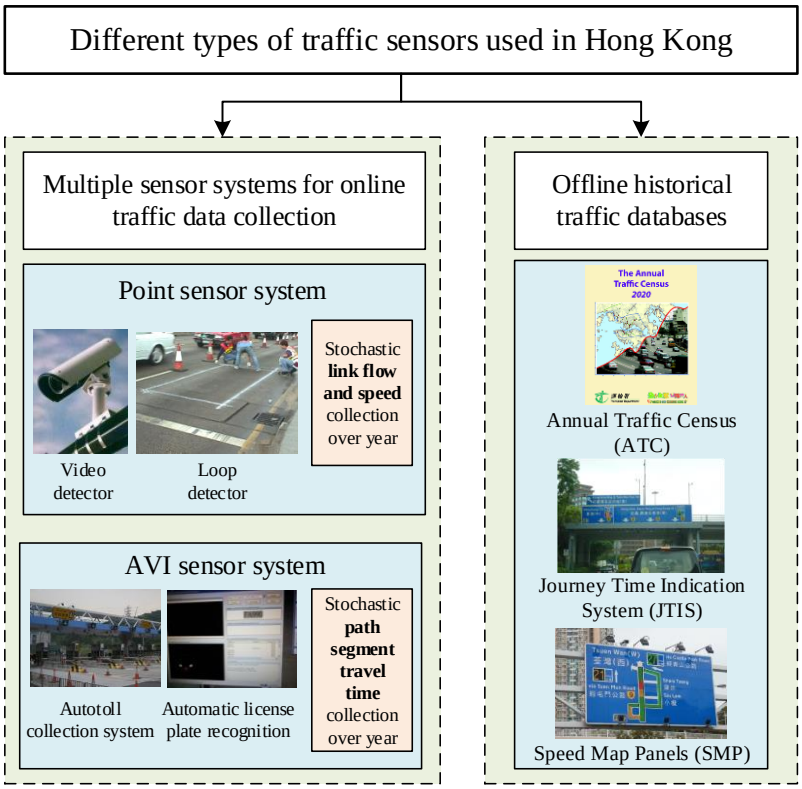

Figure 2.1 Different types of traffic sensors with various traffic databases in Hong Kong

As presented in Figure 2.1, in Hong Kong, video and loop detectors have been adopted for collecting traffic flow data by time of day and day of the year at about 180 selected locations for the establishment of the Annual Traffic Census (ATC) database. In addition, the ITS such as the Journey Time Indication System (JTIS) and the Speed Map Panels (SMP) system has been deployed in Hong Kong's major routes (http://tis.td.gov.hk/rtis/ttis/index/main_partial.jsp). These ITS have adopted AVI

technologies (RFID tags and automatic license plate recognition cameras) and video-based point sensors for the collection of different traffic data to facilitate the journey time and speed estimation on the selected paths and links.

It should be noted that each type of sensor system has its unique advantages. Hence, there is great potential by integrating different traffic information from multi-type sensor systems to consistently estimate the spatial-temporal traffic states of the entire road network (Hu et al., 2015; Wu et al., 2018). Although some previous studies have proposed novel models to install multi-type traffic sensors, this research aims to further investigate the trade-off between multi-source data from different traffic sensors and their effects on various estimation purposes with synthetic and real network data. For example, Zhou and List (2010) proposed an information theory-based sensor location model for OD demand estimation. Point sensors or AVI sensors can be optimally installed to separately estimate OD demands based on observations from either point sensors or AVI sensors. Hu et al. (2015) proposed an integrated model for OD demands and heterogeneous sensor locations including AVI sensors (camera-based license plate recognition detectors) and point sensors (vehicle detectors). However, the priority of point sensor or AVI sensors considering their cost ratios has not been addressed. These previous studies for multi-type traffic sensor location problems proposed models to separately install point or AVI sensors mainly for estimation of only mean OD demands. To accurately estimate mean OD demands, the data collected from a single sensor type should be enough. In this study, with consideration of the OD demand covariance between different time periods, more information should be captured by multi-type sensors as more unknown variables are needed to be estimated. The observed link-level information (e.g., link flows and link speeds) from point sensors can be combined with the observed path-level information (e.g., path flows and path travel time) from AVI sensors. Furthermore, the trade-off between these different sensor types in terms of the allocation of total budget can be explicitly examined.

2.2 OD demand estimation with uncertainty

Estimation of OD demands by link flow observations has been commonly used for transport planning and traffic management purposes in the past decades. The OD demand is a fundamental input for traffic assignment or traffic simulation models in order to estimate the link flows in the road networks (Caggiani et al., 2013; Antoniou et al., 2016). Traditionally, the deployment of traffic sensors deserved serious consideration for accurate estimation of the mean (or expected value) of the OD demands, as shown in Table 2.2.

Due to the daily variations in travel activity patterns, OD demands for a typical hourly period are not deterministic but actually fluctuate from day to day (Clark and Watling, 2005; Yin et al., 2009; Zhang et al., 2010; Fei et al., 2013). Shao et al. (2014) revealed that there exist day-to-day variations in hourly OD demand and traffic flow on road links, especially during morning peak hourly periods over the year.

Table 2.2 Categories of OD estimation and traffic sensor location problems

	Mean and/or variance of OD demands	Mean, variance, and **covariance of OD demands**
OD estimation problem	Yang et al. (2018); Ma et al. (2020)	Shao et al. (2014); Shao et al. (2015)
Traffic sensor location problem	Yang (1995); Yang et al. (2001)	--
Combination of traffic sensor location and OD estimation problems	Owais et al. (2019); Zhu et al. (2016)	**Chapters 3 and 4** (OD demand in a single period and multiple periods, respectively)

The covariance of stochastic OD demands is a nontrivial statistical characteristic in light of joint travel behaviors and network uncertainty (Clark and Watling, 2005; Yang et al., 2018; Z. Zhu et al., 2018). Many scholars have pointed out that joint travel

behaviors (including ridesharing and carpooling) can effectively increase vehicle occupancy and then decrease the vehicular traffic flow to potentially mitigate traffic congestion (Giuliano et al., 1990; Goel et al., 2016). Altshuler et al. (2019) and Fu et al. (2019) further demonstrated that joint travel behaviors would enlarge the covariance of vehicular traffic flow between different OD pairs.

The effects of joint travel behaviors and network uncertainty on traffic flows and their covariances are evident, particularly under congested conditions in the morning peak hour (Yin et al., 2017; Li et al., 2020). The covariance effects among different OD pairs, apart from mean values of OD flows, can provide insightful information to infer travel patterns under uncertainties. The estimation of stochastic and correlated rather than deterministic OD demands reveals significant interest, especially in a congested network.

For the deterministic OD demand estimation in the literature, the previous studies have proposed many functional methods, including maximum likelihood estimator (MLE) (Spiess, 1987), entropy maximization (EM) (Van Zuylen and Willumsen, 1980), generalized least square (GLS) (Cascetta, 1984; Yang et al., 1992), and Bayesian inference (Maher, 1983).

Some studies have assumed that link choice proportions are fixed if congestion effects are not considered (Yang and Zhou, 1998; Simonelli et al., 2012). In contrast, other studies have assumed that link choice proportions are deterministic and determined exogenously by AVI data or explicitly by traffic assignment methods and have incorporated this assumption into various traffic count location models (Zhou and List, 2010; Zhu et al., 2016; Owais et al., 2019). Updated stochastic link choice proportions should be used when considering the stochastic effects of congestion and updated OD demand estimates on traffic count location problems, because travelers select different

routes under different congestion conditions.

Thus, to account for the effects of the stochasticity of OD demand and link flow and the effects of traffic congestion, the link choice proportions are regarded as stochastic variables and updated by a traffic flow simulator during the iteration process in the second stage of the model developed in this thesis.

On the other hand, some scholars have examined the effects of variance and covariance relationship of OD demands on traffic assignment problems in a stochastic road network (Chen et al., 2002; Waller et al., 2006; Castillo et al., 2008a; Duthie et al., 2011; Ma and Qian, 2017). Shao et al. (2014), Yang et al. (2017), and Ma and Qian (2018) extended the GLS model for stochastic OD demand estimation with explicit consideration of variance and covariance of OD demands. However, an implicit or explicit probabilistic assumption has commonly been adopted in these studies for stochastic OD demand estimation. To be less contingent on a specific probabilistic assumption, Yang et al. (2019a) and Z. Zhu et al. (2019) are pioneers for stochastic OD demand estimation by proposing a hierarchical framework based on a generalized method of moment or a Bayesian model. As a probabilistic assumption can potentially be relaxed by considering Kullback–Leibler (KL) divergence, Menon et al. (2015) and Ma (2016) demonstrated that KL divergence is capable of estimating sparse OD demands under uncertainty based on multi-source data.

Furthermore, the traffic flows of different OD pairs in multiple periods are highly correlated with one another because of the phenomenon of joint travel behavior and the inter-relationships of travel patterns in different periods (Ballis and Dimitriou, 2020). Elucidating these patterns of traffic flow for multiple periods can significantly benefit transportation planning and management.

The OD demands in multiple periods show spatial, temporal, and multi-period covariance in road networks. Specifically, as depicted in Shao et al. (2014), the covariance of OD flows in a spatial manner represents the statistical correlation of traffic flows within the same time period (e.g., morning peak period) among various OD pairs. Temporal covariance of OD flows represents the correlation of vehicular flow for the same OD pair but among different time periods (i.e., 8:00 –9:00 and 17:00–18:00). In addition to spatial and temporal covariance, OD demands may also show multi-period covariance, i.e., correlation of OD demands for different OD pairs over different time periods. In fact, these three types of OD demand covariances simultaneously contribute to the stochasticity of multi-period OD demands.

In stochastic transportation networks, the covariance of OD demands in multiple periods is often overlooked in the OD demand estimation problem. Using mean OD demand estimates without consideration of variance and covariance may lead to biased outputs as the variation of travel patterns over time cannot be adequately captured (Fu et al., 2019).

In the last decade, a few studies have made important contributions in showing the importance of capturing OD trip chaining behavior and temporal interaction. For instance, to explicitly consider the trip chaining behavior, Cantelmo et al. (2020) developed a new state-space framework based on a Kalman filter for OD demand estimation. Djukic et al. (2012) and Krishnakumari et al. (2020) considered the variation of OD demand by time of day and day of the year using a principal component analysis (PCA) method to reduce the dimensionality of high-dimensional OD matrices. A quasi-dynamic extended Kalman filter was developed by Marzano et al. (2018) to estimate stochastic OD demand more efficiently. Recently, several studies have focused on estimating the covariance relationship of OD demand rather than the mean OD demand (Shao et al., 2014, 2015).

2.3 Link/path travel time estimation with uncertainty

In the literature, the travel time estimation methods have been developed depending on the available data obtained from different types of sensors. In a congested road network, travel times on different links or paths can be highly correlated. For instance, traffic congestion on an upstream link could also lead to congestion on downstream links due to spillback effects.

Many studies have demonstrated that ignoring the correlation of travel time can result in an inaccurate evaluation of transport projects (Clark and Watling, 2005; Shao et al., 2013). Guo et al. (2020) uncovered the spatial and temporal correlation of link travel speed between different links based on empirical datasets from different networks. This thesis also found that correlations increase at large with decreased distance in time and space. Zhang et al. (2019) devised a deep learning-based method to model the joint distribution of two successive links by considering the spatiotemporal correlation between travel times on different links. Tani et al. (2020) developed a novel method to structure stochastic link travel time and obtain the covariance information of link travel time by expanding the concept of risk premium.

In literature, the covariance effects of travel time or speed are investigated based on the data provided by fixed traffic sensors. How the covariance of travel time between different links influences the deployment of traffic sensors is still an opening and exciting question to be explored.

Therefore, the travel time covariance should also be considered in accounting for the variation of road traffic conditions, particularly in congested urban road networks. Estimating stochastic and correlated travel time in a territory-wide road network is more challenging due to the uncertainty of the traffic conditions and limited traffic

information from sensors (Zheng and Van Zuylen, 2013; Gentili and Mirchandani, 2018). Multi-source traffic data from emerging sensor technologies can be leveraged in this big data arena to obtain more accurate estimates of stochastic link travel times, especially for the entire road network with thousands of road links but comparatively a few traffic sensors (Shao et al., 2018). There is a need to propose a robust method to estimate stochastic and correlated link travel times in congested road networks with the use of limited multi-source data from different traffic sensors.

2.4 Sensor location problem for estimation of OD demands and travel times

To collect productive and effective information for estimation of OD demands and/or travel times in a large road network with many links, multi-type traffic sensors should be allocated systematically rather than arbitrarily. Nevertheless, the SLP has been examined in the literature to optimize the traffic sensor locations in road networks but mainly for one specific purpose or objective only, as summarized in Table 2.3.

In this thesis, SLPs are categorized into two types:

(i) *SLP for Flow Measurement:* to identify the optimum location of traffic sensors on the road network to improve the accuracy of traffic flow. They include OD flows, link flows, path flows observation, and/or estimation (Gentili and Mirchandani, 2012; Castillo et al., 2015).

(ii) *SLP for Travel Time Measurement*: to identify the optimum location of traffic sensors that enable the accurate estimation of link/path travel times on a freeway or road network (Gentili and Mirchandani, 2018).

An essential objective of SLP resides in the estimation of OD demands for strategic planning purposes (Zhou and List, 2010; Hu et al., 2015; Ye and Wen, 2017; Fu et al.,

2019). For instance, Yang et al. (1991) proposed an MPRE to quantify the relative deviation of mean OD demand estimates from their actual values. On top of that, Yang and Zhou (1998) proposed four criteria: the OD covering rule, maximum flow fraction rule, maximal flow-intercepting rule, and link independence rule to determine the sensor locations. Yang et al. (2006) extended the MPRE criterion to study the screen-line SLP. Other scholars have also proposed other criteria to measure the accuracy of OD demand estimates for SLP, such as the total demand scale (Bierlaire, 2002) and generalized demand scale (Chootinan and Chen, 2011).

Previous studies that have examined flow observability via SLPs (Castillo et al., 2012, 2015; Viti et al., 2014; Xu et al., 2016) have determined whether flows observed on links/paths in a road network by installed traffic sensors are sufficient for estimating the flows on other links/paths in the network without installed traffic sensors. Most of these studies have focused on determining optimal sensor locations by minimizing the total cost of sensor installation to enable network-wide link/path flow observation or estimation. Thus, to capture as much information as possible from installed sensors, these studies have typically modeled the flow conservation conditions—which describe the relationships between link, path, and OD flows— as constraints. For instance, Viti et al. (2014) devised a novel methodology to quantify the quality of a solution for partial observability of link flow, which occurs when traffic flow on some links of a road network cannot be observed or uniquely determined as a limited number of sensors are deployed on the network. By comparison, Xu et al. (2016) developed a robust SLP model for full observability of link flow that considers the propagation of measurement errors during the inference of link flow. More recently, Rinaldi and Viti (2017) developed a methodology to determine sensor locations on a road network by identifying optimal route sets, which enhances both full and partial observability of link flow over a road network.

Table 2.3 Categories of sensor location problems

	OD demand estimation	Link travel time estimation	Simultaneous estimation of OD demands and link travel times
Single sensor type	Simonelli et al. (2012), Fu et al. (2019)	Mirchandani et al. (2009), N. Zhu et al. (2018)	\
Multiple sensor types	Zhou and List (2010), Hu et al. (2016)	Xing et al. (2013), Shao et al. (2018)	**Chapter 5** (mean and covariance of OD demands/link travel times)

From traffic planners' aspects, traffic demands inferred from link flow observations are intrinsically fundamental traffic characteristics. However, OD demand estimation is usually an underdetermined problem because traffic sensors are often much less than the number of unknown OD pairs, especially in a large-scale road network.

Many studies have proposed various models to deal with this underdetermined system and thus confine the search space around meaningful solutions. For example, utilizing prior OD demand information obtained from surveys or simulation models as part of the model formulation incorporates important structural information related to the temporal and spatial distribution of trip-making activities. Based on the observations from traffic sensors, an EM model was first developed by Van Zuylen and Willumsen (1980) to find the most likely OD demand matrix. Using Bayesian theory, Maher (1983) proposed analytical models to update the prior mean and variance of static OD demand.

In fact, the number, type, and locations of sensors significantly affect the quality of the OD demand estimates. Most researchers have developed models to optimize traffic sensor locations concerning the accuracy of mean OD demand estimation (Bianco et al., 2001; Xiong et al., 2014). Several recent studies of the SLP have focused on the variances of OD flow to minimize the error of OD demand estimates considering the daily variation of travel patterns (Zhou and List, 2010; Simonelli et al., 2012). Fu et al.

(2019) further examined the significance of spatial covariance of OD demand during peak hour periods on SLP.

However, only the OD demands in one specific period, e.g., the morning peak was considered in these studies such that only the spatial information can be incorporated. As both spatial and temporal information about OD demands can intrinsically facilitate routing policies, transportation management, and traffic control for various periods, estimation of multi-period OD demands has assumed growing importance in the context of intelligent transportation systems (Meng and Wang, 2011; Ohazulike et al., 2013; Meng et al., 2015). Hence, there is an urgent need to generalize the traffic sensor location method for multi-period OD demand estimation, emphasizing spatial, temporal, and multi-period covariances.

In the literature, there are many indexes to measure the model performance for sensor location and OD demand estimation problems. For instance, some prominent statistical measurements, including mean absolute error, mean absolute percentage error, mean square error, root mean square error, and so forth, have been widely used (Cascetta, 2009; Hu et al., 2015). However, the true values of OD demand, which are necessary for these measurements, can hardly be obtained in practice.

Apart from these statistical measurements, some scholars have proposed other criteria to evaluate the performance of estimated OD demand without the true values. Yang et al. (1991) proposed a maximum possible relative error to measure the maximum deviation of estimated OD demand from true values. Bierlaire (2002) proposed a total demand scale to calculate the difference between the maximum and minimum possible total OD demand estimates constrained by sensor measurements. Chootinan and Chen (2011) further developed a general demand scale to assess the accuracy of OD demand estimates from traffic sensors. Zhou and List (2010) and Xing et al. (2013) proposed

the percentage of reduction in variance to measure the quality of sensor locations for OD demand estimation and travel time estimation, respectively.

In addition to algebraic methods, heuristic algorithms have been developed, such as the branch and bound algorithm and genetic algorithms (Castillo et al., 2012; Salari et al., 2019). For example, Cipriani et al. (2006) formulated two different heuristic algorithms for solving traffic sensor location problems by maximizing the OD demand fraction intercepted by installed sensors. Viti et al. (2008) devised a heuristic algorithm that considers the correlation between link flow and link travel time to optimize traffic count location for accurate travel time estimation. Owais et al. (2019) constructed a robust traffic sensor location model that minimizes the MPRE for OD demand estimates and the total cost of sensor installation. Thus, they devised a multi-criteria meta-heuristic algorithm based on a multi-objective method to examine the relationship between the accuracy of OD demand estimation and the cost of sensor installation.

A few studies on SLPs have focused on estimating network-wide link/path travel time in a road network for various ITS development (Mirchandani et al., 2009; Ban et al., 2011; Danczyk and Liu, 2011; Zhu et al., 2017). For example, Viti et al. (2008) extended the concept of MPRE for link travel time estimation to monitor the traffic states. Xing et al. (2013) further developed an information-theoretic model proposed by Zhou and List (2010) for heterogeneous sensor locations to estimate the link/path travel time with uncertainties. N. Zhu et al. (2018) proposed a data-driven link-based sensor location model to maximize the travel time information gain.

2.5 Summary

As discussed in the above sections, although some previous studies have devised

models that locate different types of traffic sensors, they have focused on the trade-off between using multi-source data from different traffic sensors and the suitability of these data for various estimation tasks. Thus, there remains a need to determine how to integrate different traffic information from multi-type sensor systems, as this would enable consistent estimates of the spatial-temporal traffic states of an entire road network.

Clearly, the above studies have demonstrated that the covariance of OD demands plays an essential role in stochastic OD demand estimation problems. However, less attention has been paid to estimating OD demand while simultaneously considering spatial, temporal, and multi-period covariances. Multi-period covariance is a statistical measurement that is essential for quantifying the interrelationship of vehicular traffic demand between different OD pairs and different time periods, considering the within-day and day-to-day variation of travel patterns. In particular, the multi-period covariance of OD demand is a critical input for transportation planning and management. Therefore, a vital extension of previous studies is to formulate the stochastic OD demand estimation with consideration of different OD demand covariances.

Previously reported models for SLPs deploy single-type or multi-type sensors primarily to obtain more accurate estimates of OD demands or link travel times than have been obtained by other methods; studies have not explicitly considered the covariance relationships of OD demands or link travel times. However, OD demands can be efficiently estimated from link flows that are highly interrelated with travel time on links, especially under congested conditions. Thus, when determining traffic sensor locations, it should be possible to simultaneously estimate OD demands and link travel times over a peak-hour period to provide coherent information for advanced traffic management and traveler information systems (Li and Ouyang, 2011; Fei et al., 2013).

In this research, multi-type sensor locations are optimized to allow simultaneous estimation of stochastic OD demands and network-wide link travel times with explicit consideration of covariance between OD demands and between link travel times. Moreover, targeted simultaneous estimates need not be limited to OD demand and/or link travel time, as heterogeneous data from multi-type sensors can be used to extend the developed sensor location model to estimate other traffic information, such as link flows, link speeds, and path travel times.

3. Optimization of traffic count locations for estimation of travel demands with covariance between Origin-Destination flows

As depicted in Chapters 1 and 2, vehicular traffic between different OD pairs for a typical hourly period may statistically correlate with each other. The OD demand covariance effect mainly generated from the daily variation of travel patterns, network topology, and trip chaining activities of household members can be particularly significant during the morning peak hour. Moreover, the hourly OD demands are not deterministic but indeed fluctuate on a daily scale.

With the increasing attention on the OD demand variance and covariance in stochastic road networks, a new criterion is proposed in this chapter for measuring the estimation accuracy of covariance OD demands. The mathematical properties of this proposed criterion are analyzed to understand better the relationship between the estimation errors of mean and covariance of OD demands.

As indicated in Table 2.2, this chapter is to investigate how to determine the traffic sensor (i.e., traffic count) locations for minimizing the weighted maximum deviation of the estimated mean and covariance of OD demands from the observed values. Different magnitudes of travel demands by OD pair are also taken into account because of the variation of travel purpose. More generally, both the weighted-sum approach and Pareto front approach are examined with the extension of the firefly algorithm (FA) to solve the single-objective and bi-objective problems. Numerical examples are presented to demonstrate the effects, with and without considering the covariance of the OD demands for the optimization of traffic sensor locations.

The rest of this chapter is organized as follows. The background and the illustration of the motivation and main contributions of the research in this chapter are presented in Section 3.1. It is followed by a problem statement in Section 3.2. A new criterion is proposed in Section 3.3 to measure the estimation accuracy of covariance of OD demands. Some properties of the new model are also investigated. In Section 3.4, model formulation for stochastic OD demand estimation and traffic sensor location optimization are introduced. A solution algorithm to solve these problems is discussed in Section 3.5. Some numerical examples are used to demonstrate the effects of the proposed models in Section 3.6. Finally, Section 3.7 summarizes the research in this chapter.

3.1 Background

3.1.1 Motivating example

As mentioned in the preceding section, the demands of different OD pairs are not deterministic and independent. The variance and covariance of OD demands generated from multiple factors do exist in the road network. The relationship among different OD pairs should be considered when allocating the traffic sensors for stochastic OD demand estimation.

It is noted that the stochastic OD demands, particularly for OD demand covariance, are affected by the trip chaining activities. An illustrative example related to the relevant trip chaining activities is used to demonstrate the existence of covariance between different OD pairs and the effects of stochastic OD demands on traffic sensor locations. Seven nodes and three OD pairs {(B,C),(C,F),(B,F)} are included in this illustrative network, given that Node C stands for a school, Node B stands for a home, and Node F stands for an office, respectively.

In this example, suppose that there are two travelers - a father (Traveler A) and his son (Traveler B), Traveler A would like to travel from home to office (B-F), and Traveler B would like to travel from home to school (B-C) respectively. Figure 3.1 illustrates the paths of the father, who has a car, in two different scenarios: (a) with no trip chaining and (b) with trip chaining, respectively. As shown in Figure 3.1(a), in the "no trip chaining" scenario, The father will travel from home (Node B) to the office (Node F) directly. In contrast, as shown in Figure 3.1(b), in the "trip chaining" scenario, he will first travel to school (Node C) together with his son and then travel to the office (Node F) alone. The father and his son will share the same car for the journey from home (Node B) to school (Node C). When trip chaining exists, a journey between (B-F) will be split into two: (i) travel between (B-C) and (ii) travel between (C-F). The overall demands between (B-C) and (C-F) will therefore be correlated.

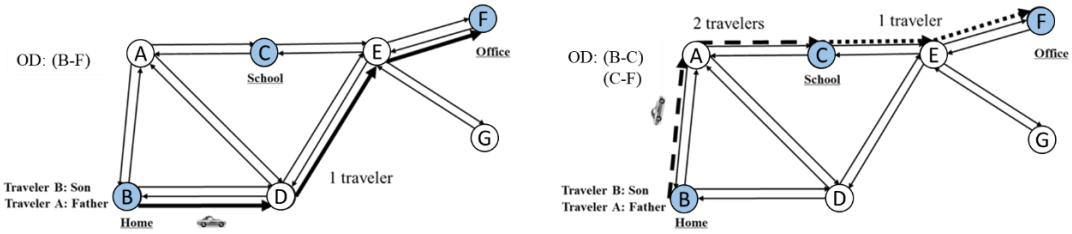

(a) No trip chaining scenario (b) Trip chaining scenario

Figure 3.1 Travel paths in (a) no trip chaining and (b) trip chaining scenarios

W_1, W_2, and W_3 are denoted as the OD demands for (B-F), (B-C), and (C-F), respectively, given that W_1, W_2, and W_3 are independent and follow normal distributions, where $W_1 \sim N(200,30^2)$, $W_2 \sim N(150,36^2)$, and $W_3 \sim N(100,25^2)$, respectively. The proportion of trip chaining users is represented by x, and the standard deviation of OD demands W_1, W_2, and W_3 as σ_1, σ_2, and σ_3, respectively. Therefore, the covariance between W_2 and W_3 could be deduced by the following equation.

$$\mathrm{cov}_{2,3} = x^2 \cdot \sigma_1^2 \tag{3.1}$$

Table 3.1 Relationship among the proportion of trip chaining users, covariance of OD demands, and average vehicle occupancy

Proportion of travelers using trip chaining	Covariance (W_2, W_3)	Average vehicle occupancy [a]
0.0%	**0.0**	**1.00**
17.8%	28.5	1.19
50.0%	225.0	1.80
100.0%	**900.0**	**2.25**

[a] average number of people in a vehicle, including the driver

As shown in Table 3.1, when the proportion of travelers using trip chaining increases, both the covariance between W_2 and W_3 and average vehicle occupancy increase. For instance, when there is no trip chaining (proportion equal to zero), covariance will be zero, and vehicle occupancy will be 1, respectively. In contrast, when everyone uses trip chaining (proportion equal to 1), covariance and vehicle occupancy will increase to 900 and 2.25, respectively. This testifies the prevalence of covariance between OD demands when trip chaining becomes popular.

3.1.2 Contributions

Different from the conventional traffic sensor location optimization models, the main contribution of this chapter is to optimize the traffic sensor locations so as to estimate **both the mean and covariance** OD demands with minimization of the overall estimation error (in terms of the relative errors of both the mean and covariance of OD demands).

In general, the main contributions of this chapter could be viewed from two aspects: theoretical and methodological developments.

For the **theoretical** development, a new concept is introduced, together with a new

model formulation, to explicitly capture the effects of covariance between OD flows on the determination of traffic sensor (i.e., traffic count) locations for OD demand estimation from link flow observations. The mathematical properties of the new model are examined and discussed. As shown in the numerical results, the conventional model is indeed a special case of the newly proposed model. With the new model presented in this research, the traffic SLP can be generalized. Therefore, the effects of covariance between OD flows can be incorporated to optimize the traffic sensor locations for simultaneous estimation of mean and covariance of OD demands. Stochastic link choice proportions are updated using an adapted traffic flow simulator to consider the effects of traffic congestion and stochastic OD demands.

As for the **methodological** development, the proposed model has been extended by considering covariance among OD pairs and different magnitudes of travel demands by OD pair. The metaheuristic solution algorithm has also been improved for solving the bi-objective optimization problem.

3.2 Problem statement

In this chapter, there are mainly two stages for modeling the traffic SLP for stochastic OD demand estimation: (i) the traffic sensor location stage and (ii) the stochastic OD demand estimation stage, as shown in Figure 3.2. The connections between these two stages relate to the observed link flows and the values of the weighted maximum possible relative error for mean OD demand (WMPREM) and weighted maximum possible relative error for covariance of OD demand (WMPREC). The observed link flows based on traffic sensor locations from the first stage are the inputs of the second stage. Conversely, the outputs of the second stage, WMPREM and WMPREC, calculated from resultant OD demand estimates, are the inputs of the first stage.

The first stage model is to generate the traffic sensor locations based on prior OD demands, where some existing traffic sensor location rules are mathematically treated as constraints. However, these traffic sensor locations may not be the optimal ones concerning the accuracy of OD demand estimation (Larsson et al., 2010). Therefore, the criteria WMPREM and proposed WMPREC for measuring OD demand estimation accuracy are incorporated to optimize the traffic sensor locations.

For validation purposes, it is assumed that the mean and covariance of observed link flows can be obtained from the "true" stochastic OD demands, which are acquired by the adapted traffic flow simulator (Lam and Xu, 1999). It should be noted that only those links equipped with traffic sensors can provide observed link flows.

At the second stage, stochastic OD demands are estimated using the Bayes method based on the observed stochastic link flows obtained from the first stage, together with prior OD demands. With the resultant stochastic OD demand estimates, the proposed WMPREM and WMPREC for each traffic sensor location scheme can be calculated to examine the accuracy of estimated results on mean and covariance of OD demands. By comparing the values of resultant WMPREM and WMPREC among the traffic sensor location schemes using the genetic algorithm (GA), the optimal traffic sensor location scheme with the minimum OD demand estimation errors can be selected, which is the output of the proposed model.

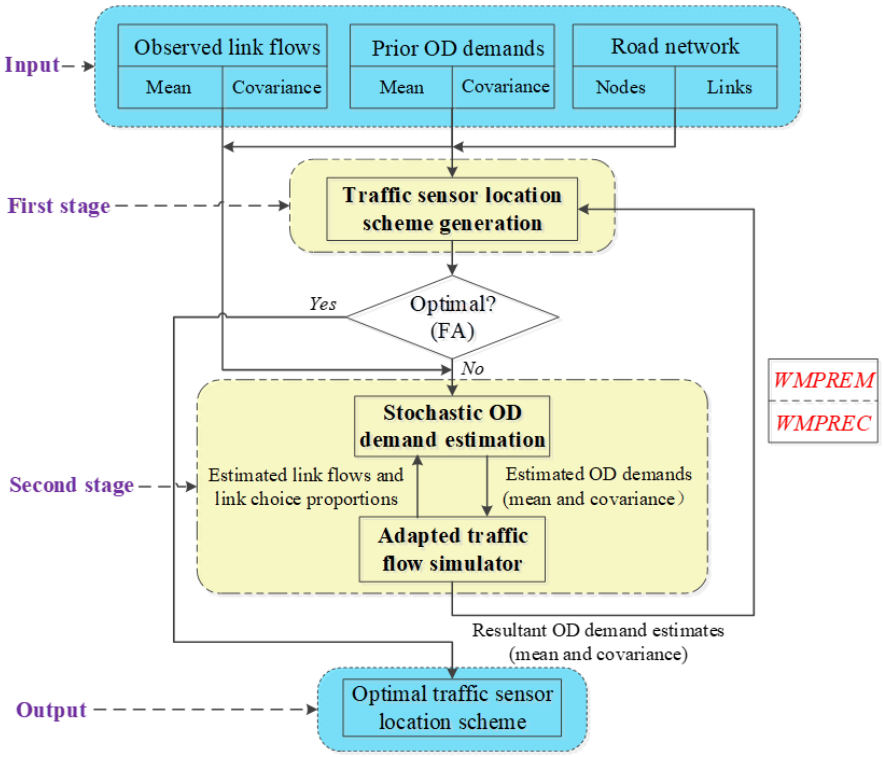

Figure 3.2 The relationship between traffic sensor location and OD demand estimation problems

3.3 Criteria for measuring OD demand estimation accuracy

3.3.1 Model assumptions

A1. It is assumed that all the observed link traffic flows are error-free (Yang et al., 1991; Yang and Zhou, 1998).

A2. The covariance of travel demands between any two arbitrary OD pairs is positive. Specifically, it is assumed that all the entries in the OD demand covariance matrix are positive.

It should be pointed out that the covariance of travel demands between any two arbitrary OD pairs could be negative theoretically. However, it is probably hard to observe the negative OD covariance in reality. Taking the trip chaining in Figure 3.1 for illustration, once traveler A chooses Destination F through Node C instead of selecting the path B-D-E-F, the covariance of travel demands between OD (B-C) and

OD (C-F) should then be positive. Nonetheless, this assumption deserves to be relaxed in further studies to propose a more generalized model.

A3. It is assumed that there is only one sensor or detector allocated at each traffic sensor location.

3.3.2 Relationship between OD demands and link flows

The traffic flows on a link are observed by a traffic sensor during the same peak hourly period (say 8:00 am - 9:00 am) for a typical weekday *l* over a given number of days *h* in the year concerned. The link with (without) traffic sensor is called "observed link" ("unobserved link") throughout this chapter. Because of the daily fluctuation in travel demand over the year, the link flows should be stochastic instead of deterministic.

The sample mean matrix of hourly traffic flows **v** on observed links over the year can be calculated as:

$$\mathbf{v} = (\cdots, v_a, \cdots)^T = \frac{1}{D}\sum_{d=1}^{D} \mathbf{v}_{(d)} \tag{3.2}$$

The sample covariance matrix of traffic flows on observed links can be calculated as:

$$\Sigma^{\mathbf{v}} = \left\{\sigma_{a,b}^{v}\right\}_{\tilde{m}\times\tilde{m}} = \frac{1}{D-1}\sum_{d=1}^{D}\left\{\left(\mathbf{v}_{(d)} - \mathbf{v}\right)\left(\mathbf{v}_{(d)} - \mathbf{v}\right)^T\right\} \tag{3.3}$$

Then, the mean of observed link flow can be obtained by the following Eq. (3.4):

$$v_a = E\left[V_a\right] = E\left[\sum_{w\in W} p_{a,w} Q_w\right] = \sum_{w\in W} p_{a,w} q_w \qquad \forall a \in \tilde{\mathbf{A}} \tag{3.4}$$

According to A2, the covariance between V_a and V_b can be deduced as:

$$\sigma_{a,b}^{v} = \mathrm{cov}\left[V_a, V_b\right]$$

$$= \mathrm{cov}[\sum_{w\in W} p_{a,w} Q_w, \sum_{w'\in W} p_{b,w'} Q_{w'}]$$

$$= \sum_{w\in \mathbf{W}}\sum_{w'\in \mathbf{W}} p_{a,w} p_{b,w'}\, \mathrm{cov}[Q_w, Q_{w'}]$$

$$= \sum_{w \in \mathbf{W}} \sum_{w' \in \mathbf{W}} p_{a,w} p_{b,w'} \sigma^{q}_{w,w'} \qquad \forall a,b \in \tilde{\mathbf{A}} \tag{3.5}$$

Then Eqs. (3.4) and (3.5) can be rewritten as the following matrix:

$$\mathbf{v} = \tilde{\mathrm{P}}\mathbf{q} \tag{3.6}$$

and

$$\Sigma^{\mathbf{v}} = \tilde{\mathrm{P}}\Sigma^{\mathbf{q}}\tilde{\mathrm{P}}^{T} \tag{3.7}$$

3.3.3 Formulation of WMPREM and WMPREC

Yang et al. (1991) proposed the MPRE to measure the reliability of the estimated OD demands. In this chapter, the MPRE is modified as WMPREM. According to assumptions A1 and A2, the true and estimated mean OD demand must satisfy the following relationships.

$$\sum_{w} p_{a,w} q_w = v_a \quad \forall\ a \in \tilde{\mathbf{A}} \tag{3.8}$$

$$\sum_{w} p_{a,w} q^{*}_w = v_a \quad \forall\ a \in \tilde{\mathbf{A}} \tag{3.9}$$

Subtracting (3.8) from (3.9), it follows that

$$\sum_{w} p_{a,w} (q^{*}_w - q_w) = 0 \quad \forall\ a \in \tilde{\mathbf{A}} \tag{3.10}$$

Denote $\lambda_w^{mean} = (q_w^* - q_w)/q_w$ as the relative deviation of the estimated mean OD demands from the "true" one for OD pair $w \in \mathbf{W}$. It follows from $q_w^* \geq 0$ and $q_w \geq 0$ that $\lambda_w^{mean} \geq -1$. Substituting λ_w^{mean} into Eq. (3.10), it follows that

$$\sum_{w} p_{a,w} q_w \lambda_w^{mean} = 0 \quad \forall\ a \in \tilde{\mathbf{A}} \tag{3.11}$$

Denote ρ_{w_0} as the weight of traffic flows in OD pair w_0.

$$\rho_{w_0} = q_{w_0} / \sum_{w} q_w \tag{3.12}$$

Define the average relative deviation of the mean OD demand as

$$G(\boldsymbol{\lambda}^{mean}) = \sqrt{\phi(\boldsymbol{\lambda}^{mean})/n} \tag{3.13}$$

where

$$\boldsymbol{\lambda}^{mean} = \left(\cdots, \lambda_w^{mean}, \cdots\right)^T \tag{3.14}$$

$$\boldsymbol{\rho}_{\mathbf{w}} = (\cdots, \rho_{w_0}, \cdots)^T \tag{3.15}$$

$$\varphi\left(\boldsymbol{\lambda}^{mean}\right) = \sum_{w \in \mathbf{R}} \rho_w \left(\lambda_w^{mean}\right)^2 \tag{3.16}$$

$G(\boldsymbol{\lambda}^{mean})$ is a measure of the estimation error of the mean OD demand. Obviously, the smaller $G(\boldsymbol{\lambda}^{mean})$, the higher the accuracy of the estimation. Therefore, the WMPREM can be defined by the following maximization problem.

$$\text{WMPREM}(\mathbf{z}) = \max_{\boldsymbol{\lambda}^{mean}} G(\boldsymbol{\lambda}^{mean}) \tag{3.17a}$$

subject to

$$\sum_{w} p_{a,w} q_w \lambda_w^{mean} = 0 \quad \forall a \in \tilde{\mathbf{A}} \tag{3.17b}$$

$$\lambda_w^{mean} \geq -1 \quad \forall w \in \mathbf{W} \tag{3.17c}$$

Similar to the definition of WMPREM, WMPREC can be defined as below. The covariance matrices of "true" and estimated OD demands must satisfy the following relationships.

$$\sum_{w \in \mathbf{W}} \sum_{w' \in \mathbf{W}} p_{a,w} p_{b,w'} \sigma_{w,w'}^{q} = \sigma_{a,b}^{v} \quad \forall \ a,b \in \tilde{\mathbf{A}} \tag{3.18}$$

$$\sum_{w \in \mathbf{W}} \sum_{w' \in \mathbf{W}} p_{a,w} p_{b,w'} \sigma_{w,w'}^{q^*} = \sigma_{a,b}^{v} \quad \forall \ a,b \in \tilde{\mathbf{A}} \tag{3.19}$$

Subtracting (3.18) from (3.19), it follows that

$$\sum_{w \in \mathbf{W}} \sum_{w' \in \mathbf{W}} p_{a,w} p_{b,w'} (\sigma_{w,w'}^{q^*} - \sigma_{w,w'}^{q}) = 0 \quad \forall \ a,b \in \tilde{\mathbf{A}} \tag{3.20}$$

Similar to the definition of λ_w^{mean}, let $\lambda_{w,w'}^{cov} = \left(\sigma_{w,w'}^{q*} - \sigma_{w,w'}^{q}\right)/\sigma_{w,w'}^{q}$ denote the relative deviation of the estimated covariance matrix of OD demands from the true one between OD pairs w and w'. According to assumption A4, $\sigma_{w,w'}^{q*}$ and $\sigma_{w,w'}^{q}$ have the same sign, i.e. $\sigma_{w,w'}^{q*}/\sigma_{w,w'}^{q} \geq 0$, it follows that

$$\lambda_{w,w'}^{\text{cov}} = \frac{\sigma_{w,w'}^{q*}}{\sigma_{w,w'}^{q}} - 1 \geq -1 \quad \forall\ w, w' \in \mathbf{W} \tag{3.21}$$

Substituting $\lambda_{w,w'}^{cov} = \left(\sigma_{w,w'}^{q*} - \sigma_{w,w'}^{q}\right)/\sigma_{w,w'}^{q}$ into Eq. (3.20), it follows that

$$\sum_{w \in \mathbf{W}} \sum_{w' \in \mathbf{W}} p_{a,w} p_{b,w'} \sigma_{w,w'}^{q} \lambda_{w,w'}^{\text{cov}} = 0 \quad \forall\ a, b \in \tilde{\mathbf{A}} \tag{3.22}$$

Denote ρ_{w_0,w'_0} as the weight of covariance between traffic flows in OD pair w_0 and OD pair w_0'.

$$\rho_{w_0,w'_0} = \sigma_{w_0,w'_0}^{q} \Big/ \sum_{w,w' \in \mathbf{W}} \sigma_{w,w'}^{q} \tag{3.23}$$

Define the average relative deviation of the OD demand covariance matrix as

$$H(\boldsymbol{\lambda}^{\text{cov}}) = \sqrt{\psi\left(\boldsymbol{\lambda}^{\text{cov}}\right)/n^2} \tag{3.24}$$

where

$$\boldsymbol{\lambda}^{\text{cov}} = \left\{\lambda_{w,w'}^{\text{cov}}\right\}_{n \times n} \tag{3.25}$$

$$\psi\left(\boldsymbol{\lambda}^{\text{cov}}\right) = \sum_{w \in \mathbf{R}} \sum_{w' \in \mathbf{R}} \rho_{w,w'} \left(\lambda_{w,w'}^{\text{cov}}\right)^2 \tag{3.26}$$

$H(\boldsymbol{\lambda}^{cov})$ is a measure of the estimation error of the OD demand covariance matrix. Obviously, the smaller $H(\boldsymbol{\lambda}^{cov})$, the higher the accuracy of the estimation. Therefore, the WMPREC can be defined by the following maximization problem, which is very similar to the definition of WMPREM.

$$\text{WMPREC}(\mathbf{z}) = \max_{\boldsymbol{\lambda}^{\text{cov}}} H(\boldsymbol{\lambda}^{\text{cov}}) \tag{3.27a}$$

subject to

$$\sum_{w \in \mathbf{W}} \sum_{w' \in \mathbf{W}} p_{a,w} p_{b,w'} \sigma_{w,w'}^{q} \lambda_{w,w'}^{\text{cov}} = 0 \quad \forall a, b \in \tilde{\mathbf{A}} \tag{3.27b}$$

$$\lambda_{w,w'}^{\text{cov}} \geq -1 \quad \forall w, w' \in \mathbf{W} \tag{3.27c}$$

In Eqs. (3.17b) and (3.27b), both the mean OD demand q_w ($\forall w \in \mathbf{W}$) and covariance variable of OD demand $\sigma_{w,w'}^{q}$ ($\forall w, w' \in \mathbf{W}$) can be estimated by traditional techniques, such as a weighted least squares method proposed by Shao et al. (2014) or the entropy maximizing method proposed by Van Zuylen and Willumsen (1980). In

this chapter, the entropy maximizing method is adapted to estimate the mean and covariance of OD demands.

3.3.4 Properties of WMPREM and WMPREC

As known in the literature, if the number of traffic sensors is less than the number of OD pairs, the mean OD demand cannot be uniquely identified. This property indicates that if the number of traffic sensors is insufficient, the sensor location scheme needs to be optimized to improve the estimation error. Such a property needs to be extended for the case of OD demand covariance estimation. To address this issue, the following property explains the relationship between the number of traffic sensors and the uniqueness of the estimated OD demand covariance matrix.

Property 3.1: If $\widetilde{\mathrm{P}}$ is a matrix with full column rank, i.e., $rank(\tilde{P}) =$ the number of columns of $\widetilde{\mathrm{P}}$, $\boldsymbol{\Sigma^{q}}$ must be uniquely identified according to Eq. (3.7).

Remark: It should be noted that the number of columns in $\widetilde{\mathrm{P}}$ is equal to the number of traffic sensors. If the number of traffic sensors is less than the number of OD pairs, $\widetilde{\mathrm{P}}$ must not be a matrix with full column rank. In other words, only under the condition that the number of sensors is less than the number of OD pairs, the solution for the estimation of OD demand covariance matrix is not unique and should be optimized. Property 3.1 is consistent with the relationship between the number of traffic sensors and the uniqueness of estimated mean OD demand.

In addition, the definition of WMPREC is different from that of WMPREM. The key difference is that WMPREC relates to a pair of traffic sensor locations ($a, b \in \widetilde{\mathbf{A}}$ in Eq. (3.27b)), while WMPREM only depends on a single traffic sensor location ($a \in \widetilde{\mathbf{A}}$ in Eq. (3.17b)). Even if the formulations are different, the mathematical properties are the same under some assumptions.

Before the investigation of the mathematical properties for WMPREC, the following definition of OD Covering Rule is introduced.

OD Covering Rule: the traffic sensors on the road network must be located in order to ensure that the traffic flows (or vehicular trips) between each OD pair can be observed.

The OD covering rule was proposed by Toi (1986). Its mathematical formulation with a clear explanation was presented by Yang et al. (1991). It is a common rule widely used for SLPs in the literature but is extended below in this chapter for consideration of the covariance between OD flows.

Property 3.2: The WMPREM ($G(\boldsymbol{\lambda}^{mean})$) and WMPREC ($H(\boldsymbol{\lambda}^{cov})$) are both finite under the following two conditions:

(i) the OD Covering Rule is satisfied (i.e., the traffic flows between any OD pair are observed by at least one traffic sensor location).

(ii) $\sigma_{w,w'} = r_{w,w'}\sigma_w\sigma_{w'}$ and $\sigma_w = c_w q_w$, where $r_{w,w'}$ is the coefficient of correlation between the travel demands of OD pairs *w* and *w'* and c_w is the coefficient of variation of OD pair *w*. In this condition, the covariance between the travel demands of any two OD pairs can be either **positive or negative**.

Property 3.3: The WMPREM ($G(\boldsymbol{\lambda}^{mean})$) and WMPREC ($H(\boldsymbol{\lambda}^{cov})$) are both finite under the following two conditions:

(i) the OD Covering Rule is satisfied (i.e., the traffic flows between any OD pair are observed by at least one traffic sensor location).

(ii) the covariance of travel demands between any two arbitrary OD pairs is **positive**. Specifically, it is assumed that all the entries in the OD demand covariance matrix are positive.

As discussed above, either the condition (ii) in Property 3.2 or the one in Property 3.3 is satisfied, the WMPREM and WMPREC are bounded. Both Properties 3.2 and 3.3 seek to ensure finite WMPREM and WMPREC so that traffic sensor locations can be optimized in the following models. The proofs of the above three properties can refer to the Appendix A.

3.4 Traffic sensor location optimization and stochastic OD demand estimation

This section firstly discusses the equivalent optimization model for optimizing the traffic sensor locations with consideration of both the WMPREM and WMPREC at the first stage. At the second stage, the extension of the formulation based on the Bayes method is presented to estimate both the mean and covariance matrix of OD demands from traffic sensors. Stochastic link choice proportions are also updated by an adapted traffic flow simulator.

3.4.1 Model formulation for traffic sensor location optimization

The purpose of this chapter is to enhance the reliability of the estimated OD demands by locating traffic sensors in the road network. As the WMPREM and WMPREC can be regarded as two measures of the estimation errors for the estimated mean and covariance OD demands, the smaller the WMPREM and WMPREC are, the higher the accuracy of the estimation is. Then, minimizing WMPREM and WMPREC can enhance the reliabilities of the estimated mean and covariance matrices of OD demands. Thus, a bi-objective model is proposed for improving the estimation reliability of the OD mean and covariance matrices. As discussed above, two objective functions can be used. The first objective function is expressed as

$$\min O_1 = \text{WMPREM}(\mathbf{z}) \tag{3.28a}$$

The second objective function is expressed as

$$\min O_2 = \text{WMPREC}(\mathbf{z}) \tag{3.28b}$$

Subject to

$$z_a = 0 \text{ or } 1 \quad \forall a \in \mathbf{A} \tag{3.28c}$$

It is well known for the traffic SLP that the more traffic sensors are used in the road network, the smaller the estimation errors are. Thus, an obvious solution for programming (3.28a) is $z_a = 1$ for all $a \in \mathbf{A}$. This solution may not be feasible in practice. In reality, there is usually a budget constraint for locating traffic sensors in the road network. Thus, the number of traffic sensors should be within a given threshold based on the budget constraint, which can be expressed as below:

$$\sum_{a \in \mathbf{A}} c_a z_a \leq B \tag{3.29}$$

where c_a is the cost for installing and maintaining one traffic sensor on link a, and B is the total budget.

However, the number of possible traffic sensors under consideration could be very large if a traffic network contains a large number of road links. For example, in a network with 100 links, there are totally $2^{100} - 1$ possible schemes. If the number of traffic sensors used for OD estimation is fixed, the number of schemes is still too large for any methodology to cope with in practice. One approach to solve this problem is to use some traffic sensor location constraints to remove the redundant schemes so as to reduce the size of possible schemes.

Yang and Zhou (1998) have proposed four traffic sensor location rules: **OD covering rule**, maximal flow fraction rule, maximal flow intercepting rule and **link independence rule**. OD covering rule is considered as a fundamental rule, so in this chapter. Note that it should always be satisfied and be treated as a constraint. The link

independence rule should also be satisfied because it could exclude the redundant links. So, in this chapter, the link independence rule is transformed into an equivalent constraint for solving the optimization problem concerned. The following two equations are the mathematical expressions of OD covering rule and link independence rule, respectively.

$$\sum_{a=1}^{m} \delta_{w,a} z_a \geq 1 \quad \forall w \in \mathbf{W} \tag{3.30}$$

$$rank(\tilde{\mathrm{P}}) = \tilde{m} \tag{3.31}$$

For every moderate road network, the above two constraints could only remove a small portion of "not too good" schemes, and there still be a large number of possible schemes for consideration. According to the maximal flow intercepting rule proposed by Yang and Zhou (1998), traffic sensors should be located on links so that the observed flows are as many as possible. In this chapter, because of the considered fluctuation and covariance of link flows, a variant maximal flow intercepting rule is proposed as a **maximal probability of flow intercepting rule**. That is, traffic sensors should be located on road links so that the probability of the observed link flows larger than a given value (e.g., mean link flow) is as much as possible. The proposed probability-based rule could be mathematically expressed as a constraint as follow:

$$\Pr(\mathbf{V} > v) > p^0 \quad \text{(the value of } p^0 \text{ varies with the number of traffic sensors)} \tag{3.32}$$

Finally, the mathematical model for optimization of traffic sensor locations can be formulated as the following constrained bi-objective problem:

$$\min \begin{cases} O_1 = \mathrm{WMPREM}(\mathbf{z}) \\ O_2 = \mathrm{WMPREC}(\mathbf{z}) \end{cases} \tag{3.33a}$$

Subject to

$$\text{(3.28c), and (3.29) – (3.32)} \tag{3.33b}$$

The optimization problem (3.33) is to find the traffic sensor locations that can minimize the estimation errors within a given budget constraint. To better understand the proposed model, a proposition should be noticed as follow:

Proposition 3.1: the value of WMPREM (or WMPREC) will be positive if the number of traffic sensors is less than the number of OD pairs; the value of WMPREM (or WMPREC) will be zero if the number of traffic sensors is no less than the number of OD pairs.

This could be proved directly from that when the number of traffic sensors is no less than the number of OD pairs, the number of equations is equal to the number of unknown variables according to the conservation law (Eq. (3.6)). Thus, **q** will be a matrix with a full column rank. The OD flows could then be calculated accurately.

3.4.2 Estimation of stochastic OD demands and update of stochastic link choice proportions

In this chapter, statistical methods such as the maximum likelihood method and Bayesian inference may be more suitable for this problem than some optimization methods, like the GLS method and EM method. The statistical methods may perform better because these methods can explicitly consider the variation of OD demands in the considered case. As such, after determining the traffic sensor locations at the first stage of the proposed model in this research, the second-stage problem is to estimate the mean and covariance of OD demands using the Bayes method and then update stochastic link choice proportions using traffic flow simulator based on the estimated stochastic OD demands.

Due to that the OD demands will change during the iteration, the stochastic link choice proportions and stochastic link flows are also updated during determining traffic

sensor locations, as shown in Figure 3.2. This information obtained from the adapted traffic flow simulator at the second stage should be consistent with the observed ones. Thus, the stochastic link flows and stochastic link choice proportions are updated iteratively until the difference between the estimated link flows from the adapted traffic flow simulator and observed link flows from traffic sensors is less than the predetermined tolerance.

The "estimated link flows" including their mean and covariance are obtained from the adapted traffic flow simulator based on the estimated stochastic OD demands at the second stage. In this chapter, the "true" OD demands are assumed so that the mean and covariance of "observed link flows" can be obtained by assigning the "true" mean and covariance of OD demands using the adapted traffic flow simulator. The "true" OD demands only serve as a reference for validation in the numerical examples.

Based on the stochastic link flows observed from traffic sensors which have been determined at the first stage, the Bayes method for estimating the stochastic OD demands is formulated as follows:

Suppose that observed link flows follow a multivariate normal distribution, $V|Q \sim MVN(PQ, \Sigma^{\mathrm{v}})$, where V is an $m \times 1$ vector of observed link flow, Q is an $n \times 1$ parameter vector of estimated OD demands, P is an $m \times n$ given matrix of link choice proportion, and Σ^{v} is an $m \times m$ observed covariance matrix of link flow. In addition, suppose the prior distribution of OD demand is also multivariate normal, $Q \sim MVN(Q^{prior}, \Sigma_{\mathrm{q}}^{\mathrm{prior}})$, where Q^{prior} is an $n \times 1$ parameter vector of prior OD demands, $\Sigma_{\mathrm{q}}^{\mathrm{prior}}$ is an $n \times n$ covariance matrix of prior OD demands. Please note that both Q^{prior} and $\Sigma_{\mathrm{q}}^{\mathrm{prior}}$ are known. From the Bayes method (Carlin et al., 2000), the marginal distribution of observed link flows V can be deduced as:

$$V \sim MVN(PQ^{prior}, \Sigma^{v} + P\Sigma_{q}^{prior}P^{T}) \tag{3.34}$$

The posterior distribution of OD demands Q can then be obtained by:

$$Q|V \sim MVN(Dd, D) \tag{3.35a}$$

Where

$$D^{-1} = P'(\Sigma^{v})^{-1}P + (\Sigma_{q}^{prior})^{-1} \tag{3.35b}$$

$$d = P'(\Sigma^{v})^{-1}V + (\Sigma_{q}^{prior})^{-1}Q^{prior} \tag{3.35c}$$

Therefore, the mean OD demands can be estimated.

$$\mathbf{q} = E(Q|V) = Dd \tag{3.36}$$

The posterior covariance matrix of OD demand can be expressed as follows:

$$\mathbf{\Sigma}^{q} = Cov(Q|V) = D \tag{3.37}$$

Based on the estimation of mean and covariance OD demands, stochastic link choice proportions together with the stochastic link flows are then updated by an adapted traffic flow simulator. The initial method can be referred to Lam and Xu (1999). In this chapter, based on the estimation of mean and covariance of OD demands from the Bayes method, it is assumed that OD demands follow a multivariate normal distribution. By sampling the OD demand from the overall population, stochastic user equilibrium (SUE) assignment is used to obtain mean and covariance of link flows and link choice proportions. Stochastic OD demands will be updated according to the proposed Bayes method. The procedure should be repeated until the difference between estimated link flows and observed link flows is less than the tolerance predetermined.

3.5 Solution algorithm

In this section, the improved FA will be used to solve the proposed bi-objective optimization problem.

3.5.1 Solution formulation

For each sensor location scheme, the optimization problem can be solved to estimate the mean OD demands $\mathbf{q}$ and the covariance matrix of OD demands $\boldsymbol{\Sigma}^{\boldsymbol{q}}$. Similar to Eqs. (3.6) and (3.7), Eqs. (3.17b) and (3.27b) can be rewritten in the following matrix form:

$$\widetilde{\mathrm{P}}\mathbf{q}^{d}\boldsymbol{\lambda}^{mean} = \mathbf{0} \tag{3.38}$$

$$\widetilde{\mathrm{P}}\Sigma^{\mathbf{q}}\boldsymbol{\lambda}^{\mathrm{cov}}\widetilde{\mathrm{P}}^{T} = \mathbf{0} \tag{3.39}$$

where $\mathbf{q}^{d}$ is a diagonal matrix whose diagonal elements are q_w.

Then the matrix form of the optimization problem (3.17) for finding WMPREM is shown as below:

$$\mathrm{WMPREM}(\mathbf{z}) = \max_{\boldsymbol{\lambda}^{mean}} G(\boldsymbol{\lambda}^{mean}) \tag{3.40a}$$

Subject to

$$\widetilde{\mathrm{P}}\mathbf{q}^{d}\boldsymbol{\lambda}^{mean} = \mathbf{0} \tag{3.40b}$$

$$\boldsymbol{\lambda}^{mean} \geq -\mathbf{1} \tag{3.40c}$$

To facilitate efficient solutions, the matrix equation constraint (3.39) can be transformed into a linear equation constraint as follow.

$$\mathrm{M}^{\lambda}\mathrm{vec}(\boldsymbol{\lambda}^{\mathbf{cov}}) = \mathbf{0} \tag{3.41}$$

Similar to matrix $\widetilde{\mathbf{M}}$, the method to obtain matrix $\mathrm{M}^{\boldsymbol{\lambda}}$ is shown in Appendix A. Subsequently, the optimization problem (3.27) should be rewritten as below:

$$\mathrm{WMPREC}(\mathbf{z}) = \max_{\boldsymbol{\lambda}^{\mathrm{cov}}} H(\mathrm{vec}(\boldsymbol{\lambda}^{\mathbf{cov}})) \tag{3.42a}$$

Subject to

$$\mathrm{M}^{\lambda}\mathrm{vec}(\boldsymbol{\lambda}^{\mathbf{cov}}) = \mathbf{0} \tag{3.42b}$$

$$\mathrm{vec}(\boldsymbol{\lambda}^{\mathbf{cov}}) \geq -\mathbf{1} \tag{3.42c}$$

Then, the bi-objective model could be formulated as below:

$$\min \begin{cases} O_1 = \text{WMPREM}(\mathbf{z}) \\ O_2 = \text{WMPREC}(\mathbf{z}) \end{cases} \tag{3.43a}$$

Subject to

$$\begin{bmatrix} \mathbf{q}^d & \\ & \mathrm{M}^{\lambda} \end{bmatrix} \begin{bmatrix} \boldsymbol{\lambda}^{mean} \\ \text{vec}(\boldsymbol{\lambda}^{\mathbf{cov}}) \end{bmatrix} = \mathbf{0} \tag{3.43b}$$

$$\begin{bmatrix} \boldsymbol{\lambda}^{mean} \\ \text{vec}(\boldsymbol{\lambda}^{\mathbf{cov}}) \end{bmatrix} \geq -\mathbf{1} \tag{3.43c}$$

To solve this constrained bi-objective optimization problem, two main approaches are used: the weighted-sum approach and the Pareto front approach.

The weighted-sum approach converts the bi-objective problem into a single objective problem as Eq. (3.44) by varying the weights of the two objectives. However, this weighted-sum approach requires good background knowledge of the problem so as to determine the weighting parameter α and then to obtain a reliable solution. The objective of the weighted-sum approach is defined as the weighted maximum possible relative error (WMPRE).

$$\text{WMPRE}(\mathbf{z}) = \min_{\mathbf{z}} \{(1-\alpha) \cdot \text{WMPREM}(\mathbf{z}) + \alpha \cdot \text{WMPREC}(\mathbf{z})\} \tag{3.44}$$

More generally, the Pareto front approach is adopted to acquire the Pareto front of this bi-objective problem without the need to determine the weighting parameter α. A set of non-dominated solutions called Pareto optimal solutions will be generated, which represents the relationship between the two objectives. Hence, no absolute unique solution could be obtained from the Pareto front approach.

To better understand the pattern of solutions from these two approaches, the results

obtained from the weighted-sum approach and Pareto front approach will be compared below. The proposed traffic sensor location optimization is a non-convex problem with binary decision variables that represent the sensor locations. This problem is NP-hard such that no global optimization algorithm can be used to solve it. For the two approaches concerned, the main difference between the two solution algorithms is the fitness function described in the following sub-section.

3.5.2 Firefly algorithm

FA is a novel and powerful nature-inspired algorithm inspired by the social behavior of fireflies (Yang, 2008). The original FA is to optimize continuous problems. Some scholars have further developed the algorithm to apply it for different areas such as mixed integer programming (Sayadi et al., 2010; Jati and Suyanto, 2011) and multi-output support vector regression (Xiong et al., 2014). This chapter has adapted the FA to solve the traffic SLP that is regarded as mixed integer programming with binary decision variables and constraints. The numerical example, as will be shown in the following section, demonstrates its efficiency with comparison to the classical GA, which is widely used in literature (see Yin, 2000).

3.5.2.1 Firefly representation

It is very convenient to represent a sensor scheme by a firefly in the platform of FA. $\mathbf{z}$ is a vector with values 0 and 1 only. The purpose of the proposed FA is to determine the value of $\mathbf{z}$. Thus one firefly represents one sensor scheme $\mathbf{z}$, and each binary variable indicates the existence of a traffic sensor on link a, i.e., 1 if a traffic sensor is located on link a and 0 otherwise.

3.5.2.2 Fitness function

Weighted-sum approach

Define $I(\mathbf{z}) = \mathrm{WMPRE}(\mathbf{z})$ as the light intensity of fireflies. $I(\mathbf{z})$ is selected as the

fitness function here. The smaller the $I(\mathbf{z})$ is, the more likely the scheme $\mathbf{z}$ will be selected.

Pareto front approach

As for the bi-objective problem, the solution is non-dominated (Pareto optimal) if there were no other feasible solutions that could improve one objective without worsening another objective. In one iteration, the non-dominated solutions but not a unique optimal solution will be determined. The population in the next iteration will be generated based on the non-dominated solutions.

3.5.2.3 Algorithm steps

Step 1 (Initialization)

After determining the number of sensors l by considering the budget constraint, generate initial population of fireflies $\mathbf{Z}^0$ randomly, the size of $\mathbf{Z}^0$ is k, and the number of variables in each firefly equals to the number of links in the road network. Set the maximum iterations (or the maximum generations) to T, and set the iteration number t to zero. (Bielli et al., 2002; Nayeem et al., 2014).

Step 2 (Conditions for the termination judgment)

If the number of iterations is larger than the threshold for maximum iteration (if $t > T$), terminate. Otherwise, go to the next step. Two different approaches are considered in this chapter. If the weighted-sum approach is used, go to Step 3a. Otherwise, go to Step 3b.

(Selection operation)

Step 3a: For each firefly $\mathbf{z}^{(i)}$ $(i = 1,2,I,k)$ of population pool $\mathbf{Z}^{(\mathrm{t}-1)}$, estimation of the mean and covariance matrix of OD demands by using the Bayesian method and then solving the bi-objective optimization problem (3.43). After calculating the value of its light intensity $I(\mathbf{z}^{(i)})$ according to the fitness function, rank the fireflies based on light intensity and find the current best. Then go to step 4a.

Step 3b: After estimation of the mean and covariance matrix of OD demands for each

individual of the population pool, calculate WMPREM and WMPREC according to the proposed criteria (formulation (3.40) and (3.42)). By comparing the values of WMPREM and WMPREC among all feasible solutions, the non-dominated solutions will be determined.

(Variation operation)

Step 4a: Vary attractiveness of fireflies $\mathbf{Z}^{(t)}$ according to the distance and light intensity, respectively, update $\mathbf{Z}^{(t)}$ that consists of k individuals based on the roulette wheel. Set $t = t + 1$, go back to step 2.

Step 4b: Based on the selected non-dominated solutions, update the population pool according to the distance and light intensity, respectively. Set $t = t + 1$, then go back to Step 2.

3.6 Numerical examples

In this section, two numerical examples are used to illustrate the applicability of the proposed model and solution algorithm for estimating the mean and covariance of OD demands. Example 1 is a small transportation network to examine: (a) effects of the sensor number and location on WMPREM and WMPREC, respectively; (b) comparison of the results between WMPREC and WMPREM; (c) effects of traffic congestion on the estimation results; and (d) sensitivity of weighting parameter α in the weighted-sum approach. Example 2 employed a medium-size transportation network to demonstrate the applicability of the proposed method and convergence of the solution.

3.6.1 A simplified road network

As shown in Figure 3.3, a small transportation network that consists of 7 nodes, 16 links, and 12 OD pairs is used. The mean and covariance of OD demand during morning peak hours for 300 days were estimated for this Example 1 network.

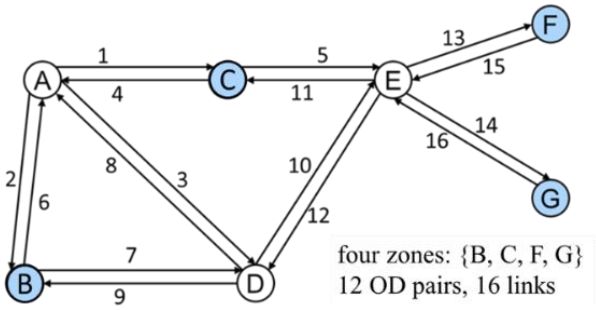

Figure 3.3 Example 1 network

In this example, the prior mean and var-cov (variance-covariance) matrix of OD demands are set the following $\mathbf{q}^{prior} = 0.5\mathbf{q}^*$, $\mathbf{\Sigma}^{\boldsymbol{q}prior} = 0.5^2\mathbf{\Sigma}^{\boldsymbol{q}*}$, which are given in Table 3.2 and Table 3.4, respectively. For example, the travel demand from origin C to destination F is numbered OD 2, in which the prior mean OD demands in OD 2 are assumed **240**; the demand from origin B to destination C is numbered OD 4, in which the prior mean OD demands are assumed **208**. The covariance between OD 2 and OD 4, the maximum covariance among all OD pairs, is **1996.1**.

Table 3.2 Network parameters

OD number	Origin-Destination	Paths	Prior mean OD demands
1	C–B	4-2; 4-3-9	168
2	**C–F**	4-3-10-13; 5-13	240
3	C–G	4-3-10-14; 5-14	96
4	**B–C**	6-1; 7-8-1; 7-10-11	208
5	B–F	6-1-5-13; 6-3-10-13; 7-10-13	223
6	B–G	6-1-5-14; 6-3-10-14; 7-10-14	240
7	F–C	15-11; 15-12-8-1	144
8	F–B	15-12-9; 15-12-8-2	168
9	F–G	15-14	184
10	G–C	16-11; 16-12-8-1	120
11	G–B	16-12-8-2; 16-12-9	136
12	G–F	16-13	208

Table 3.3 Prior link choice proportions by OD pair

OD No. / Link	1	2	3	4	5	6	7	8	9	10	11	12	Link Flow
1				0.9	0.2	0.3	0.4			0.4			485.6
2	0.8							0.4			0.5		350.0
3	0.2	0.2	0.2	0.1	0.4	0.3							358.1
4	1.0	0.2	0.2										284.0
5		0.8	0.8		0.2	0.3							477.0
6				0.9	0.6	0.6							565.9
7				0.1	0.4	0.4							274.1
8				0.1			0.4	0.4		0.4	0.5		343.9
9	0.2							0.6			0.5		240.0
10		0.2	0.2	0.1	0.8	0.75							560.1
11				0.1			0.6			0.6			235.4
12							0.4	1.0		0.4	1.0		511.8
13		1.0			1.0							1.0	840.0
14			1.0			1.0			1.0				650.0
15							1.0	1.0	1.0				620.0
16										1.0	1.0	1.0	580.0

With respect to the "true" covariance matrix of OD demands, the following re-sampling method is used (Lo et al., 1996). First, the "true" traffic flows for each OD pair during the morning peak hours during a sequence of days (e.g., 300 days) are generated from a normal distribution with mean q and variance $(0.2q)^2$. The OD demands are re-sampled with a sampling fraction of ten %. From the enlarged samples, the covariance of different OD demands, which is considered as the "true" covariance OD demands, could then be calculated for the numerical examples in this chapter. However, with the recent advancement of AVI technologies such as Bluetooth, Wi-Fi, RFID, and ALPR technologies, the sample prior OD mean and covariance matrices can now be estimated based on these AVI data. In addition, the databases of online trip chaining platforms, e.g., Uber and DiDi, are also useful for generating the prior mean and covariance of OD demands.

The parameters of the adapted traffic flow simulator model are set to be the same as those in Lam and Xu (1999). A Monte Carlo-based algorithm is used for the adapted traffic flow simulator in this chapter. It should be noted that to save the computation time for searching the feasible paths by OD pair in numerical examples, the path choice set for each OD pair is assumed to be known and fixed.

In addition, the prior mean link choice proportion matrix obtained from prior stochastic OD demands using the adapted traffic flow simulator is given in Table 3.2. Table 3.3 shows the other network parameters for Example 1 network.

Table 3.4 Prior covariance matrix of OD demands

OD No.	1	2	3	4	5	6	7	8	9	10	11	12
1	1129.0											
2	1240.2	2304.0										
3	366.6	450.1	368.6									
4	820.6	**1996.1**	354.9	1730.6								
5	831.5	996.1	333.1	648.2	1989.0							
6	1526.3	1877.5	596.7	1461.7	1384.5	2304.0						
7	824.5	954.7	354.9	678.6	709.0	1089.7	829.4					
8	973.4	1151.3	429.8	841.6	960.2	1565.1	758.9	1129.0				
9	1049.1	1287.0	407.9	884.5	1282.3	1745.6	943.0	1077.9	1354.2			
10	490.6	514.0	123.2	325.3	471.1	756.6	274.6	447.7	544.4	576.0		
11	782.3	765.2	322.1	706.7	599.0	1205.9	570.2	769.1	780.8	279.2	739.8	
12	825.2	1047.5	295.6	819.0	726.2	1522.6	618.5	861.9	959.4	397.8	556.9	1730.6

3.6.1.1 Effects of OD demand covariance on the optimal traffic sensor locations

In this subsection, the effects of OD demand covariance on the optimal traffic sensor locations are examined by considering different scenarios for using the WMPREC. Different values of weighting parameter α reflect different levels of importance considered for estimating the mean OD demand and its covariance. Therefore, three scenarios are proposed by setting three values of the α in the weighted-sum approach (e.g., Eq. (3.44)). The three scenarios are listed below:

- $\alpha = 1$ represents the scenario that only WMPREC is considered;
- $\alpha = 0$ represents the scenario that only WMPREM is considered;
- $\alpha = 0.5$ represents the scenario that both WMPREC and WMPREM are considered.

In this example, the network, as shown in Figure 3.3, is adopted. The "real" relative errors of mean and covariance of OD demands are used to compare the estimated mean and covariance of OD demands with the assumed "true" OD demands. The "real" relative errors of mean and covariance OD demand are calculated by Eqs. (3.13) and (3.24), respectively, with the assumption that the "true" mean and covariance OD demands are known (Zhou and List, 2010).

As shown in Table 3.5 – Table 3.7, links traversed by OD pairs with larger covariance values should be covered by traffic sensors if WMPREC is considered in the objective function. For instance, as depicted in Table 3.4, the covariance between OD 2 (C – F) and OD 4 (B – C) is the greatest. If WMPREC is considered in the objective function, more traffic sensors should be located on the set of links $\{6,1,5,13\}$. It could be seen from Table 3.5 – Table 3.7 that when the number of traffic sensors is 7, one link (link 13) in the set $\{6,1,5,13\}$ is covered by a traffic sensor if only WMPREM is considered ($\alpha = 0$); three links (link 1, 5, and 13) in this set are covered by traffic sensors if both

WMPREM and WMPREC are considered ($\alpha = 0.5$); and four links in this set are covered by traffic sensors if only WMPREC is considered ($\alpha = 1$) respectively.

In addition, if only WMPREM is considered ($\alpha = 0$), WMPRE is **1.71** when the number of traffic sensors is 8. However, if estimation accuracy of both mean and covariance are considered, to achieve comparable estimation accuracy of WMPRE (**1.79**), only 7 traffic sensors are needed on the network. Furthermore, even only 5 traffic sensors are needed when $\alpha = 1$. Therefore, it concludes that the number of traffic sensors required can be reduced when the estimation accuracy of covariance is considered in the objective function, given that the change in overall estimation accuracy is marginal.

As shown in Table 3.7, when there are 7 traffic sensors, the "real" relative error of covariance of OD demands (**0.07**) is the least when $\alpha = 1$, as compared to that (e.g., **0.39** and **0.21**) using other weighting parameters. Hence, the estimation error of the covariance of OD demands can be reduced when WMPREC is adopted. In other words, WMPREC could be more applicable to the situation that both the mean and covariance of OD demands are needed to be estimated.

Table 3.5 Results of the optimal traffic sensor location scheme selected in accordance to WMPREM ($\alpha = 0$)

Number of traffic sensors	WMPRE	"Real" relative error of mean OD demands	"Real" relative error of covariance of OD demands	The optimal traffic sensor location scheme selected by WMPREM
5	3.84	0.31	0.55	3,10,13,15,16
7	2.59	0.27	**0.39**	***3,4,7,10,13,14,16***
8	**1.71**	0.20	0.31	1,4,7,10,12,13,14,15
11	0.17	0.11	0.19	2,3,4,7,8,9,10,11,12,13,15,16

Table 3.6 Results of the optimal traffic sensor location scheme selected in accordance to WMPRE ($\alpha = 0.5$)

Number of traffic sensors	**WMPRE**	"Real" relative error of mean OD demands	"Real" relative error of covariance of OD demands	The optimal traffic sensor location scheme selected by WMPRE
5	2.99	0.35	0.29	3,5,10,15,16
7	**1.79**	0.31	**0.21**	***1,2,4,5,7,13,16***
8	1.36	0.24	0.17	1,3,6,9,11,12,13,14
11	0.15	0.12	0.09	1,2,3,4,5,7,9,11,12,13,15

Table 3.7 Results of the optimal traffic sensor location scheme selected in accordance to WMPREC ($\alpha = 1$)

Number of traffic sensors	WMPRE	"Real" relative error of mean OD demands	"Real" relative error of covariance of OD demands	The optimal traffic sensor location scheme selected by WMPREC
5	**1.78**	0.40	0.11	3,5,10,15,16
7	0.84	0.39	**0.07**	***1,5,6,9,12,13,14***
8	0.77	0.25	0.06	2,5,6,9,11,13,14,16
11	0.05	0.15	0.02	1,5,6,9,10,11,12,13,14,15,16

3.6.1.2 Effects of the number and location of traffic sensors on estimation reliability

In this subsection, the weighted-sum approach is used to obtain a unique solution and to investigate the effects of the number and location of traffic sensors on estimation reliability. For this sensitivity test, the value of the weighting parameter α is set to be 0.5. $\alpha = 0.5$ implies that in optimizing the traffic sensor locations, the estimation reliability of the mean and covariance OD demands have equal importance.

As shown in Figure 3.4, it can be observed that when the number of traffic sensors increases, both the Pareto optimal solutions for WMPREM and WMPREC decrease because more traffic sensors deployed contribute to more information acquired. The

estimation accuracy for both the mean and covariance of OD demands is enhanced.

It is, however, noted in Figure 3.4 that the reduction range of WMPREM is more remarkable than that of WMPREC when the number of traffic sensors increases. In other words, WMPREM is more sensitive to the number of traffic sensors deployed compared to WMPREC. For instance, when five traffic sensors are deployed, WMPREM (**1.85**) is almost 50% greater than WMPREC (**1.16**). In contrast, when the number of traffic sensors increases to 11, WMPREM reduces to **0.08**, while WMPREC only reduces to **0.21**.

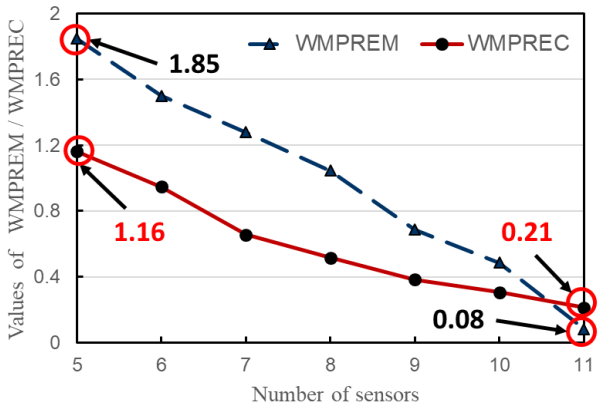

Figure 3.4 Effects of number of traffic sensors on WMPREM and WMPREC

Figure 3.5 illustrates the ranges of WMPREM and WMPREC for different traffic sensor locations, stratified into groups of 500 feasible schemes in the descending order of WMPRE for different numbers of traffic sensors (i.e., 7, 9, and 11, respectively).

As shown in Figure 3.5, the ranges of both WMPREM and WMPREC vary with both the number and location of traffic sensors. When the number of traffic sensors is 7, the values of WMPREM are, in general, much greater than that of WMPREC. In addition, the ranges of both WMPREM and WMPREC are large. When the number of traffic sensors increases, values of WMPREC and WMPREM both reduce in general. Notably,

the reductions of WMPREM value are more remarkable than that of WMPREC. When the number of traffic sensors is 11, the values of WMPREM are even less than that of WMPREC in general.

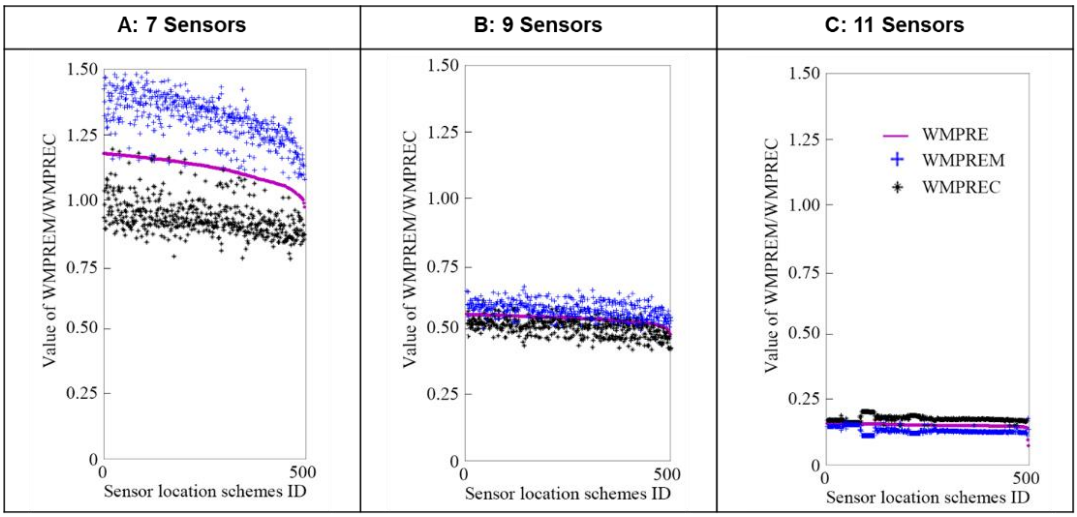

Figure 3.5 Effects of location of traffic sensors on WMPREM and WMPREC

In addition, the newly proposed criteria (WMPREM and WMPREC) in this chapter are intended to weigh the conventional criteria by considering different magnitudes of travel demands by OD pair during the morning peak hours. The proposed model is validated by comparing with the previous non-weighted method, MPREM in Yang et al. (1991), as well as the MPREC in this chapter.

As shown in Table 3.8, when the number of traffic sensors in the Example 1 network is greater than or equal to 12 (number of OD pairs), the estimates of both the mean and covariance of OD demands can be absolutely accurate (with zero MPREM and MPREC). Table 3.8 also indicates that the proposed weighted maximum possible relative errors are much smaller than that based on the non-weighted criterion with the same number of traffic sensors. For instance, the relative increase for WMPREM is **-91%** when the number of traffic sensors is 11; the relative increase for WMPREC is **-82%** with five traffic sensors. Thus, it could conclude that considering different

magnitudes of travel demands by OD pair effectively reduces the estimation errors for both mean and covariance of OD demands, compared to the original method (MPRE).

Table 3.8 Comparison between the methods with and without weight on MPREM or MPREC

Number of traffic sensors	MPREM	WMPREM	Relative increase [a]	MPREC	WMPREC	Relative increase
5	3.38	1.85	-45%	6.50	1.16	**-82%**
7	2.68	1.28	-52%	3.44	0.66	-81%
8	2.02	1.04	-48%	1.92	0.52	-73%
11	0.88	0.08	**-91%**	0.56	0.21	-62%
12,13,14,15,16	0	0	**--**	0	0	--

[a] Relative increase = (WMPRE-MPRE)/MPRE

3.6.1.3 Effects of traffic congestion on the proposed model

Intuitively, when the number of private cars grows faster than road capacity, the traffic network is more likely to be congested. Under such circumstances, different OD demands are more likely to be correlated.

To illustrate the importance of considering WMPREC, two scenarios: (i) uncongested condition (Scenario A) and (ii) congested condition (Scenario B) are set out below. Under uncongested conditions, the mean and covariance of OD demands are set to be half of that, as given in Table 3.2 and Table 3.4. In contrast, under congested conditions, the mean and covariance of true OD demands are doubled. The weighted-sum approach is adopted again in this sub-section to have a unique Pareto optimal solution and then to compare different results conveniently. The weighting parameter α is set to be 0, which implies that only WMPREM is considered in the objective function.

It is noticed from Table 3.9 that the estimation error of covariance of OD demand could be enormous if only the WMPREM is used to determine the traffic sensor locations

for both uncongested and congested conditions. For instance, under congested conditions, when there are five traffic sensors in the Example 1 network, the value of WMPREM is 2.40, and the value of WMPREC is 6.62, much larger than that of WMPREM. This phenomenon is also observed when seven traffic sensors are deployed. Hence, even though the mean OD demands could be accurately estimated, it is difficult to estimate the covariance of OD demands accurately when only the WMPREM is chosen as the criterion. Such a phenomenon is much more apparent under congested conditions. Table 3.9 shows that when there are only five traffic sensors under congested conditions, the resultant WMPREC is 15.13, which is more than double the result (6.62) under uncongested conditions.

Table 3.9 Results of the model under different traffic conditions

Number of sensors	Uncongested condition (**half** actual OD demands)			Congested condition (**double** actual OD demands)		
	WMPRE	WMPREM	WMPREC	WMPRE	WMPREM	WMPREC
5	2.40	**2.40**	**6.62**	2.28	2.28	**15.13**
7	1.67	1.67	2.52	1.62	1.62	3.18
8	1.38	1.38	1.66	1.32	1.32	2.52
11	0.48	0.48	0.60	0.54	0.54	0.96

Intuitively, the larger the value of WMPREC implies that the covariances between OD flows could not be adequately captured by the resultant sensor scheme. As for the illustrative example given in Section 3.2, it will be difficult to assess the effects of carpooling, ridesharing, and other trip chaining strategies in the traffic network based on OD estimation from traffic sensors. Therefore, WMPREC is essential for stochastic OD demand estimation, particularly under congested conditions.

To testify the performance of the newly proposed index, WMPREC, especially under the congested condition, a sensitivity test has been carried out for both WMPREM and WMPREC in the following subsection. In this comparison, the weighting parameter

α is set to be **0.5**. Scenario **A** and **B** stand for the uncongested and congested conditions, respectively. Table 3.10 shows the resultant relative increases in WMPREM and WMPREC, between congested and uncongested conditions (i.e., Relative increase = ($WMPRE_B$ – $WMPRE_A$)/ $WMPRE_A$), for different numbers of traffic sensors.

Table 3.10 Relative increase for WMPREM and WMPREC under congested conditions compared to that under uncongested conditions

Number of sensors	WMPREM			WMPREC		
	Scenario A	Scenario B	Relative increase of mean	Scenario A	Scenario B	Relative increase of covariance
5	3.64	4.13	13.5%	4.01	6.88	71.5%
7	2.56	3.26	27.4%	2.72	2.97	9.1%
8	2.04	2.26	11.0%	1.99	1.77	-10.9%
11	0.95	0.97	1.9%	0.87	0.88	1.0%

A negative relative increase implies that estimation under congested conditions is more accurate than that under uncongested conditions. It can be found from Table 3.10 that estimation of mean OD demand is less accurate under congested conditions (using the Example 1 network), as compared to that under uncongested conditions. However, it is possible for the estimation of covariance OD demands to be more accurate when the traffic network becomes congested, as implied by the negative relative increase of WMPREC. For example, when there are eight sensors, the accuracy of OD covariance estimation under congested conditions improves by **10.9%**. It could be concluded that WMPREC should be considered, especially when the traffic network is congested. Under congested conditions, the observed data might provide more information about the covariance of OD demands as more travelers may use the carpooling and trip chaining strategies. Therefore, the estimation error could be minimized with the proposed model.

3.6.1.4 Sensitivity of weighting parameter α in the weighted-sum approach

The proportion of joint travel activities (e.g., carpooling, ridesharing, and other trip chaining strategies) could affect the weighting parameter α, intuitively. In addition, as depicted in the illustrative example in Section 3.2, the covariance between OD demands increased with the proportion of joint travel activities during the typical period (e.g., peak hour) concerned. Therefore, the weighting parameter α can be estimated given the covariance. Figure 3.6 illustrates the relationship between covariance and optimal values of weighting parameter α that minimizes WMPRE with 8 sensors using the OD pair 2 and OD pair 4 as an example (with the maximum covariance among all OD pairs).

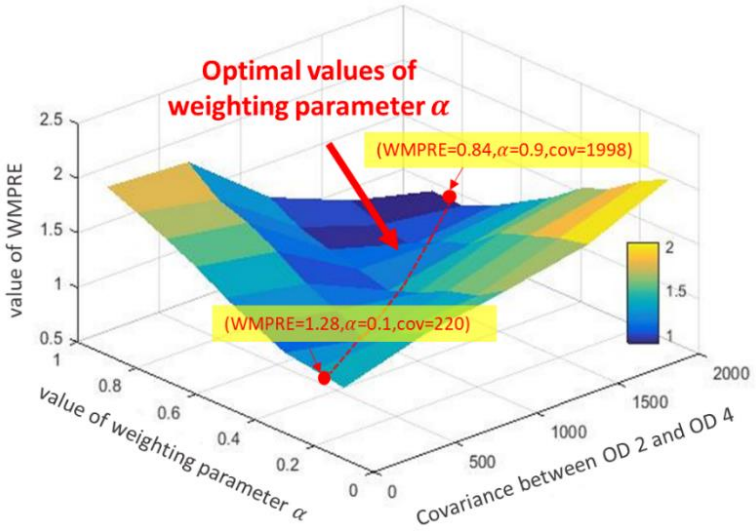

Figure 3.6 Effects of covariance between OD pair 2 and OD pair 4 on the value of weighting parameter α

(The red line in the graph depicts the relationship between optimal weight parameter α and covariance when WMPRE is minimized)

Figure 3.6 reveals that when the covariance between OD pair 2 and OD pair 4 is small, the optimal value of weighting parameter α is also small, and vice versa. For instance, when the covariance between OD pair 2 and OD pair 4 is **220**, WMPRE is minimum

at **1.28**, and the corresponding weighting parameter is **0.1**. When the covariance between OD pair 2 and OD pair 4 is **1998**, WMPRE is minimum at **0.84**, and the corresponding weighting parameter α is **0.9**. This finding can be intuitively interpreted as that when covariance increases, the covariance of OD demands should be more important than the mean OD demands when evaluating the estimation accuracy, and therefore weighting parameter α also increases. Thus, a larger weighting parameter α should be chosen to improve the estimation accuracy of the OD covariance under this circumstance.

From the perspective of formulation, the weighting parameter α just quantifies the trade-offs between mean and covariance. If the road is more congested, more emphasis should be placed on the covariance. Therefore the weighting parameter α should be larger. As depicted in subsection 3.6.1.1, different values of weighting parameter α reflect different levels of importance for estimating the mean and covariance of OD demands. For instance, $\alpha = 1$ implies that only the estimation accuracy of OD demand covariance is taken into consideration for optimization of the traffic sensor locations. The larger the value of α, the more accurate the estimated covariance of traffic flows, and vice versa. The choice of the value of α depends on the degree of covariance between OD flows. If one focuses on estimating the covariance matrix of OD demands, a larger value of α should be used and vice versa.

In view of the above discussion, assessing the Pareto efficiency (Tan et al., 2014) becomes another exciting research question. Another method with the use of the Pareto front approach is also adopted to investigate further this traffic SLP with consideration of the effects of both the mean and covariance OD demands. The FA has also been improved accordingly, as shown in Section 5 of this chapter. Using the Example 1 network, the results from the weighted-sum and the Pareto front approaches are compared to examine their relationship, as depicted in Figure 3.7.

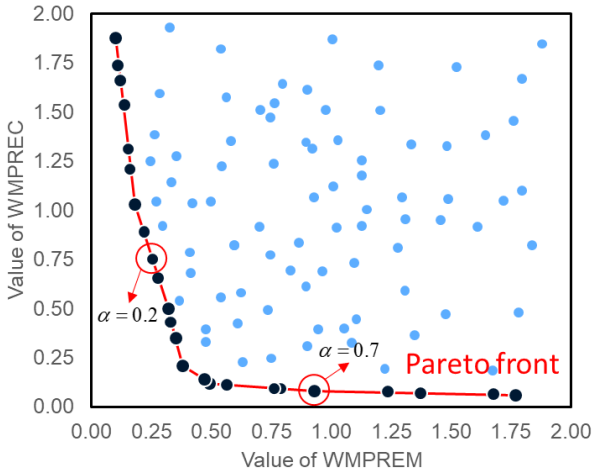

Figure 3.7 Pareto optimal solutions obtained from the Pareto front approach

In Figure 3.7, if the value of WMPREM (or WMPREC) is equal to 1, it means that the relative error of the mean OD demand estimation (or covariance OD demand estimation) is 100%.

As shown in Figure 3.7, for instance, the Pareto optimal solution when the weighting parameter α is set to be **0.2** falls on the Pareto Front. Another example when α is set to be **0.7** could also demonstrate this finding. It concludes that the solutions obtained from the weighted-sum approach are the sub-set of that from the Pareto front approach. A unique optimal solution could be acquired from the weighted-sum approach, given the specified value of weighting parameter α. However, from the Pareto front approach, much more than one Pareto optimal solution would be acquired. As such, it is more challenging to make the final decision on the sensor location scheme by using the Pareto front approach. Thus, given the weighting parameter, the weighted-sum approach is more effective for finding the optimal sensor location scheme in practice.

3.6.2 A medium-size road network

In this subsection, the well-known medium-size Sioux Falls network, as shown in Figure 3.8(a), is used to examine the performance of the proposed model and solution algorithm. This Example 2 network consists of 24 nodes, 76 links, and 30 OD pairs. Based on the budget constraint, the maximum number of sensors is 12. The effects of OD covariance on the overall estimation accuracy are shown in Table 3.11.

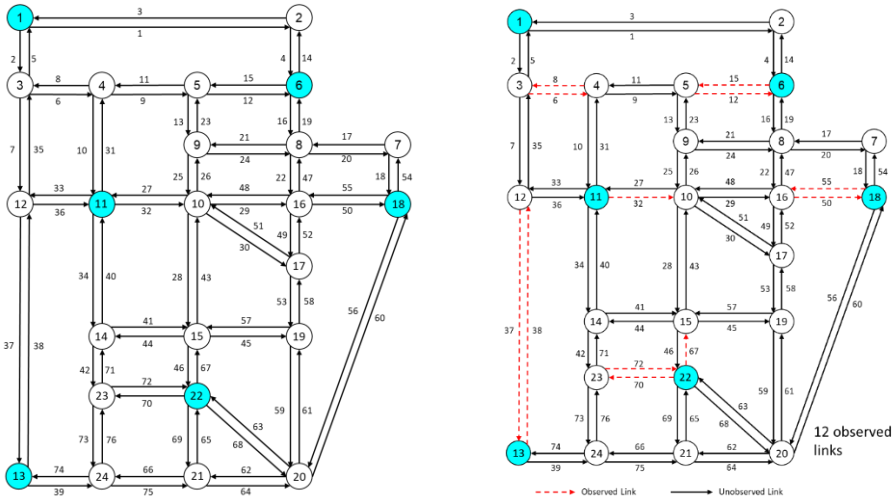

(a) Origin Sioux Falls network (b) Optimal location scheme of Sioux Falls network

Figure 3.8 The Sioux Falls network – Example 2 network

Table 3.11 Effects of OD covariance on objective function in the Sioux Falls network

Consider OD covariance in the objective or not	WMPRE	Relative increase [a]	WMPREM	WMPREC
No ($\alpha = 0$)	**12.32**	--	12.32	7.72
Yes ($\alpha = 0.5$)	8.26	**-33.0%**	13.01	3.51
Yes ($\alpha = 1$)	2.17	**-82.4%**	13.98	2.17

[a] Relative increase=(WMPRE(α=0.5 or α=1)− WMPRE(α=0))/WMPRE(α=0)

Table 3.11 shows that WMPREC is the largest (i.e., **12.32**) when the OD covariance is not taken into consideration ($\alpha = 0$). Compared with the relative increase in error in this case ($\alpha = 0$), when the OD covariance is taken into consideration ($\alpha = 1$ and $\alpha = 0.5$), the relative increase in error decreases to **-82.4%** and **33.0%**, respectively.

This is an additional demonstration that considering covariance in the objective function reduces error in the estimation of covariance between OD demands. It also shows that this novel model is particularly effective under the following circumstances: (i) there are relatively few traffic sensors; (ii) the covariance between different OD pairs is very large; and (iii) the prior OD demand is not particularly close to the actual OD demand.

When using a desktop computer with the system of Intel Core i7-2600 CPU, 3.40GHz, and 8 GB RAM, the convergence time required for solving the traffic SLP is 807 seconds by the weighted-sum approach given that the weighting parameter α is 0.5. The Pareto optimal traffic sensor location scheme is shown in Figure 3.8(b). To demonstrate the efficiency of the proposed improved FA, the convergence with 12 traffic sensors is shown in Figure 3.9(a) compared to that of the classical GA as shown in Figure 3.9(b). Figure 3.9 depicts that even though both of these two algorithms can obtain the same optimal target value, it converges at the 3rd iteration by the improved FA, while at the 48th iteration by the GA. In addition, the convergence time of the improved FA (807s) is much less than that of the conventional GA (18193s). The above descriptions have demonstrated the efficiency of the improved FA.

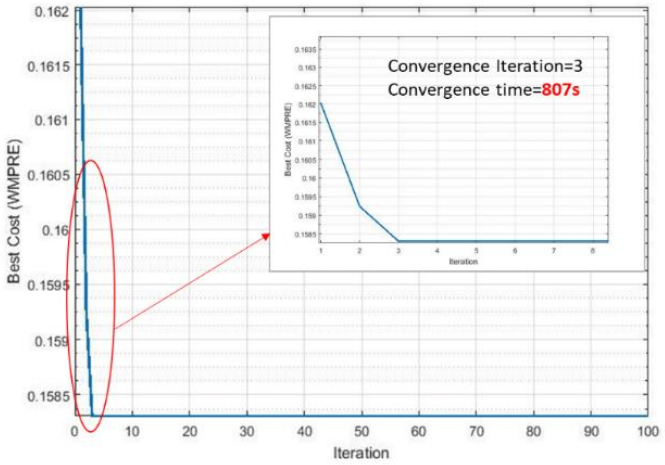

a. Firefly algorithm

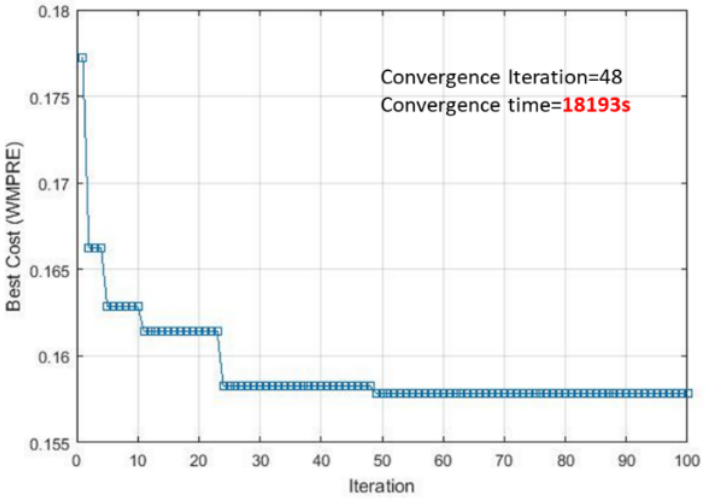

b. Genetic algorithm

Figure 3.9 Convergence of the solution algorithm

3.7 Summary

The covariance effects are increasingly crucial as vehicular traffic flows between different OD pairs in a typical period (such as morning peak hour) from day to day could be statistically correlated with each other in reality. The covariance is mainly generated from the daily variation of travel patterns, network topology, and trip chaining activities of household members. The trip chaining activities are evidenced by the vehicle occupancy of a private car that is larger than one (e.g., 1.4 persons/vehicle on average reported by ATC 2020).

As the covariance between different traffic demands by OD pairs is not considered in the conventional approach, the bias of OD demand estimation from traffic sensors will increase. When traffic sensor locations are determined without considering the covariance effect, the OD demand estimation accuracy will be reduced dramatically, and hence the traffic sensors may be located inefficiently.

In this chapter, the traffic SLP has been investigated for OD demand estimation by explicitly considering the covariance of traffic demand between different OD pairs during the morning peak hour period. A new criterion, WMPREC, is proposed and can measure the estimation accuracy of OD demand covariance without the need for its ground truth. Similarly, a WMPREM is used to qualify the mean OD demand estimates.

Based on the proposed criteria measuring the quality of mean and covariance of OD demand estimates, a novel traffic sensor location model has been developed in this chapter. The peak-hour OD demands, including both mean and covariance between different OD pairs, can be estimated more accurately with the optimum traffic sensor locations. Two numerical examples have been conducted to demonstrate the efficiency of the proposed model by comparison with previous models. Numerical results in Section 3.6 indicate that the proposed traffic sensor location model outperforms the traditional models, especially on the estimation accuracy of OD demand covariance.

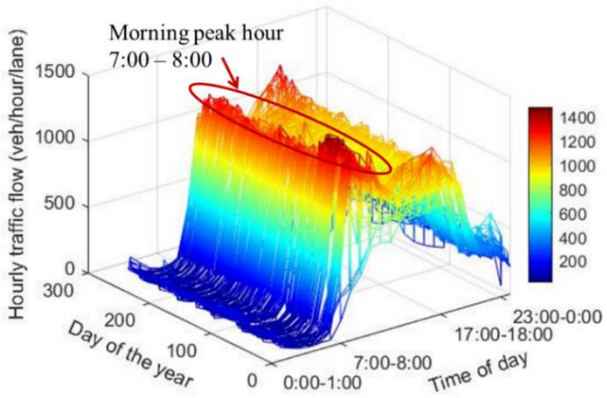

Figure 3.10 Traffic flow variation by time of day and day of the year

It should be noted that the covariance effects of OD demand modeled in this chapter indeed refer to the spatial covariance of traffic demand between different OD pairs during the same time period. However, due to the variation of travel patterns by time of day and day of the year, as depicted in Figure 3.10, the vehicular traffic demands

could correlate with one another during different time periods. In other words, the temporal covariance of OD demand between different time periods can also affect the OD demand estimation and traffic sensor locations. In the following Chapter 4, the traffic sensor (i.e., traffic count) location model will be extended to the allocation of multi-type traffic sensors with considering spatial and temporal covariance of vehicular traffic demands between different OD pairs during different hourly periods of the day.

4. Optimization of multi-type traffic sensor locations for estimation of multi-period origin-destination demands with covariance effects

In Chapter 3, traffic sensor (i.e., traffic count) locations are optimized for estimation of stochastic OD demands with taking into account the spatial covariance of vehicular traffic demand between different OD pairs within the morning peak hour period on a daily scale. However, the travel patterns of OD demand could vary significantly during different hourly periods of the day. For instance, in the morning peak hour, travelers use their cars to commute from residential areas to city centers for work. These commuters would travel back home by car from their workplaces in the evening peak hour. As such, the vehicular traffic demands by OD pairs are indeed correlated in morning and afternoon peak hours.

In this Chapter 4, the traffic sensor location model proposed in Chapter 3 is extended to the allocation of multi-type traffic sensors for multi-period OD demand estimation. The extended model considers the spatial and temporal covariances of OD demand for different OD pairs during different hourly periods of the day.

This chapter is organized as below. A brief introduction, motivation, and contributions are given in Section 4.1. In Section 4.2, the model assumptions and problem statement are clarified. In Section 4.3, the relationship between observations and multi-period OD demand estimates is presented to give the basis of the proposed models in the following sections. The multi-period OD demand estimation model and multi-type sensor locations models are developed in Sections 4.4 and 4.5, respectively. In addition, numerical examples are conducted in Section 4.6 to demonstrate the merits of considering the multi-period covariance of OD demand on SLPs. The summary of this

chapter is given in Section 4.7.

4.1 Background

4.1.1 Motivating example

As mentioned above, covariance effects of hourly OD demand in multiple periods can result from factors such as the hourly and daily variation of travel patterns, network topology, and joint travel behavior. For an intuitive explanation, the illustrative example related to joint travel behavior is presented to demonstrate the existence of OD demand covariance in multiple periods.

Joint travel behavior refers to how people consider other household memb'rs' travel behaviors/choices or persons in their social networks when making their own travel choices (Bhat et al., 2013). Household members often need to decide how to share the jointly owned vehicle(s) to conduct their daily activities. In this chapter, joint travel behaviors include more than one trip with at least two household members (Cascetta, 2009). In other words, if a joint travel behavior is conducted, there should be at least two different OD pairs.

An example is presented in this subsection to intuitively illustrate the relationship between joint travel behavior and OD demand, and to manifest the significance of spatial, temporal, and multi-period covariance. As shown in Figure 4.1, the example network consists of six OD pairs {(B,C), (C,F), (B,F), (C,B), (F,C), (F,B)} with Node C, Node B, and Node F respectively representing the school, home, and office. The weekday morning peak hour and evening peak hour are represented by h_1 and h_2, respectively. For convenience, six OD pairs in the illustrative network are numbered from 1 to 6 with OD(1) = (B,C), OD(2) = (C,F), OD(3) = (B,F), OD(4) = (C,B), OD(5) = (F,C) and OD(6) = (F,B). $q_{w(h_x)}$ $(w = 1, \dots, 6 \text{ and } x = 1,2)$ represents traffic

demand of OD pair *w* in time period h_x. $\sigma_{1(h_1),2(h_1)}$ stands for the OD demand covariance between OD pairs 1 and 2 in time period h_1. Similarly, $\sigma_{2(h_1),6(h_2)}$ stands for the OD demand covariance between OD pair 2 in time period h_1 and OD pair 6 in time period h_2.

Consider a joint travel behavior conducted by a spouse and a child as an example. Specifically, in the weekday morning peak hour (h_1), a spouse will drive the child to school first (i.e., OD pair (B, C)) and then drive to the office alone to work (i.e., OD pair (C, F)). As such, two OD demands (i.e., one is from Node B to Node C, and another is from Node C to Node F) will be generated by such joint travel behavior in the weekday morning peak hour (h_1). In the weekday evening peak hour (h_2), the spouse has two options: (i) going back home directly (i.e., OD pair (F, B)) while his/her child could take public transit or school bus to go back home, or (ii) going to school to pick up his/her child (i.e., OD pair (F, C)), then back home together (i.e., OD pair (C, B)). Option (i) generates only one OD demand traveling from Node F to Node B directly, while option (ii), a joint travel behavior, splits the original demand into two OD demands (i.e., one is from Node F to Node C, and another is from Node C to Node B) and is similar to that in the morning peak hour.

Under such circumstances, there exists a spatial covariance relationship between OD pairs (B,C) and (C,F) in the morning peak hour (i.e., $\sigma_{1(h_1),2(h_1)}$) due to the joint travel behavior by the spouse and the child. On the one hand, in the evening peak hour, if the spouse chooses option (i), the covariance relationship between OD pair (C,F) in the morning peak hour and OD pair (F,B) in the evening peak hour denoted as $\sigma_{2(h_1),6(h_2)}$ will be outstanding. On the other hand, if the spouse chooses option (ii), the covariances among OD pair (C,F) in the morning peak hour, OD pair (F,C), and OD pair (C,B) in the evening peak hour will be significant.

Note that the joint travel behavior can be reflected by the vehicle occupancy data reported from "The Annual Traffic Census 2017" of Hong Kong (Transport Department, 2018). Vehicle occupancy is the number of persons in a vehicle, including both driver and passengers. It has been pointed out in the literature that joint travel behaviors (including both carpooling and ridesharing for travel with or without the same OD pair) would lead to a larger vehicle occupancy (Giuliano et al., 1990; Goel et al., 2016; Yin et al., 2017). For instance, Goel et al. (2016) mentioned that the vehicle occupancy could be approximately calculated by (1 + number of passengers / number of drivers). In other words, without joint travel behaviors, the vehicle occupancy for the private car is 1. However, with joint travel behaviors, the vehicle occupancy should be larger than 1. Under the assumption that a joint travel behavior only includes two persons, when the vehicle occupancy is 1.3 person/vehicle, the proportion of joint travel behavior of total demand should then be about 30%.

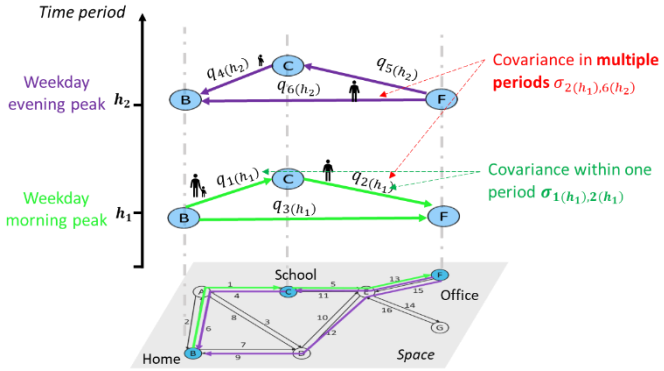

Figure 4.1 Different activities and travel patterns in different periods

In this chapter, the research models the effects of multi-period OD demand covariance on the installation of multi-type sensors, including both point and AVI sensors. Point sensors are assumed to be able to count the number of vehicles passing through the link. AVI sensors can only identify the tagged vehicles and match them with the records from other locations. The similarity between point and AVI sensors is that both types of sensors can count vehicles at a certain point installed with a sensor. However, they differ in that point sensors can count all the vehicles, while AVI sensors can detect

(or count) only the portion of vehicles equipped with AVI tags. Another difference is that AVI sensors are also able to cover a spatial area, namely count partial path flows by matching the tagged vehicles at different locations.

In summary, AVI and point sensors provide complementary information. While the point sensors can detect complete link flow observation for all vehicles at the installed locations (i.e., point coverage), AVI sensors can detect (i) partial link flow (i.e., point coverage) and (ii) partial path flow for the tagged vehicles (i.e., spatial coverage).

4.1.2 Contributions

With explicit consideration of covariance relationships of various traffic sensor data in multiple periods, this chapter proposes a novel model to locate multi-type traffic sensors (point sensors and AVI sensors) for estimation of multi-period OD demands. Generally, the major contributions of this chapter can be summarized as follows.

(C1) The **covariances** of multi-period OD flows are explicitly incorporated into the SLP in response to the effects of joint travel behaviors, inter-relationships of the travel patterns in different periods, and significant changes in the network topology or land use. For example, as displayed in Figure 4.1, the covariance between OD demands during different time periods exists due to the joint travel behavior by the spouse and the child. This joint travel behavior can be evidenced by the average vehicle occupancy larger than 1.4 persons per private car from 7:00 am to 11:00 pm (Transport Department, 2018).

(C2) **Multi-period OD demands**, particularly under congested conditions, should be estimated based on various but co-related traffic sensor data over time because of the time-to-time variation of hourly OD demands. Furthermore, the consequence of traffic congestions for hourly OD demand may carry over into the next hourly period. With

taking into account the spatial-temporal covariance of OD demands in multiple time periods, the research in this chapter proposes a new model to optimize the multi-type traffic sensor locations for multi-period OD demand estimation.

(C3) In this chapter, both the number and locations of **multi-type traffic sensors**, including point sensors and AVI sensors, can be optimized simultaneously. The coordination of different traffic data provided by various sensor types can help to elucidate the inter-relationship of travel patterns over time. The trade-off between these two different sensor types is analyzed to provide more insights into the determination of sensor type priority as analytically demonstrated in Proposition 4.2 in the model formulation section.

(C4) A more generalized criterion to allocate multi-type traffic sensors for OD demand estimation in multiple periods has been proposed in this chapter. By using the proposed model, as proved in Proposition 4.1, fewer sensors will be needed to achieve a similar quality of OD demand estimates for different time periods, as compared to the results of the previous models.

4.2 Model assumptions and problem statement

To focus on the main ideas of this chapter, the following assumptions are adopted:
(A1) The partial information of prior OD demands and their covariances by hourly period can be obtained and regarded as historical data (Parry and Hazelton, 2012).

(A2) Point sensors and AVI sensors are installed on the selected links in a road network.

(A3) The vehicles equipped with AVI tags are a representative subset of the total vehicles traveling in the road network (Zhou and List, 2010).
Basically, it is assumed that the linear function of observed traffic flow of tagged

vehicles is unbiased and can be used to estimate total vehicular flow on this particular link. Two underlying assumptions are included: (i) the AVI sensors can correctly identify each tagged vehicle without matching errors. (ii) the average penetration rate of tagged vehicles over the road network is considered. Note that the penetration rate can vary by location of AVI sensors due to the uncertainties in travel behaviors and traffic demand. However, it is difficult to get the penetration rate for each location of AVI sensors. To clearly demonstrate the key contributions of this chapter, an average penetration rate is adopted for the entire network.

For instance, in Hong Kong, there were approximately 785,000 registered vehicles, including 167,300 commercial vehicles, at the end of 2018. Approximately 350,000 vehicles had been installed with Autotoll tags to enable automatic toll charge payments. Therefore, the overall penetration rate of all tagged vehicles is approximately 45% in Hong Kong.

(A4) The amount of traffic in operation during the studied period is of interest. This means it is possible that OD demands starting before and/or ending after the studied period are taken into account.

The traffic SLP for OD demand estimation contains two main inter-related stages as presented in Figure 4.2: (i) multi-type traffic sensor location generation and (ii) multi-period OD demand estimation (Mirchandani et al., 2009; Fei et al., 2013; Hu et al., 2015).

Given the prior OD demand information for a network (represented by nodes, links, and paths), PCA is adopted in this chapter to extract the principal OD demand components from the prior OD demand. More specifically, these principal OD demand components can be pre-determined before starting the two-stage model. After

performing the PCA, the prior OD demand matrix is divided into principal OD demand components and a matrix of eigenvectors. The former represents the essential features in the original OD demand matrix. The latter stands for a transformation direction between the original OD demand matrix and the principal OD demand component.

At the first stage, the inputs are the network topology and the prior principal OD demand components. Given the total budget, the focus of the first stage is to generate candidate point sensor and AVI sensor locations in the road network. Point sensors can provide counts of all vehicles passing the locations (or roads) installed with this type of sensor. AVI sensors, in addition to the partial link flow data of tagged vehicles, can provide partial path flows by matching records of identified vehicles at different locations.

At the second stage, based on the observations from the traffic sensors planned by the first-stage model, multi-period stochastic OD demands can be estimated. On the basis of these estimates, the uncertainties of the estimations calculated from the total trace of the OD demand matrix and weighted by their covariance values can be evaluated. The calculated uncertainties of OD demand estimates serve as a feedback mechanism so that the candidate sensor location scheme will then be adjusted accordingly. By comparing the uncertainties of OD demand estimates among all of the candidate traffic sensor location schemes using the FA (Fu et al., 2019), the optimal scheme contributing to the minimum uncertainty of multi-period OD demand estimates can be selected.

The problem studied at the second stage is to estimate the multi-period OD flows from measured link/path flows by using network and path choice models. Specifically, the second-stage problem for OD demand estimation is indeed a bi-level problem, as shown in Figure 4.2 (Bierlaire, 2002; Cascetta, 2009; Jones et al., 2018). The upper level, given that the link/path choice proportion matric is known, estimates OD

demand with observed link flows obtained from point sensors and partial path flows obtained from the AVI sensors. The lower level updates the link/path choice proportions by assigning the OD demand estimated in the upper level by using an adapted traffic flow simulator (which is developed based on SUE) (Lam and Xu, 1999). The link and path flow obtained from the adapted traffic flow simulator at the second Stage should be consistent with the observed ones from traffic sensors. Thus, the bi-level OD estimation model iterates until the difference between the estimated link/path flow from the adapted traffic flow simulator and observed link/path flows from traffic sensors is less than the predetermined tolerance.

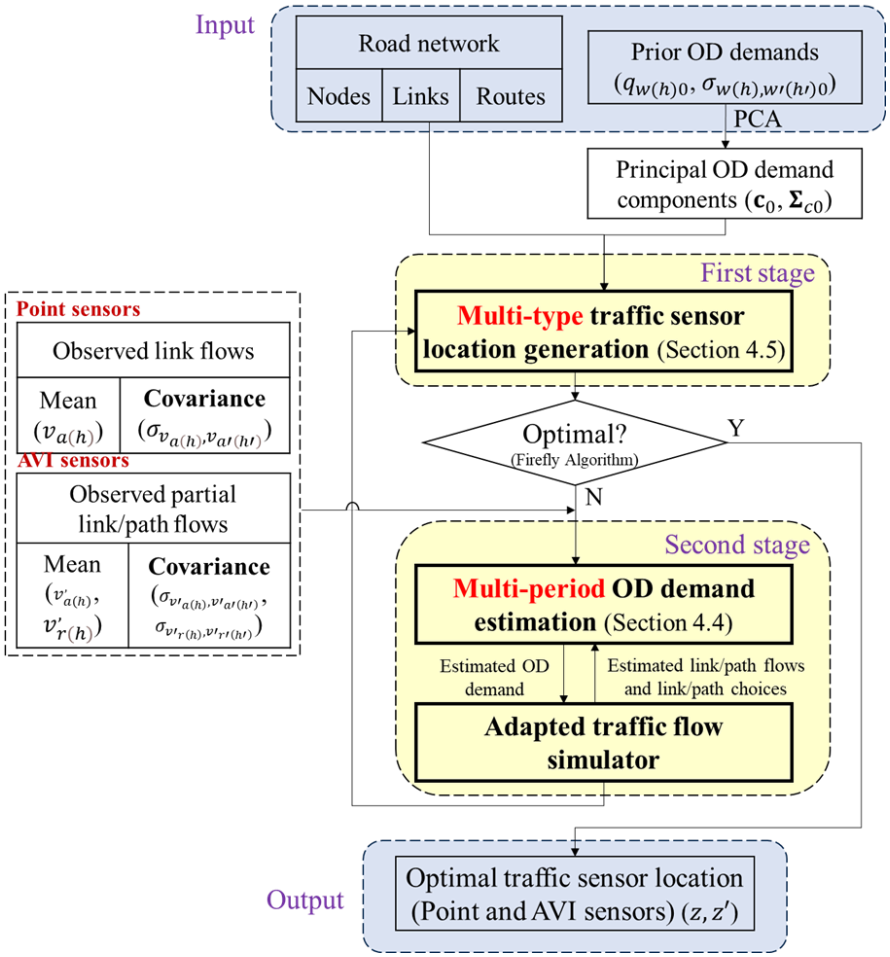

Figure 4.2 The flowchart of the traffic sensor location model

During iterations of the two-stage model, the proposed multi-period OD demand

estimation model at the second stage updates the values of principal OD demand components. Taken directly from these principal OD demand components, the OD demand matrix can then be inferred based on the eigenvectors extracted by the PCA procedure. Note that these eigenvectors do not change during the iterative process, and the PCA only needs to perform once.

4.3 Relationship between observations and multi-period OD demand estimation

In this chapter, some typical hourly periods have been chosen to reflect the variation of travel patterns during multiple periods over the year. Consider a road network with a set of links **A,** set of OD pairs **W**, and set of paths or path segments **R**. The determinant function $|\cdot|$ of the set represents the number of the corresponding network features. For instance, $|\mathbf{A}|$ means the number of links in the road network. The typical periods denoted as a set **H** in this chapter include the morning peak hour (i.e., 8:00–9:00) and the evening peak hour (i.e., 17:00–18:00) on weekdays together with a typical peak hour (i.e., 12:00–13:00) on weekends.

The **observations** include those from both point and AVI sensors. Specifically, for point sensor observations, $v_{a(h)}$ represents the mean of observed hourly traffic flow on link a from point sensors in period h. $\sigma_{v_{a(h)},v_{a\prime(h\prime)}}$ represents the covariance of observed hourly traffic flow between link flows v_a during period h and $v_{a\prime}$ during period h' by point sensors. For AVI sensor observations, $v'_{a(h)}$ stands for the mean of observed partial hourly traffic flow on link a by an individual AVI sensor in period h. $v'_{r(h)}$ stands for the mean of observed partial traffic flow on path or path segment r by a pair of AVI sensors in period h. $\sigma_{v\prime_{a(h)},v\prime_{a\prime(h\prime)}}$ and $\sigma_{v\prime_{r(h)},v\prime_{r\prime(h\prime)}}$ are the

covariance of observations corresponding to the partial link flows $v'_{a(h)}$ and partial path flows $v'_{r(h)}$, respectively. The corresponding vector or matrix of the observations (e.g., $\mathbf{v}_{a(h)}$, $\mathbf{v'}_{a(h)}$, $\mathbf{\Sigma}_{v_a}$, $\mathbf{\Sigma}_{\mathbf{v'}_a}$) are boldfaced.

The **unknown variables** needed to be estimated are the mean and covariance of OD demands. $q_{w(h)}$ is denoted as the traffic demand of OD pair *w* during period *h*. $\sigma_{w(h),w'(h')}$ is denoted as the covariance estimate of traffic demands between OD pairs *w* in period h and OD pair w' in period h'. In addition, the decision variables also include the point and AVI sensor location indexes represented by z and z', respectively. Both z and z' are binary variables. The boldface of these observations (e.g., $\mathbf{q}_{(h)}$, $\mathbf{\Sigma}_q$) represents the corresponding vector or matrix.

The sample mean of observed vehicular flow during the period *h* ($h \in \mathbf{H}$) within a studied year is calculated as

$$\mathbf{v}_{(h)} = \frac{1}{|\mathbf{D}|}\sum_{d\in\mathbf{D}}\mathbf{v}_{(h,d)}\,, \tag{4.1}$$

where $\mathbf{v}_{(h)} = \left[v_{1(h)}, v_{2(h)}, \ldots, v_{|\mathbf{A}|(h)}\right]^T$ is the column vector of sample mean link flows on all links during time period *h*, in which $v_{a(h)}$ is the sample mean link flow on link *a* during time period *h*. $\mathbf{v}_{(h,d)} = \left[v_{1(h,d)}, v_{2(h,d)}, \ldots, v_{|\mathbf{A}|(h,d)}\right]^T$ is a column vector of traffic flows on all links in period *h* on day *d* ($d \in \mathbf{D}$) over the days of interest. $\mathbf{D}$ is the set of days considered, and $|\mathbf{D}|$ is the number of days.

The sample covariance of observed flows among different links during multiple periods within the year is calculated as

$$\Sigma_v = (\sigma_{v_a(h),v_{a'}(h')})_{mr\times mr} = \frac{1}{|\mathbf{D}|-1}\sum_{d\in\mathbf{D}}\{(\mathbf{v}_{(d)}-\mathbf{v})(\mathbf{v}_{(d)}-\mathbf{v})^T\}, \tag{4.2}$$

where $\sigma_{v_a(h),v_{a\prime}(h\prime)}$ represents the sample covariance between vehicular flows on the links a in period h and a' in period h', respectively. $\mathbf{v}$ is a vector of mean hourly traffic flow during all periods obtained by vertically concatenating $\mathbf{v}_{(h)}$, $\mathbf{v} = (\dots(\mathbf{v}_{(h)})^T\dots)^T$. $\mathbf{v}_{(d)}$ is a vector of traffic flows on all links during all periods of interest on day d ($d \in \mathbf{D}$) obtained by vertically concatenating $\mathbf{v}_{(h,d)}$, $\mathbf{v}_{(d)} = (\dots(\mathbf{v}_{(h,d)})^T\dots)^T$.

4.3.1 Observation from point sensors

As described in Section 2.3, point sensors supply entire traffic flows on selected links in a road network, including their mean and covariance. The observed traffic flows on link *a* during period *h* can be expressed by the OD demands and link choice proportions.

$$v_{a(h)} = \sum_{w\in\mathbf{W}} p_{aw(h)} q_{w(h)} \quad \forall a \in \mathbf{A}, h \in \mathbf{H}, \tag{4.3}$$

where $p_{aw(h)}$ is the link choice proportion of OD pair *w* passing through link *a* in period *h*. $q_{w(h)}$ is traffic demand in OD pair *w* during period *h*. For any link installed with a point sensor in any time period, the Eq. (4.3) means that the observed link flow by a point sensor ($v_{a(h)}$) equals the summation of OD demand passing through this link ($\sum_{w\in\mathbf{W}} p_{aw(h)} q_{w(h)}$).

The covariance between the observed link flows v_a during period h and $v_{a\prime}$ during period h' can be obtained as follows:

$$\sigma_{v_a(h),v_{a'}(h')} = \sum_{w'\in\mathbf{W}} \sum_{w\in\mathbf{W}} p_{aw(h)} p_{a'w'(h')} \sigma_{w(h),w'(h')} \quad \forall a, a' \in \mathbf{A}, h, h' \in \mathbf{H}, \tag{4.4}$$

where $\sigma_{w(h),w\prime(h\prime)}$ is the covariance estimate of traffic demands between OD pairs *w* in period h and w' in period h'.

For simplicity, Eqs. (4.3) and (4.4) are expressed in the matrix form:

$$\mathbf{v}_{(h)} = \mathbf{P}_{(h)}\mathbf{q}_{(h)}, \text{ and} \tag{4.5}$$

$$\Sigma_v = \mathbf{P}\Sigma_q(\mathbf{P})^T . \tag{4.6}$$

4.3.2 Observation from AVI sensors

From the assumption (A3), the penetration rate of tagged vehicles can serve as a representative index of all vehicles, allowing one to estimate path flow and OD demand even though only those tagged vehicles can be matched by AVI sensors.

To estimate the OD demands using observations from AVI sensors, two different cases can be summarized as follows, based on the information observed by (I) only one AVI sensor and (II) more than one AVI sensor.

(I) Similar to point sensors, the information obtained from an individual AVI sensor in period h can be used for OD estimation as follows:

$$v'_{a(h)} = \pi \cdot \sum_{w \in \mathbf{W}} p_{aw(h)} q_{w(h)} \quad \forall a \in \mathbf{A}, h \in \mathbf{H} . \tag{4.7}$$

$v'_{a(h)}$ is the observation from an individual AVI sensor on link a. $q_{w(h)}$ is the unknown OD demand of OD pair w in time period h needed to Be estimated. $p_{aw(h)}$ is the link choice proportion that represents the proportion of OD demand of OD pair w in time period h going through link a. The link choice proportion is assumed to be known in the upper level of the OD demand estimation problem, while this proportion will be updated by a traffic flow simulator (which is developed based on SUE) at the lower level with a given OD demand. π is the average penetration rate of tagged vehicles. Specifically, for link a equipped with a point sensor and an AVI sensor, partial link flows passing through (v_a) together with the number of tagged vehicles (v'_a) can both be observed. The penetration rate for tagged vehicles on link a can then be estimated from $\pi_a = v'_a / v_a$. Therefore, the average penetration rate for tagged vehicles for all links equipped with AVI sensors π can be calculated.

For any link installed with an AVI sensor in any time period, the Eq. (4.7) holds and is

used to describe the linear relationship between the observation from the individual AVI sensor ($v'_{a(h)}$) and estimated OD demand ($q_{w(h)}$). An intuitive explanation of Eq. (4.7) is that the observed partial link flow by an individual AVI sensor ($v'_{a(h)}$) equals the summation of OD demand passing through this link ($\sum_{w\in\mathbf{W}} p_{aw(h)} q_{w(h)}$) multiplied by the penetration rate (π) of tagged vehicles.

(II) The tagged vehicles observed by more than one AVI sensor sequentially can also be used for OD demand estimation considering the penetration rate of tagged vehicles. To incorporate the information obtained from paired AVI sensors, i.e., AVI sensors that identify the same tagged vehicle on different links, the relationship between the observations from paired AVI sensors and OD demand in period h can be described as follows:

$$v'_{r(h)} = \pi \times \sum_{w\in\mathbf{W}} p'_{rw(h)}\, q_{w(h)} \quad \forall r \in \mathbf{R}, h \in \mathbf{H}, \tag{4.8}$$

where $p'_{rw(h)}$ denotes the proportion of traffic demand in OD pair w passing through path or path segment r in period h. The path or path segment r is defined by the sequence of traversed AVI sensors. Eq. (4.8) means that for any path that can be observed by matching AVI sensors at different locations in any time period, the observed partial path flow ($v'_{r(h)}$) equals the summation of OD demand passing through this specific path ($\sum_{w\in\mathbf{W}} p'_{rw(h)} q_{w(h)}$) multiplied by the penetration rate (π) of tagged vehicles. Note that AVI sensors can also be installed at the entry and exit links before the origin and destination nodes, in which case the relationship between AVI observations and OD demand in period h can be represented as following Eq. (4.9):

$$v'_{r(h)} = \pi \times q_{w(h)} \quad \forall r \in \mathbf{R}, h \in \mathbf{H}. \tag{4.9}$$

Furthermore, information including flow and travel time detected by AVI sensors can further improve the estimation of link or path segment choice proportions. Interested readers can refer to Zhou and List (2010) for the update of link choice proportion from observed flow information and Zhu et al. (2019) for the update of path choice proportion from observed travel time information.

4.4 Multi-period OD demand estimation

4.4.1 Principal component analysis for OD demand estimation

The OD demands generated in multiple periods present significant variability in both spatial and temporal manners. For instance, at the morning peak hour on weekdays, most traffic demand is directed from residences to places of work, while the direction of demand is reversed during the evening peak hour. In contrast, on weekends and public holidays, people seldom travel to places of work. When considering multiple periods, the number of OD demand variables needed to be estimated increases dramatically. However, because only a subset of OD pairs is dominant in any specific period, these OD pairs of particular importance can be taken to represent the overall characteristics of all OD pairs.

Using PCA, the dominant OD demands, i.e., those which exhibit the greatest dynamics can be extracted from the covariance of OD demand in multiple periods (Djukic et al., 2012; Krishnakumari et al., 2020). Mathematically, assuming that there are n OD pairs in a road network and k periods of interest, the traffic demand of OD pair w during period h is denoted as $q_{w(h)}$. A column vector is denoted as $\mathbf{q_w} = \left[q_{w(h_1)}, q_{w(h_2)}, \ldots, q_{w(h_k)}\right]^{\boldsymbol{T}}$ representing the traffic demands in OD pair w during the observation periods from h_1 to h_k.

As proposed by Djukic et al. (2012), one can extract the essential features of the multi-period OD demand matrix to improve the effectiveness of the method for OD demand estimation and sensor location optimization. The PCA method has been used in this chapter to extract the principal OD demand components in multiple periods.

The multi-period OD demand matrix can be written as the following matrix considering the spatial and temporal information of OD demands.

$$\mathbf{q} = [\mathbf{q_1}, \mathbf{q_2}, \ldots, \mathbf{q_n}] = \begin{bmatrix} q_{1(h_1)} & q_{2(h_1)} & \cdots & q_{n(h_1)} \\ q_{1(h_2)} & q_{2(h_2)} & \cdots & q_{n(h_2)} \\ \vdots & \vdots & \ddots & \vdots \\ q_{1(h_k)} & q_{2(h_k)} & \cdots & q_{n(h_k)} \end{bmatrix}. \tag{4.10}$$

By reformulating the multi-period OD demand matrix to a column vector $[\mathbf{q_1}^T, \mathbf{q_2}^T, \ldots, \mathbf{q_n}^T]^T$, the covariance matrix of the multi-period OD demand with the size of $(n \times k) \times (n \times k)$, which is real and symmetric, can then be calculated and expressed as follows:

$$\mathbf{\Sigma_q} = \begin{bmatrix} \mathbf{\Sigma}_{\mathbf{q}(h_1)} & & sym. \\ \vdots & \ddots & \\ \mathbf{\Sigma}_{\mathbf{q}(h_1,h_k)} & \cdots & \mathbf{\Sigma}_{\mathbf{q}(h_k)} \end{bmatrix} = \begin{bmatrix} \sigma_{1(h_1)} & & & & & & \\ \vdots & \ddots & & & sym. & & \\ \sigma_{1(h_1),n(h_1)} & \cdots & \sigma_{n(h_1)} & & & & \\ \vdots & \vdots & \vdots & \ddots & & & \\ \sigma_{1(h_1),1(h_k)} & \cdots & \sigma_{n(h_1),1(h_k)} & \cdots & \sigma_{1(h_k)} & & \\ \vdots & \ddots & \vdots & \cdots & \vdots & \ddots & \\ \sigma_{1(h_1),n(h_k)} & \cdots & \sigma_{n(h_1),n(h_k)} & \cdots & \sigma_{1(h_k),n(h_k)} & \cdots & \sigma_{n(h_k)} \end{bmatrix}, \tag{4.11}$$

where $\mathbf{\Sigma}_{q(h_1)}$ and $\mathbf{\Sigma}_{q(h_k)}$ are the $n \times n$ covariance matrices of OD demand within the period h_1 and h_k, respectively, and $\mathbf{\Sigma}_{q(h_1,h_k)}$ is the $n \times n$ covariance matrix of OD demand between periods h_1 and h_k. The entry $\sigma_{w(h),w\prime(h\prime)}$ represents the multi-period covariance of traffic demand between OD pair w in period h and OD pair w' in period h'. $\sigma_{w(h),w\prime(h)}$ represents the spatial covariance between OD pairs w and w' in the same period h. $\sigma_{w(h),w(h\prime)}$ represents the temporal covariance for the same OD pair w between time periods h and h'.

Remark 1

When different OD pairs are assumed to be independent at all times, the covariance matrix of OD demands in Eq. (4.11) can be simplified as a diagonal matrix, in which diagonal elements are the variances while all other elements are zero:

$$\sigma_{w(h),w'(h')} = 0 \quad \forall w, w' \in \boldsymbol{W}, w \neq w', and \ \forall h, h' \in \boldsymbol{H}. \tag{4.12}$$

Alternatively, when different OD pairs are statistically correlated only within the same period, the covariance matrix of OD demands in Eq. (4.11) can be simplified as a block diagonal matrix:

$$\sigma_{w(h),w'(h')} = 0 \quad \forall w, w' \in \boldsymbol{W}, \ and \ \forall h, h' \in \boldsymbol{H}, h \neq h'. \tag{4.13}$$

Remark 2

The elements in the multi-period covariance matrix can be positive, zero, or negative. When the covariance is positive (i.e., $\sigma_{w(h),w'(h')} > 0$), the traffic demand of OD pair w in period h has a positive relationship with that of OD pair w' in period h', and vice versa.

As illustrated in Figure 4.1, the statistical covariance relationship between OD pairs (B,C) and (C,F) at the morning peak hour is positive, whereas the covariance between OD pairs (F,C) and (F,B) in the evening peak hour is negative.

However, the incorporation of multi-period statistical OD demands dramatically increases the number of OD demand variables that need to be estimated. Therefore, it is challenging to directly infer the mean and covariance of multi-period OD demand accurately with a limited number of traffic sensors. To take advantage of additional information provided by the spatial and temporal covariance of OD demand in multiple periods, PCA is adopted to extract the essential features of the multi-period OD flow matrix. For instance, if the covariance of traffic flows between OD pair w in period

h and OD pair w' in period h' is relatively large, these two OD demands are highly correlated, as shown in Figure 4.3. With the negligible loss of information, a vector e_i, the eigenvector corresponding to the largest eigenvalue, can be used to represent the traffic demands of these two OD pairs, thereby reducing the dimensionality of the multi-period OD demands.

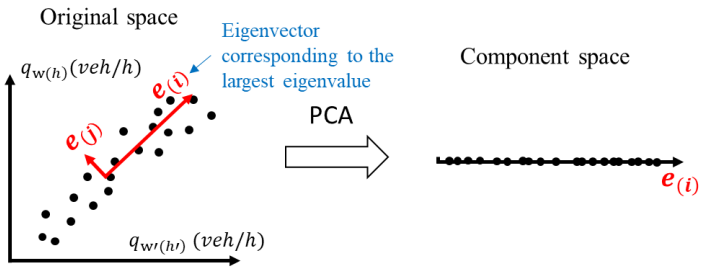

Figure 4.3 PCA to extract the principal OD demand components

The eigenvectors of the centered and scaled OD demand covariance matrix contain important information that can be obtained from the singular value decomposition of the covariance matrix. Based on linear algebra, because the $(n \times k) \times (n \times k)$ covariance matrix $\mathbf{\Sigma_q}$ in multiple periods is real and symmetric, the matrix $\mathbf{\Sigma_q}$ can be factorized as follows:

$$\mathbf{\Sigma}_q = \mathbf{\Lambda Y \Lambda}^{-1} \quad , \tag{4.14}$$

where $\mathbf{\Lambda}$ is the square $(n \times k) \times (n \times k)$ matrix whose column vector is the eigenvector $\mathbf{e_i}$ of $\mathbf{\Sigma_q}$, and $\mathbf{Y}$ is the diagonal matrix whose diagonal elements are the corresponding eigenvalues. The eigenvectors $\{\mathbf{e_1}, \mathbf{e_2}, \ldots, \mathbf{e_{nk}}\}$ of the multi-period OD demand matrix can be considered as an orthonormal basis because the covariance matrix is real and symmetric. Therefore, the centered traffic demands in any OD pair with column-wise zero empirical mean $(\mathbf{q_{w(h)}} - \bar{\mathbf{q}})$ can be expressed by a linear combination of the set of orthonormal vectors as follows:

$$\boldsymbol{q_{w(h)} - \bar{q} = c_1 e_1 + c_2 e_2 + \cdots c_{kn} e_{kn} = \sum_{i=1}^{kn} c_i e_i} \quad , \tag{4.15}$$

where c_i is the coefficient of the eigenvector representing the principal OD demand component in The coordinate system. $\bar{\mathbf{q}}$ is the mean OD demand for all OD pairs over all periods. Eq. (4.15) can be concerned as a simple rotation of the coordinate system from the original OD demands to a new set of coordinates represented by c_i and eigenvectors. By sorting the corresponding eigenvalues in decreasing order, the original OD demand can be retained with M $(M < kn)$ eigenvectors with the maximum variance. Therefore, the information given by the OD demand can be maintained with the least possible information loss after dimensionality reduction by the PCA. A new representation of OD demand with a lower dimension can be expressed as follows:

$$\tilde{\mathbf{q}}_{\mathrm{w(h)}} - \bar{\mathbf{q}} = \mathbf{c_i E}, \tag{4.16}$$

where $\tilde{\mathbf{q}}_{\mathrm{w(h)}}$ is the approximate OD demand in period h represented by M eigenvectors and the principal OD components $\{c_1, c_2, \ldots, c_M\}$. $\mathbf{E}$ is the matrix containing all of the eigenvectors.

The principal OD demand components with M dimensions are extracted to capture the main contribution of the original OD demand matrix with $n \times k$ dimensions. The extraction by PCA can potentially make full use of the additional information arising from the consideration of multiple periods. Instead of directly estimating the original traffic demand in all OD pairs, the OD demand estimation problem first shifts the focus to estimating principal OD demand components from traffic sensors. The multi-period traffic SLP becomes that of locating point sensors and AVI sensors to estimate the principal OD demand components first, then to estimate the traffic demand in all of the OD pairs.

4.4.2 Multi-period OD demand estimation based on PCA

The multi-period OD demand in a road network can be uniquely represented by the principal OD demand components c_i in the *M*-dimensional space on the basis of the

PCA. By taking account of the measurement errors from point sensors, the relationship between OD demand and observed link flow from point sensors can be represented as follows:

$$v_{a(h)} = \sum_{w \in \mathbf{W}} p_{aw(h)} q_{w(h)} + \varepsilon_a \quad \forall a \in \mathbf{A}, h \in \mathbf{H}, \tag{4.17}$$

where ε_a denotes the measurement error of traffic flow on link a from a point sensor.

Substituting the principal OD demand components representing the approximate multi-period OD demands into Eq. (4.17), the following relationship can be obtained:

$$v_{a(h)} = \sum_{w \in \mathbf{W}} \sum_{i=1}^{M} p_{aw(h)} c_i e_i + \bar{v} + \varepsilon_a = \Theta_{(h)} \mathbf{c}_i + \bar{v} + \varepsilon_a \quad \forall a \in \mathbf{A}, h \in \mathbf{H}, \tag{4.18}$$

where $\Theta_{(h)}$ denotes the matrix of transformed link choice proportion in period h, that is, the transformation of the original link choice proportions to the orthonormal basis matrix of eigenvectors $\mathbf{E}$. $\bar{v}$ is the mean link flow on all links observed by point sensors over all periods.

Furthermore, AVI sensors represent an additional data source to provide path or path segment flows for multi-period OD demand estimation. Based on the principal OD demand components, the observations from AVI sensors in multiple periods can be formulated as follows:

$$\begin{aligned} v'_{r(h)} &= \pi \times \sum_{w \in \mathbf{W}} p'_{rw(h)} q_{w(h)} \\ &= \pi \times \left(\sum_{w \in \mathbf{W}} \sum_{i=1}^{M} p'_{rw(h)} c_i e_i + \bar{v}' \right) + \varepsilon'_r \\ &= \pi \cdot \Theta'_{(h)} \mathbf{c}_i + \pi \cdot \bar{v}' + \varepsilon'_r \quad \forall r \in \mathbf{R}, h \in \mathbf{H} \end{aligned}, \tag{4.19}$$

where $\Theta'_{(h)}$ denotes the matrix of transformed path or path segment choice proportion in period h, that is, the transformation of the original path or path segment choice proportions to the orthonormal basis matrix of eigenvectors $\mathbf{E}$. ε'_r denotes the measurement error of traffic flow on path r from an AVI sensor. $\bar{v}'$ is the mean traffic flow observed by AVI sensors over all periods.

Given the prior information, including mean and covariance of OD demand (i.e., $\mathbf{q}_0$ and $\mathbf{\Sigma}_{q0}$, respectively), the prior principal OD demand components $\mathbf{c}_0$ and their covariance matrix $\mathbf{\Sigma}_{c0}$ can be estimated by PCA. Similarly, the transformed prior link or path choice proportions (i.e., Θ_0 and Θ'_0, respectively) can also be obtained. It is assumed that the measurement errors from point and AVI sensors belong to uncorrelated white noise processes. With the knowledge of the observations from point sensors $\mathbf{v}$ and AVI sensors $\mathbf{v}'$, as well as their variance and covariance matrices $\mathbf{\Sigma}_e$ and $\mathbf{\Sigma}'_e$, the optimal principal OD demand component estimator can be derived using a Kalman filter. More comprehensive descriptions of the initial Kalman filter method can be found in Ashok and Ben-Akiva (1993). To combine the information observed from both point and AVI sensors, the following formulation of the Kalman filter is adopted:

$$\mathbf{c} = \mathbf{c}_0 + \mathbf{K}(\mathbf{v} - \Theta_0\mathbf{c}_0) + \mathbf{K}'(\mathbf{v}' - \pi \cdot \Theta'_0\mathbf{c}_0) \text{ and} \tag{4.20a}$$

$$\mathbf{\Sigma}_{\mathrm{c}} = (\mathbf{I} - \mathbf{K}\Theta_0)(\mathbf{I} - \mathbf{K}'\Theta'_0)\mathbf{\Sigma}_{\mathrm{c0}} \ , \tag{4.20b}$$

where

$$\mathbf{K} = \mathbf{\Sigma}_{\mathrm{c0}}{\Theta_0}^T(\Theta_0\mathbf{\Sigma}_{\mathrm{c0}}{\Theta_0}^T + \mathbf{\Sigma}_{\mathrm{e}})^{-1} \text{ and} \tag{4.20c}$$

$$\mathbf{K}' = \mathbf{\Sigma}_{\mathrm{c0}}{\Theta'_0}^T(\Theta'_0\mathbf{\Sigma}_{\mathrm{c0}}{\Theta'_0}^T + \mathbf{\Sigma}'_{\mathrm{e}})^{-1}. \tag{4.20d}$$

The above equations are regarded as the update phase in a Kalman filter, where the observations from traffic sensors (i.e., $\mathbf{v}$ and $\mathbf{v}'$), regarded as measurements, are used to update the prior principal OD demand components and obtain their mean by Eq. (4.20a) and covariance by Eq. (4.20b). The terms $\mathbf{K}$ and $\mathbf{K}'$ are known as the optimal Kalman gain and yield the minimum mean square error of the estimates. $\mathbf{v} - \Theta_0\mathbf{c}_0$ and $\mathbf{v}' - \pi\Theta'_0\mathbf{c}_0$, called the measurement residual, are the errors of the estimate incorporating observed information from point and AVI sensors, respectively.

To improve the efficiency of the solution algorithm, substitute Eqs. (4.20c) and (4.20d) into Eq. (4.20b). Recall the matrix inversion lemma: given the invertible matrices A,

D, and $D + CA^{-1}B$, the following equation can be obtained: $(A + BD^{-1}C)^{-1} = A^{-1} - A^{-1}B(D + CA^{-1}B)^{-1}CA^{-1}$. A is an n-by-n, D is a k-by-k, B is an n-by-k, and C is a k-by-n matrix. Based on this lemma, it can be deduced as:

$$\boldsymbol{\Sigma}_{\mathrm{c}}{}^{-1} = \boldsymbol{\Sigma}_{\mathrm{c0}}{}^{-1} + \Theta_0^T \boldsymbol{\Sigma}_{\mathrm{e}}^{-1} \Theta_0 + \Theta'^T_0 \boldsymbol{\Sigma}'^{-1}_{\mathrm{e}} \Theta'_0. \tag{4.21}$$

The terms $\Theta_0^T \boldsymbol{\Sigma}_e^{-1} \Theta_0$ and $\Theta'^T_0 \boldsymbol{\Sigma}'^{-1}_e \Theta'_0$ in Eq. (4.21) represent the value of the additional information from point sensors and AVI sensors, respectively. Note that the estimation of principal OD demand components and their covariance can be further used to obtain the OD demand in multiple periods by applying Eq. (4.16) (see Djukic et al. (2012)). Importantly, due to the variation of the multi-period OD demands at different iterations, the link choice proportions are also updated during the OD demand estimation process. This means a bilevel optimization framework is needed for multi-period OD demand estimation, especially for congested networks (Zhou and List, 2010). Detailed information on bilevel OD demand estimation can be found in Shao et al. (2014). An adapted traffic flow simulator has been used in this chapter to update the link choice proportions in multiple periods (Lam and Xu, 1999).

4.5 Multi-period traffic sensor locations

To account for the hourly and daily variation of traffic flow, traffic sensor locations should be adapted to different situations in various time periods, rather than for one single period as typically considered in the literature. In this chapter, for multi-period OD demand estimation, the number, type, and locations of traffic sensors can be optimized simultaneously while considering the budget constraint.

As stated in Section 4.4, if link flows are available after the installation of traffic sensors, the principal OD demand components, and the multi-period OD demand, can be estimated using the Kalman filter. However, for the traffic SLP, it is impossible to

observe the link flows from traffic sensors in the planning stage before the installation of the sensors. To deal with this, it is noticed from Eq. (4.21) that the covariance matrix of the principal OD demand components can be estimated based solely on the traffic sensor locations and without exact observations from the sensors (Zhou and List, 2010; Simonelli et al., 2012). In other words, the *variation* of the multi-period OD demand estimates can be obtained before installing any sensors.

In addition to the variance information, the additional information provided by the covariance of OD demand in multiple periods can also help to optimize the traffic sensor locations and estimate the multi-period stochastic OD demands. For instance, given two OD pairs with relatively large demand covariance in multiple periods, it can be statistically inferred that these two OD pairs should have a strong linear relationship with each other (Castillo et al., 2008b). Therefore, the OD pairs with the greatest demand covariance values between one another should be assigned higher importance for multi-period OD demand estimates. Mathematically, to incorporate both the variance and covariance of OD demand in multiple periods, the summation of absolute values of OD demand covariances between OD pair w and other OD pairs is considered as the weight on OD pair w.

To present the model formulation more clearly, this research first defines two mapping functions $\Gamma(A)$ and $D(A)$. The function $\Gamma(A)$ obtains a new matrix whose elements are the absolute values of all of the elements in matrix A. The function $D(A)$ obtains a column vector whose elements are the same as the corresponding diagonal elements in matrix A. The mathematical explanations of these functions can be found in Appendix B. In addition, define a $1 \times M$ row vector $\mathbf{I}$ whose elements are all ones. Therefore, the multi-period traffic sensor locations can be modeled by minimizing the uncertainty of the resultant multi-period OD demand estimates, considering the trace

of the covariance matrix[1] to be the estimation uncertainty, as follows:

$$\min_{z,z'} \sum_{w\in \boldsymbol{W},h\in \boldsymbol{H}}\left(\sum_{w'\in \boldsymbol{W},h'\in \boldsymbol{H}} |\sigma_{w(h),w'(h')}|\right)\sigma_{w(h)}$$

$$= \min_{z,z'} \left[\boldsymbol{I}\cdot \Gamma(\boldsymbol{\Sigma}_c)\cdot D(\boldsymbol{\Sigma}_c)\right], \tag{4.22a}$$

subject to a budget constraint:

$$\beta \sum_{a\in \boldsymbol{A}} z_a + \beta' \sum_{a\in \boldsymbol{A}} z'_a \le B, \tag{4.22b}$$

where z_a and z'_a are binary variables representing point sensor locations and AVI sensor locations, respectively. $z_a = 1$ means that a point sensor is installed on link a, $z'_a = 1$ if an AVI sensor is installed on link a, and both z_a and z'_a are 0 otherwise. β and β' represent installation and maintenance costs for a point sensor and an AVI sensor, respectively. B refers to the total budget for the sensor installation. The multiplication $\mathbf{I}\cdot \Gamma(\Sigma_c)$ is to calculate the weights of all OD pairs w.

The above traffic sensor location model is used to identify the locations of point sensors and AVI sensors by minimizing the expected uncertainty of the multi-period OD demand estimation. Spatial and temporal covariance are explicitly considered when estimating the uncertainty of the multi-period OD demands based on the traffic sensor locations. The uncertainty reduction is a measurement of reduction in OD demand variance achieved by considering the observations from point sensors and AVI sensors. It should be noted that estimation uncertainty can refer to the weekly, monthly, and annual changes of the OD demand if the time interval is set as a week, month, and year.

To study the traffic SLP for multi-period OD demand estimation, the following two important propositions are analyzed.

[1] In linear algebra, the trace of a square matrix is the sum of elements on its main diagonal.

Proposition 4.1: Effects of multi-period OD demand covariance on the optimum number of sensors

Under congested conditions, the covariances of OD demands among different time periods should be non-zero, as clarified in the introduction section. By taking account of the covariance of OD demand in multiple periods, it can then be achieved that the same uncertainty reduction with fewer sensors than considering the OD demand covariance in one period only or neglecting the covariance completely.

Mathematically, for the purpose of illustration, only one type of sensor (i.e., point sensors) is considered in this proposition. Denote the optimal traffic sensor locations by considering OD demand covariance effects in multiple periods as z^*_{mcov}. Likewise, the corresponding locations by taking into account the covariance of OD demand in single period only are denoted as z^*_{bcov}, and that without consideration of any covariance effect as z^*_{nocov}. Proposition 4.1 can be expressed mathematically as below: Given $tr(\Sigma_c - \Sigma_{c0})$, $\sum z^*_{mcov} \leq \sum z^*_{bcov} \leq \sum z^*_{nocov}$.

Proposition 4.2: Trade-off between AVI and point sensors

If the value of additional information from each AVI sensor ($\Theta'^{T}{\boldsymbol{\Sigma}'_e}^{-1}\Theta'$) is smaller than that from the equivalent number of point sensors ($\Theta^{T}{\boldsymbol{\Sigma}_e}^{-1}\Theta$), only point sensors should be chosen for the multi-period OD demand estimation. Conversely, if the value of additional information from each AVI sensor is larger than that from the equivalent number of point sensors, only AVI sensors should be chosen. Otherwise, both AVI and point sensors are needed.

The mathematical explanation and proof of Propositions 4.1 and 4.2 can be found in Appendix B.

4.5.1 Solution algorithm

The multi-period OD demands and the spatial and temporal covariance information have been explicitly considered in the proposed solution algorithm to solve the multi-type SLP in this chapter. By taking advantage of this additional valuable information, the sensor locations can be optimized for the estimation of more accurate multi-period OD demands. It should be remarked that the proposed multi-period traffic sensor location model in formulation (4.22a) is an integer programming model in which binary decision variables stand for the point and AVI sensor locations. The proposed SLP is NP-hard so that no optimization algorithm can guarantee a global optimum solution, especially for a large-scale problem. Therefore, some meta-heuristic algorithms, such as a variable neighborhood search algorithm, GA, or Pareto front approach, should be adopted to efficiently solve the proposed SLP.

As demonstrated in Chapter 3.5, there are three main reasons to support the use of FA to solve the proposed model: (i) high efficiency to solve complex problems; (ii) low time complexity; (iii) includes not only a self-improving process with the current space but also improvement among its own space from the previous stages. In this chapter, the FA described in Section 3.5.2 is further adapted to deal with the proposed multi-type SLP, which is considered as an integer programming problem.

In the FA framework, the point sensor and AVI sensor location schemes can be conveniently represented by a firefly analogy. Specifically, $\mathbf{z}$ and $\mathbf{z}'$ are vectors whose elements are binary variables having allowable values of 1 or 0 only. The improved FA is to decide the values of all elements in $\mathbf{z}$ and $\mathbf{z}'$.

The objective of the traffic sensor location model is represented by the light intensity of the fireflies (i.e., $In(\mathbf{z}, \mathbf{z}') = \mathbf{I} \cdot \Gamma(\mathbf{\Sigma}_c) D(\mathbf{\Sigma}_c)$), which is regarded as the fitness

function. In the improved FA, light absorption coefficients α_{m} and α_{cov} corresponding to the estimation accuracy of the mean and covariance of multi-period OD demand are defined. A more accurate OD demand estimate in the previous iteration will lead to a larger light absorption coefficient. These light absorption coefficients are considered as the weights on the attractiveness of fireflies. A smaller light intensity indicates a larger likelihood that the represented sensor location schemes will be selected. The attractiveness of a firefly is proportional to its brightness, which is determined by the fitness function. Attractiveness and distance are determined as in Chapter 3.5.

Algorithm steps

Step 0 (Preprocessing)

Map the prior multi-period OD demand by utilizing the adapted traffic flow simulator to obtain prior link choice proportions $\mathbf{P}_{0(h)}$ and path or path segment choice proportions $\mathbf{P'}_{0(h)}$ in all periods. Perform the PCA for the prior multi-period OD demands to obtain $\mathbf{c}_0$ and $\mathbf{\Sigma}_{c0}$. Calculate the relevant Θ_0 and Θ'_0 as shown in Eqs. (4.18) and (4.19).

Step 1 (Initialization)

Randomly generate the initial point sensor and AVI sensor locations ($\mathbf{z_0}$ and $\mathbf{z'_0}$, respectively) on the basis of the budget constraint. The maximum generation (or iteration) is set to T, and the current iteration is initialized as $t = 0$ (Nayeem et al., 2014). Define the light absorption coefficients α_{m} and α_{cov} corresponding to the estimation accuracy of mean OD demand and multi-period covariance of OD demand, respectively. Define the step size parameter β.

Step 2 (Stopping criterion)

The algorithm will terminate and output the optimal solutions under one of the following conditions:

(a) the gap of objective values between two successive iterations is not larger than the

predetermined threshold.

(b) the iteration number exceeds the maximum iteration (i.e., $t > T$).

Otherwise, move on to step 3.

Step 3 (Selection operation)

For each firefly $\mathbf{z_{(t)}}$ and $\mathbf{z'_{(t)}}$, calculate the uncertainty of estimation (using formulation (4.20)), transform the estimation of principle OD demand components to multi-period OD demand by applying Eq. (4.16) and update the link choice proportions by the adapted traffic flow simulator, then solve the problem (4.22). On the basis of the calculated light intensity $In(\mathbf{z_{(t)}}, \mathbf{z'_{(t)}})$, the local optimum ($\mathbf{z^*_{(t)}}$) can be determined by ranking the fireflies.

Step 4 (Variation operation)

Vary the attractiveness of fireflies $\mathbf{z_{(t)}}$ and $\mathbf{z'_{(t)}}$ on the basis of light intensity, light absorption coefficients, and the distance between fireflies. The attractiveness is directly proportional to the light absorption coefficient and light intensity, but inversely proportional to the distance. Update $\mathbf{z_{(t)}}$ and $\mathbf{z'_{(t)}}$ consisting of m individuals according to their attractiveness (i.e., $\mathbf{z_{(t+1)}} = \mathbf{z_{(t)}} + \mathrm{e}^{-(\alpha_m + \alpha_{cov})\mathbf{r}}(\mathbf{z^*_{(t)}} - \mathbf{z_{(t)}}) + \beta^i$). Update the iteration indicator $t = t + 1$, then move back to step 2.

4.6 Numerical examples

In this section, three example networks are examined to demonstrate the effectiveness and efficiency of the proposed methodology of the SLP for multi-period OD demand estimation. Efficiency reflects that the optimum sensor location scheme can be achieved by the proposed model with the most accurate multi-period OD demand estimates. Effectiveness defines the ability of the proposed model for solving the SLP for both small and medium-size road networks. Examples 1 and 2 are to numerically demonstrate the contributions of this chapter, as described in section 4.1.2, while example 3 is to further explore the effects of joint travel behavior through empirical

data collected in Hong Kong. The main experiments are listed as follows:

Example 1

(1) The effects of the covariance of multi-period OD demand on the SLP.

The covariance of OD demand, especially in multiple periods, can significantly affect the results of OD estimation and traffic sensor locations because of the variation of joint travel behaviors over a period of time.

(2) Benchmark comparison among different sensor location models.

The results of sensor locations and OD demand estimation can vary significantly depending on different sensor location models in which whether one-period or multi-period OD demands in SLPs are considered particularly under congested conditions.

(3) The effects of traffic congestion on multi-period OD demand estimation.

Traffic congestion can last a long time and impact travel patterns and OD demands in different periods.

Example 2

(4) The efficiency of multi-type traffic sensors for OD demand estimation.

Partial path and even OD flows observed by AVI sensors can be regarded as a supplement to entire link flows only on selected links provided by point sensors for OD demand estimation. These multi-source data from different sensor types can cooperate with each other to clarify the variation and correlation relationship of multi-period OD demand.

(5) Sensitivity analysis of the cost ratio between point and AVI sensors.

The cost ratio between point and AVI sensors also affects the determination of the budgetary allocation for these different sensor types.

(6) Sensitivity analysis of the number of principal OD demand components.

The PCA method is used for stochastic OD demand estimation to take full advantage of the additional information obtained from the covariance of OD demand, especially in multiple periods. The number of principal OD demand components must be predetermined and can affect the estimation results.

Example 3

(7) Effects of joint travel behavior on the traffic SLP.

Joint travel behavior is one of the key factors contributing to the covariance of OD demand in multiple periods. Based on empirical data in Hong Kong, the effects of travel behavior patterns on multi-type traffic sensor locations are explored.

(8) Convergence test of the solution algorithm.

The convergence of the solution algorithm is tested in this numerical example to demonstrate the effectiveness of the improved FA.

4.6.1 A small-size transportation network: Example 1

A small-size road network, as exhibited in Figure 3.3, consists of 7 nodes, 16 links, and 12 OD pairs. The OD demands in three different periods, including the weekday morning peak hour (8:00–9:00), weekday evening peak hour (17:00–18:00), and peak hour on Sunday (12:00-13:00), are considered in this example. Note that it is not necessary to incorporate the afore-mentioned periods only, any period can be included in the proposed model; in this example, these three periods are adopted for illustration.

For validation purposes, the “true” OD flows, including mean and var-cov matrix in multiple periods, shown in Table 4.1 and Table 4.2, are assumed to be known and are obtained using the re-sampling method (Cascetta and Nguyen, 1988; Lo et al., 1996). Specifically, the “true” hourly OD demands during three different periods over a sequence of days (e.g., 365 days) are simulated from a multivariate normal distribution

with the desired mean, coefficient of variation, and correlation coefficient. In this example, the desired mean and coefficient of variation correspond to the Hong Kong Annual Traffic Census data. The desired coefficients of correlation are assumed according to plausible travel behaviors in the road network. The OD demands are then re-sampled with a sampling fraction of 10% so that the mean, variance, and covariance of multi-period OD demands, considered the "true" OD demand information, can be obtained.

On the basis of true multi-period OD demands, the observation of link flows from point or AVI sensors and partial path flows from AVI sensors can be simulated using an adapted traffic flow simulator. Note that to avoid the need to spend too much computation time searching for the feasible paths of the OD pairs, the path set in the road network is predetermined and fixed. The parameters in the traffic flow simulator are identical to those in Lam and Xu (1999).

Table 4.1 Assumed true OD demands in multiple periods

OD number	OD pair	True mean OD demands		
		Weekday morning peak hour (h_1)	Weekday evening peak hour (h_2)	Peak hour on Sunday (h_3)
1	C–B	168	121	90
2	**C–F**	240	180	88
3	C–G	96	142	110
4	**B–C**	208	170	120
5	B–F	223	173	115
6	B–G	240	158	280
7	F–C	144	180	105
8	F–B	168	210	111
9	F–G	184	151	124
10	G–C	120	190	185
11	G–B	136	155	171
12	G–F	208	201	190

Table 4.2 Assumed true covariance between OD pairs (B,C) and (C,F) in multiple periods

Covariance		Weekday morning peak hour (h_1)		Weekday evening peak hour (h_2)		Peak hour on Sunday (h_3)	
		(B,C)	(C,F)	(B,C)	(C,F)	(B,C)	(C,F)
Weekday morning peak hour (h_1)	(B,C)	432.64	339.46	-123.76	37.44	29.95	87.86
	(C,F)	339.46	576.00	40.80	-95.04	34.56	25.34
Weekday evening peak hour (h_2)	(B,C)	-123.76	40.80	289.00	116.28	85.68	17.95
	(C,F)	37.44	-95.04	116.28	324.00	38.88	66.53
Peak hour on Sunday (h_3)	(B,C)	29.95	34.56	85.68	38.88	207.36	121.65
	(C,F)	87.86	25.34	17.95	66.53	121.65	111.51

In this example, the prior multi-period OD flows are set to have the following relationship with their true values: $q_{w(h)0} = (1 - \mu \cdot cv_{w(h)}) \cdot q^*_{w(h)}$ and $\sigma_{w(h),w\prime(h\prime)0} = (1 - \mu \cdot cv_{w(h)})(1 - \mu \cdot cv_{w\prime(h\prime)}) \cdot \sigma^*_{w(h),w\prime(h\prime)}$, where $q^*_{w(h)}$ and $\sigma^*_{w(h),w\prime(h\prime)}$ are the simulated true mean OD demand for OD pair w in period h and the covariance of OD demand between OD pairs w in period h and w' in period h', μ is an independent random variable following a normal distribution $N(0,1)$, and $cv_{w(h)}$ represents the coefficient of variation of the true traffic flows for OD pair w during period h (Yang et al., 1992).

The initial link choice proportions for each OD pair are simulated using the stochastic user equilibrium traffic assignment model with the dispersion parameter set to be $\theta = 0.2$. In practice, except for the covariance information, the prior OD demand information can be obtained from surveys or previous models. Furthermore, in a road network with existing traffic sensors or other data sources, prior information, including covariance information, can be inferred and updated directly from the available data for more accurate estimation, especially when considering multiple periods.

As an extension to Zhou and List (2010) and Simonelli et al. (2012), the percentage of reduction in variance of the multi-period OD demand estimates is used as the model performance index in this chapter. This measurement is more suitable for the

considered case than the others because the objective of the proposed model is to determine the sensor locations by minimizing the uncertainty of multi-period OD demand. A smaller uncertainty of OD demand estimates will lead to a larger percentage of reduction in variance, given the prior OD demand information. Hence, the more accurate the multi-period OD demand estimates, the better the sensor location scheme.

4.6.1.1 Effects of covariance of multi-period OD demand on SLP

The covariances of OD demand in multiple periods play a significant role in the OD estimation problem. The effects of multi-period OD demand covariance on the SLP are examined by considering the following three scenarios:

- Scenario A: No covariance among OD demands.
- Scenario B: Covariance among OD demands only within the same period.
- Scenario C: Covariance among OD demands in multiple periods.

Different covariance relationships among OD pairs are considered in each scenario, but all of them include the same three peak hour periods for comparison. In this sensitivity test, the percentages of reduction in OD variance based on the resultant traffic sensor location schemes are compared to evaluate the performance of the proposed model under different scenarios. The reduction in OD variance is represented by the difference in uncertainty between the estimated and prior OD demands (Zhou and List, 2010). The uncertainty is evaluated by the square root of the total trace value for the OD demand covariance matrix. In addition, the mean absolute percentage error (MAPE) of the OD demand estimation is used to assess the acccuracy of the estimation results based on these three scenarios.

The results of these three scenarios in Table 4.3 indicate that the “best” traffic sensor locations depend on the assumptions regarding the covariance relationship of OD demand. It can be seen that in scenario C, where the covariance information in multiple

periods is considered, the percentage of uncertainty reduction is 65.45%. Furthermore, the MAPE of OD demand estimation is improved by more than 20% compared with scenario A. Therefore, interestingly, this experiment shows that the consideration of OD demand covariance in multiple periods can efficiently reduce the uncertainty of OD estimates and increase the estimation accuracy.

Table 4.3 Effects of OD demand covariance in multiple periods on SLPs

Scenario	Covariance consideration	Optimum traffic sensor locations	Percentage of reduction in variance (%)	MAPE (%)
A	No covariance	Point: [3,10] AVI: [4,9,16]	35.66	31.01
B	Consideration of covariance only in the same period	Point: [3,5] AVI: [2,9,16]	57.71	17.58
C	Consideration of covariance in multiple periods	Point: [3,5] AVI: [2,15,16]	**65.45**	9.88

To further gain insights on the performance of the optimum sensor configurations under different covariance scenarios, the OD estimation accuracy in terms of MAPE is tested based on these three sensor configurations for each covariance scenario.

Table 4.4 Performance of different sensor locations under different covariance scenarios

MAPE (%)	Optimum in A Point: [3,10] AVI: [4,9,16]	Optimum in B Point: [3,5] AVI: [2,9,16]	Optimum in C Point: [3,5] AVI: [2,15,16]
A. No covariance	31.03	35.26	32.41
B. One-period covariance	27.19	17.58	20.30
C. Multi-period covariance	23.05	**15.51**	**9.88**

It can be found in Table 4.4 that when multi-period covariance is taken into account, the MAPE decreases to 15.51% under the sensor configuration of the optimum in scenario B, and changes to 9.88% under the sensor configuration of the optimum in scenario C. The results in Table 4.4 testify again that even though different optimum sensor configurations are required at different covariance scenarios, multi-period

covariance of OD demands leads to efficient improvement of estimation accuracy. This highlights the need to systematically consider the multi-period covariance of OD demand in SLPs.

4.6.1.2 Benchmark comparison among different sensor location models

For benchmark comparison, the chosen models include model I proposed in Hu et al. (2016), model II proposed in Simonelli et al. (2012), and model III proposed in Fu et al. (2019). The reason why these three models are chosen is that these three models fully cover different types of sensor location models in the literature. Specifically, concerning the SLP for OD demand estimation, existing models can be categorized into three types:

(i) SLP with consideration of the mean OD demand only (Yang and Zhou, 1998; Bianco et al., 2001; Hu et al., 2015),

(ii) SLP with taking into account the mean and variance of OD demand (Zhou and List, 2010; Simonelli et al., 2012), and

(iii) SLP considering mean, variance, and covariance of OD demand in one time period (Fu et al., 2019).

However, the covariance of OD demands in multiple time periods should also be incorporated in SLP to capture better the joint travel behaviors and variation of travel patterns in multiple periods. The proposed model in this chapter fills the gap and is categorized as the fourth type, (iv) SLP taking into account the mean, variance, and covariance of OD demand in multiple periods.

These existing models (e.g., modes I, II, and III) focus on estimating one-period OD demand (e.g., morning peak hour). For comparison of OD demand estimation accuracy in different time periods, the optimum sensor locations for the morning peak hour h_1 in these previous models will be used for OD demand estimation in other time periods. Notably, the models proposed in Simonelli et al. (2012) and Fu et al. (2019) would

optimize the locations of point sensors only. This experiment maintains the same settings (e.g., sensor type, time period of interest) consistent with these existing models. When multi-type sensors are deployed, the cost ratio between point and AVI sensors is set to 1:2 based on the cost data from the Speed Map Panel project in Hong Kong (Transport Department, 2021a).

Table 4.5 displays that for the OD demand estimation accuracy, model IV proposed in this chapter contributes to the best sensor locations with the most significant average percentage of reduction in variance (**65.45%**) and smallest average MAPE (**9.88%**) for different time periods. This finding can be elucidated as that model IV explicitly takes into account the mean and covariance of OD demand in multiple periods when determining the multi-type sensor locations. As a result, more available data from multi-type traffic sensors, including mean and covariance of multi-period link flow observations, can be incorporated. The other three existing models, however, spotlight one of the most congested periods (e.g., morning period h_1). The observed information has not been fully utilized when allocating traffic sensors for the estimation of single-period OD demand. Only the proposed model IV can capture the OD demand uncertainty and correlation in different time periods.

It is also found in Table 4.5 that the largest percentage of reduction in variance (**79.31%**) is achieved by model II in time period h_1 because the outstanding feature of model II is to reduce the uncertainty of OD demand in the period of interest. This model II puts effort into decreasing the variation of OD demand in a specific time period by installing additional sensors. Furthermore, the best MAPE of OD demand estimates in time period h_1 is **5.42%** resulting from model III. Model III determines the sensor locations by directly minimizing the OD demand estimation error considering the covariance of vehicular demand among different OD pairs in the single period of interest. On the other hand, model I is particularly applicable to the situation

without prior traffic flow information, even though it is not accomplished in improving OD demand estimation accuracy.

Table 4.5 Benchmark comparison for sensor location and OD estimation problems

Consideration of OD demand	Optimum traffic sensor locations	Period	Percentage of reduction in variance (%)	MAPE (%)
Model I (Hu et al., 2015)	Point: [7,13] AVI: [5,6,14]	h_1	5.01	20.85
		h_2	3.94	32.47
		h_3	3.26	29.34
		Average	4.07	27.55
Model II (Simonelli et al., 2012)	Point: [3,5,6, 7,10,12,13,14]	h_1	**79.31**	16.59
		h_2	14.12	28.16
		h_3	9.86	24.23
		Average	34.43	22.99
Model III (Fu et al., 2019)	Point: [1,3,6, 9,11,12,13,14]	h_1	41.79	**5.42**
		h_2	12.43	26.78
		h_3	10.17	23.05
		Average	21.46	18.42
Model IV **(this chapter)**	Point: [3,5] AVI: [2,15,16]	h_1	76.08	12.24
		h_2	71.15	11.12
		h_3	49.11	6.27
		Average	**65.45**	**9.88**

In summary, when traffic managers intend to make sufficient use of the information observed from installed traffic sensors in different time periods, especially including congested peak hour periods, the proposed model with considering covariance of multi-period OD demand should be chosen with priority over the other existing sensor location models.

4.6.1.3 Effects of traffic congestion on the multi-period OD demand estimation

As explained in section 4.6.1.2, the proposed multi-period model outperforms the single-period model in its own period of h_1 because of the strong correlation among multi-period OD demands, especially during the congestion periods in the daytime. To numerically justify this explanation, a supplementary experiment for multi-period SLP

under uncongested conditions is conducted for comparison purposes. To imitate the uncongested conditions such as in the mid-night period denoted as h'_1, the mean and coefficient of correlation of original OD demand in the period of h_1 is reduced by five times to decrease the magnitude and correlation relationship of OD demand.

Table 4.6 SLP for one period vs. SLP for multiple periods under uncongested conditions

Consideration of OD demand	Period	MAPE (%)
Existing model: One-period SLP	h'_1	**25.71**
Proposed model: Multi-period SLP	h'_1	34.64
	h_2	13.17
	h_3	18.25
	Average	**22.02**

Table 4.6 illustrates that under the specified set of traffic conditions, the MAPE of OD demand estimates during time period h'_1 in the proposed model is 34.64%, which is larger than that from the existing model (i.e., 25.71%). This result confirms the justifications in the preceding subsection 6.1.2, in which when the multi-period correlation relationship is very weak, the single-period model outperforms the multi-period model in its own period of h'_1. Furthermore, Table 4.6 proves again that regardless of traffic conditions, the proposed model considering multi-period OD demand outperforms the existing model by improving the average accuracy of the multi-period OD demand estimation regarding MAPE.

4.6.2 A medium-size transportation network: Example 2

Due to the explicit consideration of multi-period OD demands, PCA is adopted to extract the essential features of the OD demands so as to improve the effectiveness of the solution algorithm. The proposed methods are particularly suitable for a road network with a large number of OD pairs.

As shown in Figure 3.8 of Chapter 3, the Sioux Falls network, including 76 links and 24 nodes with consideration of 48 OD pairs, is adopted. The corresponding origin and destination nodes are marked with the same color. The periods of interest are the same as those in Example 1 of this chapter. The OD demands in these three periods for each OD pair are set to be 300 veh/hour, 200 veh/hour, and 120 veh/hour, respectively. Other parameters are assumed to be identical to those in Shao et al. (2014). The penetration rate of tagged vehicles detected by AVI sensors is supposed to be 45%. It is assumed that this road network is already equipped with four AVI sensors on links 1, 38, 43, and 70, and four point sensors on links 11, 20, 40, and 62.

4.6.2.1 Efficiency of multi-type traffic sensors for OD demand estimation

Recall Proposition 4.2, in which the decision to prioritize AVI sensors or point sensors is determined by the value of additional information obtained when installing these two traffic sensor types, given their relative costs. To provide insight into this proposition clearly and intuitively, the trade-off between AVI sensors and point sensors is examined in this experiment.

In practice, given realistic sensor cost and physical environments, it is difficult to guarantee that an additional AVI sensor can consistently outperform the equivalent number of additional point sensors concerning OD demand estimation accuracy. Therefore, the efficiency of combining the observations from point sensors and AVI sensors should be further tested. This experiment assumes that the standard deviations of the measurement errors for point sensors and AVI sensors are 5% and 2.5%, respectively, of the corresponding true traffic flows (Zhou and List, 2010). The unit cost of an AVI sensor and a point sensor is assumed to be β' = United States dollars (US$)6,500 and β = US$1,300, respectively. In other words, the unit cost of an AVI sensor is five times that of a point sensor. The optimal number and locations of AVI

sensors and point sensors are determined by different total budgets based on the proposed models.

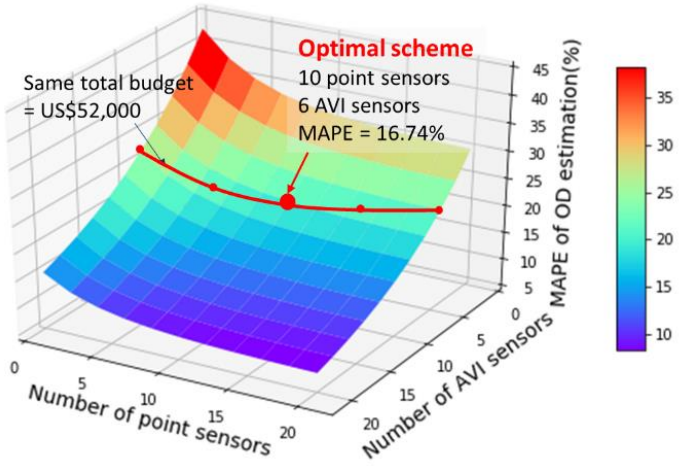

Figure 4.4 Efficiency of the combination of point sensors and AVI sensors

From Figure 4.4, it can be seen that when the total budget is US$52,000, the optimal traffic sensor location scheme includes 10 point sensors and 6 AVI sensors. The MAPE of OD estimation is then 16.74%, which is the smallest among all location schemes with the same total budget. However, for schemes with only AVI or point sensors, OD estimation accuracy (e.g., 28.81% MAPE for AVI sensors and 20.04% for point sensors) is poorer than that for the combination of information from both types of sensors. The results imply that when measurement errors of AVI and point sensors do not substantially differ, a combination of information from both types leads to a more accurate OD estimation in multiple periods, with smaller MAPE.

4.6.2.2 Sensitivity analysis of the cost ratio between point and AVI sensors

It has been presented in section 4.6.2.1 that the optimum number and type of traffic sensors are highly dependent on their measurement errors. In addition, because the total budget is usually given and fixed, the cost ratio between AVI and point sensors can also affect the budget allocation for the number of each sensor type. Practically,

AVI sensors are normally more expensive than point sensors, as they provide more information and are more reliable. Therefore, the effects of the cost ratio between these two sensor types should be examined to rationalize the budget allocation for the number of each sensor type.

In this experiment, the unit cost of a point sensor is assumed to be fixed (i.e., $\beta = US\$1{,}300$). The unit cost of an AVI sensor varies from $\beta' = US\$1{,}300$ to $\beta' = US\$9{,}100$ so that the cost ratio ranges from 1:1 to 1:7. The total budget is $B = US\$31{,}200$. The proposed model is used for different cost ratios between point and AVI sensors to optimize the number of multi-type traffic sensors and obtain the OD demand estimation results. The MAPEs of the resultant OD demand estimates based on different cost ratios are compared in Table 4.7.

Table 4.7 Effects of cost ratio between point and AVI sensors

Cost ratio (point/AVI)	Optimal number of sensors		MAPE (%)
	Number of point sensors	Number of AVI sensors	
1:1	0	24	**4.08**
1:3	6	6	9.17
1:5	9	3	13.61
1:7	24	0	17.93

It is plausible to witness from Table 4.7 that when the AVI sensor is as cheap as the point sensor, only high accuracy AVI sensors need to be installed in the road network and contribute to the highest OD demand estimation accuracy with a MAPE of 4.08%. The estimation accuracy regarding MAPE decreases monotonically with the increment of AVI sensor cost. It is also interesting to discover that the cost ratio between point and AVI sensors smaller than 1/7 makes AVI sensors unattractive under the specified settings. These findings can generally help public agencies better understand the priority of different sensor types on the basis of their cost ratio, especially for multi-period OD demand estimation.

4.6.2.3 Sensitivity analysis of the number of principal OD demand components

The sections above have shown that consideration of covariance in multiple periods can provide additional information for OD demand estimation. To make full and proper use of this additional valuable information, the PCA method is adopted in this chapter to improve the effectiveness of the proposed model. However, the number of principal OD demand components must be predetermined. This predetermined variable can also affect the estimation results. Thus, a sensitivity test of the number of principal OD demand components is conducted to elucidate the effectiveness of the PCA method, as presented in Table 4.8.

In this experiment, it is supposed that four additional point sensors and four additional AVI sensors are to be installed in the road network to cooperate with eight existing traffic sensors. The contribution of the principal OD demand components is calculated as total variances of the selected number of principal OD demand components divided by that of the original OD demands (Jolliffe, 2002).

As can be found from Table 4.8 that with an increasing number of principal OD demand components, the contribution of those components, percentage of reduction in variance, and the computation time all increase, whereas the MAPE decreases monotonically. However, when the number of principal OD demand components increases from 82 to 144, the percentage of reduction in variance does not increase substantially (i.e., from 79.35% to 86.13%). The decrease of MAPE from 7.03% to only 6.10% is much smaller than in the other cases. This small change indicates that when the number of principal OD demand components is large enough, the PCA-based model can guarantee an optimum sensor location scheme and maintain a satisfying level of estimation accuracy.

Table 4.8 Effectiveness of PCA for the Sioux Falls network

Number of principal OD demand components	Contribution of principal OD demand components	Optimum traffic sensor locations	Percentage of reduction in variance (%)	MAPE (%)	Computation time (s)
25	36.11%	Point: [3,14,45,51] AVI: [5,30,39,66]	21.54	27.14	2,083
50	72.15%	Point: [2,21,44,73] AVI: [10,17,29,60]	53.09	17.66	2,608
82	96.20%	**Point: [2,7,44,51]** **AVI: [10,30,33,61]**	**79.35**	**7.03**	3,705
144	100.00%	**Point: [2,7,44,51]** **AVI: [10,30,33,61]**	**86.13**	**6.10**	12,611

It is also worth noting that the optimum traffic sensor location scheme ceases to change when the number of OD demand components reaches 82. In this scheme, the point sensors and AVI sensors are located on links 2, 7, 44, and 51, and links 10, 30, 33, and 61. However, computation time increases dramatically with the increasing number of OD demand components, significantly exceeding 82. This experiment reveals that even though the PCA-based OD estimation method may lead to partial information loss in multi-period OD demand, it can contribute to sufficiently accurate estimates and significantly reduce computation time while guaranteeing an optimal scheme of multi-type traffic sensors.

4.6.3 A transportation network in Hong Kong: Example 3

This numerical example demonstrates the effects of travel behavior patterns on multi-type traffic sensor locations and multi-period OD demand estimation results using empirical data in the real world. The Tuen Mun Road Corridor Network in Hong Kong (Figure 4.5) is used herein as the study network. The road network consists of 487 links, 382 nodes, and 18 zones. These 18 zones include two external zones (S1 and S2) and 16 internal zones (S3-S18) and can be either origins or destinations. Tuen Mun Road (TMR) is an expressway with a higher speed limit than Castle Peak Road (CPR),

a rural road. The internal zones S3-S18 connect only to Castle Peak Road. In this road network, 19 Autoscope point sensors have been installed by the Transport Department in Hong Kong to detect traffic flow and travel speed by time of day and day of the year. The weekday morning peak hour and weekday evening peak hour are the two time periods considered in this experiment.

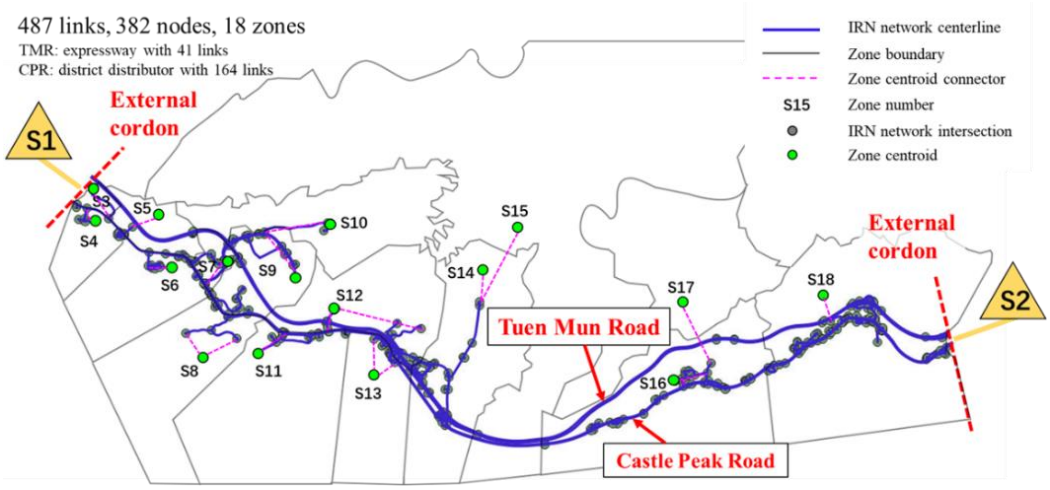

(a) Tuen Mun Road Corridor Network

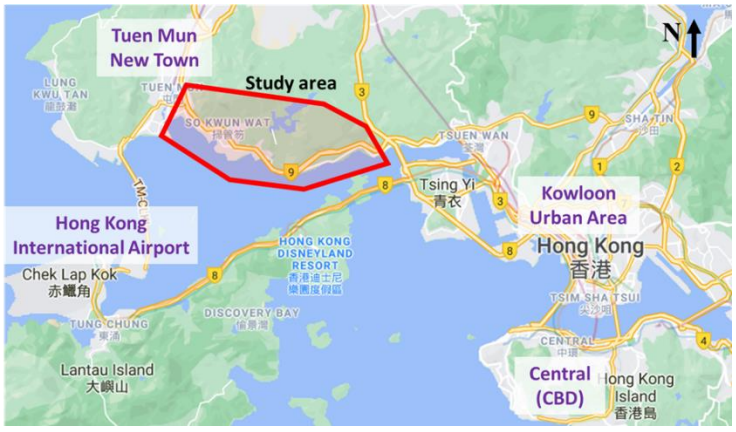

(b) Hong Kong map © Google Maps

Figure 4.5 Example 3 network: Tuen Mun Road Corridor Network in Hong Kong

In this experiment, prior OD demand is obtained from the Base District Traffic Modal data issued by the Hong Kong Transport Department (Transport Department, 2004)

and updated using Autoscope point sensors (e.g., control total at external cordons). "True" OD demand is estimated from the data obtained from all available Autoscope point sensors. In the study road network, nine different link speed-flow curves by link type are calibrated using hourly flow rate and hourly average speed detected by Autoscope point sensors. For instance, Figure 4.6(a) and Figure 4.6(b) show two of these speed-flow curves on Tuen Mun Road and Castle Peak Road calibrated by the data from Autoscope point sensors TMR-19 and CPR-3, respectively. For the link installed with sensor TRM-19, it is found that the capacity is 1,408 veh/hour/lane, and the free flow speed is 70 km/hour. For the location installed with sensor CPR-3, the capacity and free flow speed are 943 veh/hour/lane and 50 km/hour, respectively.

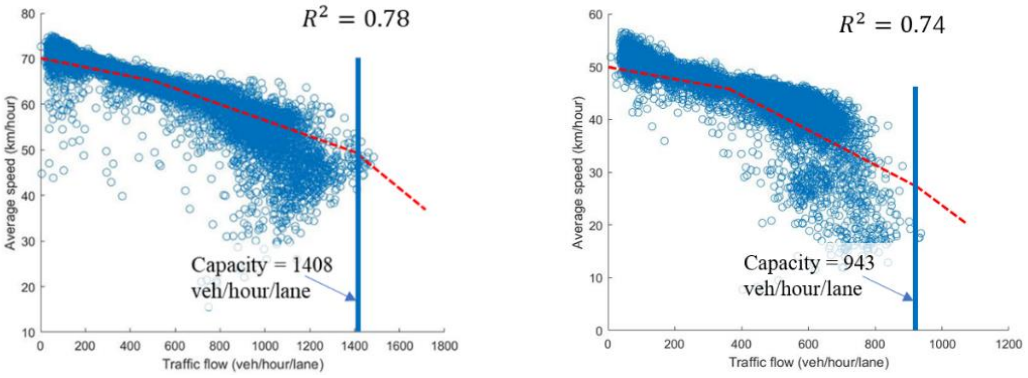

(a) Autoscope point sensor TMR-19 (b) Autoscope point sensor CPR-3

Figure 4.6 Speed-flow curves calibrated by data observed from Autoscope point sensors

In this road network, Tuen Mun New Town (S1) and Kowloon Urban Area (S2) primarily serve as residential and commercial areas, respectively. Some primary schools and kindergartens are located in internal zones S3-S18. Most traffic demand travels from zone S1 to zone S2 in the morning peak hour, while from zone S2 to zone S1 in the evening peak hour.

4.6.3.1 Effects of joint travel behavior on traffic sensor location problem

As illustrated in the motivating example, joint travel behaviors significantly impact

OD demand covariance in multiple periods. Consider the travel pattern of a spouse and child similar to the motivating example. Two scenarios (i.e., with and without joint travel behaviors) can be established in the morning peak hour. (i) Without joint travel behaviors, the spouse will drive alone from home to the office (S1-S2), and the child will go to school by public transport (only one OD demand from S1 to S2 is generated in this scenario). (ii) With joint travel behaviors, the spouse will drive the child to the school first (S1- an internal zone) and then go on to the office alone (an internal zone – S2) (two OD demands, i.e., one from S1 to the internal zone, the other from the internal zone to S2, will be generated by such joint travel behavior).

The joint travel behaviors can be approximately measured using vehicle occupancy data. According to the report in ‘‘The Annual Traffic Census 2017’’ of Hong Kong (Transport Department, 2018), vehicle occupancy fluctuates from time to time. As only one sensor in the study area can provide the vehicle occupancy data, it is assumed that vehicle occupancy in the study area remains the same when illustrating the effects of joint travel behavior. In principle, if there is a need to obtain more precise vehicle occupancy data by time and location, a roadside survey can be conducted.

As shown in Chapter 3.1, the relationship between the covariance of OD demand and the proportion of joint travel behavior of total demands can be theoretically calculated as in Eq. (3.1). It can be seen from Eq. (3.1) that the more joint travel behaviors, the larger the covariance of OD demand between the corresponding OD pairs. Due to the lack of empirical data on the covariance of OD demand, Eq. (3.1) is used to simulate the prior OD demand covariance based on the proportion of joint travel behaviors.

To demonstrate the effects of travel behavior patterns, the proposed model is implemented under different proportions of joint travel behavior. In this experiment, given the target OD demand estimation accuracy (e.g., MAPE = 10%), the objective

is to determine the number and locations of traffic sensors under different proportions of joint travel behavior.

Table 4.9 shows that to satisfy the target OD demand estimation accuracy, more traffic sensors are needed in view of the increasing number of joint travel behaviors conducted by travelers. It indicates that with more joint travel behaviors, more information is required for the estimation of both the mean and covariance of OD demand. Therefore, more traffic sensors should be installed to achieve similar accuracy in OD demand estimation.

Table 4.9 Effects of joint travel behavior on optimal number and locations of traffic sensors

Proportion of joint travel behavior	Optimal number of sensors in total	Optimal traffic sensor location scheme	
		Number of sensors on CPR	Number of sensors on TRM
0%	19	6	13
30%	24	12	12
50%	29	19	10
100%	41	33	8

Table 4.9 also indicates that when the proportion of joint travel behavior increases in this specific study network, more traffic sensors should be installed on Castle Peak Road. The topology of the study network could explain this finding. Note that the internal zones (S3-S18) are only connected to Castle Peak Road, a rural road. As joint travel behaviors will increase the traffic flow on Castle Peak Road (to the internal zones), the covariance between the OD demands of external zone S1 to internal zones (S3-S18) and internal zones to external zone S2 will be enlarged. Thus, more traffic sensors on Castle Peak Road are needed to reduce the uncertainty of the estimated OD demands.

4.7 Summary

The research in this chapter proposes a new model for optimizing multi-type traffic sensor locations with a particular emphasis on both spatial and temporal covariance relationships of OD demand. Due to the within-day and day-to-day variations of traffic demands, the multi-period OD demands are statistically correlated with one another. The effects of OD demand covariance, especially in multiple hourly periods, have become increasingly significant in multi-type SLPs with multi-source data under the big data arena.

By leveraging sensor data from multiple sources, the uncertainty of multi-period OD demand estimates can be minimized. The dominant OD demands, i.e., those exhibit the greatest dynamics, can be extracted by an adapted PCA method from the covariance of OD demand in multiple periods. Relying on the dominant OD demands, a multi-type sensor location model is proposed by minimizing the estimation uncertainty of the resultant multi-period OD demand. The estimation uncertainty is measured by the trace of the OD demand covariance matrix. Two propositions of the proposed model have been extensively analyzed to show that: (i) the superiority by taking into account the covariance of OD demand in multiple periods, and (ii) the trade-off between AVI and point sensors.

Several case studies using a synthetic road network and a real road network in Hong Kong with empirical data were presented in Section 4.6 to illustrate the merits and efficiency of the proposed model. The case studies suggest that traffic planners consider the multi-period covariance relationship of OD demand, particularly in congestion periods, when designing a multi-type traffic sensor network.

The results presented in Chapters 3 and 4 reveal that the spatial and temporal

covariance of OD demand can be used to enhance the deployment of traffic sensors for strategic planning purposes. Apart from traffic demands, vehicular travel times also take a vital role to benefit travelers better understand the traffic condition and congestion levels. In addition, traffic sensors can normally provide not only traffic flow information but also travel time (or travel speed) information. To fully utilize observations from multi-type traffic sensors, it needs an integrated traffic sensor location model to benefit both OD demand and link travel time estimations. This integrated model will be studied in Chapter 5.

Therefore, the following Chapter 5 is to investigate multi-type SLPs for simultaneous estimation of stochastic link travel times and OD demands. Based on these results, traffic planners can easily deploy efficient sensor systems to monitor traffic conditions and assess congestion levels in the road network with uncertainty.

5. Optimization of multi-type sensor locations for simultaneous estimation of origin-destination demands and link travel times with covariance effects

It is demonstrated in Chapters 3 and 4 that the SLP for estimation of vehicular traffic demands by OD pairs has been widely used in strategic transport models and intelligent transportation systems. Initially installed for OD estimation, these traffic sensors can provide additional information for link travel time estimation to assess the road network performance. Such a link travel time estimator is traditionally based on single-source traffic data (e.g., point sensor data) at the selected location(s) only. However, multi-source data are now available and can be used for network-wide travel time estimation and OD estimation by installing different types of traffic sensors on the study road networks.

Chapter 5 investigates the multi-type traffic SLP for estimating OD demands and link travel times simultaneously while considering two sources of spatial covariance effects with uncertainties, as highlighted in Table 2.3. The first source is the statistical correlation of the vehicular traffic demands for different OD pairs in a typical hourly period (e.g., morning peak hour) on a daily scale, as the travel activity patterns vary from day to day over the year. The second source is the stochastic nature of the link travel times on different road links during the peak hour period and their correlation with adjacent links in congested conditions. By considering these aspects, a novel model is formulated to optimize the number and locations of multi-type traffic sensors.

Based on the integrated observations from multi-type traffic sensors, a KL divergence-based model is developed to accommodate different probability distributions of OD demands and link travel times in various traffic conditions. Numerical examples of

synthetic and real-world road networks are used to illustrate the applications and merits of the developed multi-type sensor location model for simultaneously estimating the stochastic OD demands and link travel times.

The remainder of this chapter is structured as below. Section 5.1 introduces the SLPs related to link travel time estimation and OD demand estimation. The problem statement and model assumptions are presented in section 5.2. Section 5.3 describes the novel model proposed for estimating stochastic OD demands and link travel times and solving multi-type SLPs. A solution algorithm that efficiently solves the SLP is developed in section 5.4. Section 5.5 displays numerical results for synthetic and real-world road networks to demonstrate the advantages of the proposed model and solution algorithm. Section 5.6 summarizes the research in this chapter.

5.1 Background

5.1.1 Contributions

The four key contributions (**C1**–**C4**) of the research described in this chapter are as follows:

C1. A novel measurement method incorporating the covariances of OD demands and link travel times is developed to reflect the variability (uncertainty) in day-to-day OD flow and link travel time estimates in the same hourly period over a year. The relationship between the mean values of the link flow and link travel time and that between the covariances of link flow and link travel time are examined, which enables the integration of stochastic OD demand and link travel time estimates.

C2. The multi-type sensor location model is extended by minimizing the variability (uncertainty) of OD demand and link travel time estimates, and considering the tradeoffs between various sensor types in the context of budget constraints. Numerical

examples are presented to demonstrate that the conventional models are a special case of the developed model. Thus, based on a generalized model, the accuracies of the stochastic OD demand and link travel time estimates can be increased.

C3. A novel model is developed based on the KL divergence, as an extension of the traditional GLS and EM models, that simultaneously estimates the stochastic OD demands and link travel times for any probability distribution. Unlike the models described by Ma and Qian (2018) and Zhu et al. (2019), this KL divergence-based optimization model determines (i) OD demands and link travel times for various distributions in different traffic conditions, (ii) addresses the inconsistency between different dimensions, and (iii) reveals the connection between stochastic OD demand and link travel time.

C4. An improved variant of the FA is developed as a metaheuristic algorithm to efficiently solve the considered optimization problem: a nonconvex integer-programming problem. The search strategy of the improved FA algorithm is enhanced by using an adaptive parameter that can be iteratively updated, as this enables a near-to-global optimum to be obtained and ensures rapid convergence.

The three advantages of KL divergence-based methods are summarized.

(i) The developed KL divergence-based model can be flexibly applied in various traffic conditions involving different probability distributions of traffic measures. In contrast, the commonly used GLS approach can only be applied when the approximation error is normally distributed, as its application may lead to biased results when other types of distributions exist (Olsson et al., 2000). In practice, the distribution of traffic parameters varies with traffic conditions, and travel times generally follow Gaussian and log-normal distributions in clear and congested conditions, respectively (Li et al., 2006b). Therefore, the KL divergence can be used to consider various traffic

conditions.

(ii) The dimensionless property of KL divergence can help to avoid inconsistency problems, especially when different traffic information (such as OD demands and link travel times) are considered in the objective function for solving the SLP. Furthermore, stochastic features, such as variance, skewness, and kurtosis can be incorporated into the KL divergence-based method.

(iii) The novel model developed in this chapter can be used to simultaneously estimate stochastic OD demands and link travel times by examining the relationship between the mean and covariance values of link flows and link travel times. In addition, the model does not simply integrate the various features obtained using existing models. Rather, the model clarifies the relationship between the mean traffic flow and mean travel time and that between the covariance of the link flow and link travel time. This relationship is achieved by using a stochastic Bureau of Public Roads (BPR) link performance function as a constraint or condition for simultaneously estimating the stochastic OD demands and link travel times.

5.2 Problem statement and model assumptions

5.2.1 Problem statement

The multi-type sensor location optimization problem is examined to estimate the stochastic OD demands and link travel times in a road network. As shown in Figure 5.1, the framework consists of two stages: the first stage is the development of a multi-type traffic sensor location model; and the second stage is the development of a model for simultaneously estimating stochastic OD demands and link travel times.

The first stage involves the development of the multi-type traffic sensor-location

model, whose inputs are the network topology, the prior OD demands, and the prior link travel time information. The locations of multi-type sensors are selected based on the topology of the road network and updated in accordance with the estimations of the OD demands and link travel times obtained in the second stage. Based on the multi-type traffic sensors, the travel times and traffic flows on the links with point sensors and the path travel times between any two installed AVI sensors are observed.

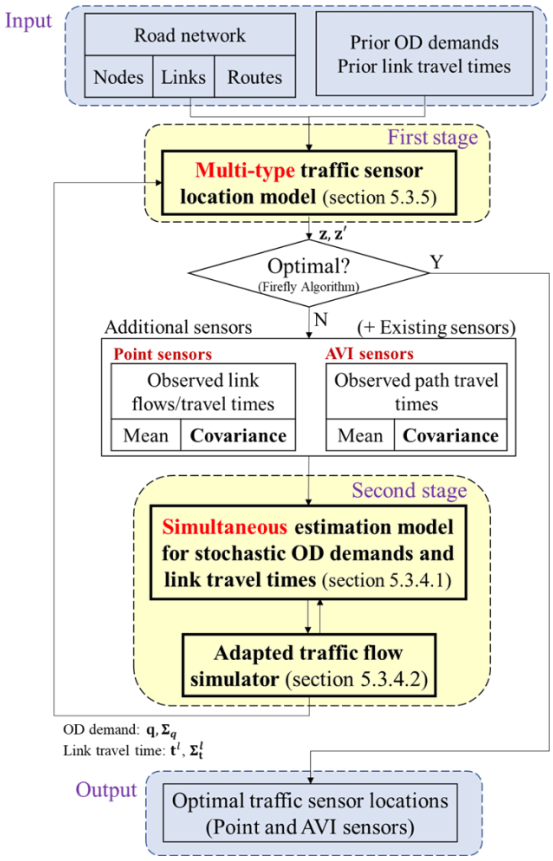

Figure 5.1 Flowchart of the proposed models

The second stage involves the development of a bi-level model to estimate stochastic OD demands and link travel times. The upper level of the model combines the observations from point and AVI sensors (i.e., the link flow/travel times and path travel times) to estimate the stochastic OD demands and link travel times for a fixed proportion of links/path choices. The upper-level model uses the KL divergence-based optimization to achieve this simultaneous estimation task while also considering

covariance effects and alleviating the inconsistency between the OD demands and link travel times due to their different dimensions. The lower level of the model—an adapted traffic flow simulator—uses the estimated OD demands to update the link/path choice proportions. The traffic flow simulator is adapted from the stochastic user equilibrium traffic assignment model developed by Lam and Xu (1999).

The output of the bi-level model consists of the mean and covariance of estimated OD demands and link travel times. The uncertainties (variances) in the OD demand and link travel time estimates measured by the trace of the var–cov matrix serve as a feedback mechanism that updates the sensor location scheme determined in the first stage. The application of this feedback mechanism and iterative updates enables the determination of locations for multi-type sensors to afford data that minimizes the uncertainties in the stochastic OD demand and link travel-time estimates.

5.2.2 Model assumptions

To facilitate the presentation of the core concepts of proposed models, the model formulation and numerical studies are based on the following six assumptions (**A1**–**A6**), without loss of generality.

A1. The covariance of OD demands refers to the spatial covariance relationship between different OD pairs within the same time period. In this chapter, the vehicular traffic in a single time period (i.e., the morning peak hour) on a daily scale over a year is considered. In general, for transport planning, traffic planners primarily focus on the most congested period in a day (e.g., the morning peak hour) (Shao et al., 2014; Ma and Qian, 2018).

A2. The variations of link flow/link travel time result only from the variation of recurrent OD demands on a daily scale. Other factors such as network supply

uncertainties (e.g., traffic incidents, adverse weather conditions) are not considered in this chapter (Shao et al., 2014; Ma and Qian, 2018).

A3. Point sensors, such as microwave radar detectors, are located on links (i.e., road segments) in a road network, and AVI sensors are located on nodes (i.e., junctions or intersections) in a road network (Park and Haghani, 2015).

To ensure that the sensor location model can be applied to different types of point sensors and road networks, it is assumed that point sensors can detect the link flow and speed in one direction over a link equipped with a sensor (Li et al., 2006a). AVI sensors can observe the path travel time for tagged vehicles moving in different directions between each pair of AVI sensors installed at both ends of a path. The cost of an AVI sensor depends on the number of directions covered by a chosen node.

A4. All of the observed data (i.e., link flows, link travel times, and partial path travel times) are error-free (Yang et al., 1991; Simonelli et al., 2012), and missing data is not considered in this chapter.

A link travel time can be inferred from the vehicle speed detected by a point sensor (Li et al., 2006a; Xing et al., 2013; Gentili and Mirchandani, 2018). AVI sensors such as RFID readers and ALPR cameras can correctly identify tagged vehicles without generating matching errors (Zhou and List, 2010). Sufficient samples of AVI data are available to obtain travel time information for the peak-hour periods on a path with AVI sensors installed at both ends.

A5. The link choice proportion is deterministic and varies with the OD demands on a daily scale (Shao et al., 2014; Yang et al., 2019). The link choice proportion is the ratio of the mean link flow to the mean OD demands associated with the considered link and can be updated by traffic assignment models. In practice, additional data sources such as probe vehicle data can be used to partially update the link choice proportions

on certain links with observed data (Guo et al., 2019).

A6. The path set is known prior to the assignment process. To alleviate the problem of the independence of irrelevant alternatives in the logit-based model, paths for a specific OD pair are generated with as low a similarity (e.g., as few overlapped links) as possible (Akamatsu, 1996; Shao et al., 2014).

5.3 Model formulation

A road network is defined as $\mathbf{G} = (\mathbf{N}, \mathbf{A})$, where **N**, sized $|\mathbf{N}|$, and **A**, sized $|\mathbf{A}|$, are the sets of nodes and links, respectively. The observed link set is $\widetilde{\mathbf{A}}$ ($\widetilde{\mathbf{A}} \subseteq \mathbf{A}$), sized $\left|\widetilde{\mathbf{A}}\right|$ in which the link flow and travel time can be observed by point sensors. Let *n* be a specific node in the road network ($n \in \mathbf{N}$). $\mathbf{W}_r$ represents a set of node pairs in which w_r is a node pair, and $\widetilde{\mathbf{W}}_r$ is a set of observed node pairs with AVI sensors installed on both end nodes. If two nodes in $\mathbf{W}_r$ are the origin and destination nodes, they can be considered an OD pair expressed as $\mathbf{W}$ ($\mathbf{W} \subseteq \mathbf{W}_r$), sized $|\mathbf{W}|$. Moreover, the path set for the road network is $\mathbf{K}$ (sized $|\mathbf{K}|$). $\widetilde{\mathbf{K}}$ (sized $\left|\widetilde{\mathbf{K}}\right|$) represents an observed path set, in which the travel times for vehicles equipped with AVI tags can be observed. In addition, the non-empty path set for node pair w_r is $\mathbf{K}_r$. All variables are defined when they first appear in the text.

5.3.1 Observed day-to-day link flow, link travel time, path travel time

Using point sensors, link flows can be observed for the same peak-hour period on weekdays. In this chapter, the links with and without a point sensor are referred to as the "observed link" and "unobserved link", respectively. Suppose that the link flow in the peak-hour period (e.g., between 8:00 a.m. and 9:00 a.m.) is observed on a sequence of (not necessarily consecutive) weekdays. Denote $\tilde{v}^{l}_{a(d)}$ as a sample of observations corresponding to the average hourly traffic flow on link *a* ($a \in \widetilde{\mathbf{A}}$) in the morning peak-

hour on day d ($d = 1,2,3,\ldots,D$). A superscript "l" represents the information on links. For convenience, a column vector $\tilde{\mathbf{v}}_{(d)}^{l} = (\ldots, \tilde{v}_{a(d)}^{l}, \ldots)^{T}$ represents the traffic flow for all $a \in \widetilde{\mathbf{A}}$. The day-to-day sample mean of link flows on the observed links in the morning peak-hour over a year ($\tilde{\mathbf{v}}^{l}$) can be calculated by (3.2). The day-to-day sample var–cov matrix of the observed link flows between different links in the morning peak-hour over a year can be calculated by Eq. (3.3).

In addition to the link flow, the average hourly link travel times on the observed links in the peak-hour period can be determined based on assumption **A4** (Xing et al., 2013; N. Zhu et al., 2018). $\tilde{t}_{a(d)}^{l}$ represents a sample of the observed link travel time corresponding to the mean travel time on link a ($a \in \widetilde{\mathbf{A}}$) in the peak-hour period on day d. The observational window is restricted to an hour, although it can be easily extended to other time intervals. For convenience, a column vector $\tilde{\mathbf{t}}_{(d)}^{l} = (\ldots, \tilde{t}_{a(d)}^{l}, \ldots)^{T}$ is defined for all $a \in \widetilde{\mathbf{A}}$. The day-to-day sample mean of the link travel times on the observed links in the peak-hour period on a daily scale can be calculated by:

$$\tilde{\mathbf{t}}^{l} = (\ldots, \tilde{t}_{a}^{l}, \ldots)^{T} = \frac{1}{D}\sum_{d=1}^{D} \tilde{\mathbf{t}}_{(d)}^{l}, \tag{5.1}$$

where $\tilde{\mathbf{t}}^{l}$ is a column vector of the sample mean travel time on all observed links, and $\tilde{t}_{a}^{l}$ represents the observed mean travel time on link a ($a \in \widetilde{\mathbf{A}}$).

Similarly, the day-to-day sample var–cov matrix of the observed travel time between different links in the peak-hour period over a year can be calculated by:

$$\tilde{\mathbf{\Sigma}}_{t}^{l} = (\tilde{\sigma}_{t_a, t_{a'}}^{l})_{\tilde{m}\times\tilde{m}} = \frac{1}{D-1}\sum_{d=1}^{D} \{(\tilde{\mathbf{t}}_{(d)}^{l} - \tilde{\mathbf{t}}^{l})(\tilde{\mathbf{t}}_{(d)}^{l} - \tilde{\mathbf{t}}^{l})^{T}\}, \tag{5.2}$$

where $\tilde{\sigma}_{t_a, t_{a'}}^{l}$ is the sample covariance between travel times on observed links a and a' ($a, a' \in \widetilde{\mathbf{A}}$).

Based on assumption **A3**, AVI sensors must be installed on the nodes of a road network to detect the path travel times by recognizing the vehicle information at the start and end points of paths. Consider a general case in which multiple paths may be used by different travelers between a node pair. The mean travel time between nodes with AVI sensors can be determined for all detected vehicles in the observational window. According to Eq. (5.1), the day-to-day sample mean of travel times between node pairs in the study period ($\tilde{\mathbf{t}}_{w_r}$) can be calculated by:

$$\tilde{\mathbf{t}}_{w_r} = \frac{1}{D}\sum_{d=1}^{D}\tilde{\mathbf{t}}_{w_r(d)}\,, \tag{5.3}$$

where $\tilde{\mathbf{t}}_{w_r(d)}$ is the column vector of sample travel times between all observed node pairs on day *d*.

Similar to Eq. (5.2), the day-to-day sample var–cov matrix of the observed travel times between different node pairs ($\tilde{\boldsymbol{\Sigma}}_t^{w_r}$) can be obtained as:

$$\tilde{\boldsymbol{\Sigma}}_t^{w_r} = \frac{1}{D-1}\sum_{d=1}^{D}\{(\tilde{\mathbf{t}}_{w_r} - \tilde{\mathbf{t}}_{w_r(d)})(\tilde{\mathbf{t}}_{w_r} - \tilde{\mathbf{t}}_{w_r(d)})^T\}\,. \tag{5.4}$$

In summary, the mean and covariance of the link flows and link travel times on the observed links can be determined from point sensor observations. The mean and covariance of the travel times between node pairs with AVI sensors on both ends can be calculated from AVI sensor observations. These observations serve as the input measurements for the estimation of the mean and covariance of the OD demands and link travel times on the unobserved links in the study network.

5.3.2 Mean and covariance of link flows and OD demands

In a road network, the relationship between the OD demand and path flows is given by:

$$q_w = \sum_{k \in \mathbf{K}_w} f_w^k \quad \forall w \in \mathbf{W}, \tag{5.5}$$

where q_w is the mean value of the traffic demand for OD pair *w*, and f_w^k is the mean path flow through path *k* in OD pair *w*. The path choice proportion is $p_{kw}^p = f_w^k / q_w$, which is the proportion of the traffic flow in OD pair w choosing path *k*.

The link flow on link *a* can be determined by summing the path flows through this link (Eq. (5.6)):

$$v_a^l = \sum_{w \in \mathbf{W}} \sum_{k \in \mathbf{K}} \delta_{ak} f_w^k \quad \forall a \in \mathbf{A}, \tag{5.6}$$

where v_a^l is the mean value of the traffic flow on link *a* ($a \in \mathbf{A}$), and δ_{ak} is the link-path incidence; $\delta_{ak} = 1$ if path *k* traverses link *a*; otherwise, $\delta_{ak} = 0$.

With $f_w^k = p_{kw}^p q_w$, the relationship between the mean link flow (v_a^l) and mean OD demand (q_w) can be established based on Eq. (5.6):

$$v_a^l = \sum_{w \in \mathbf{W}} \sum_{k \in \mathbf{K}} \delta_{ak} f_w^k = \sum_{w \in \mathbf{W}} \sum_{k \in \mathbf{K}} \delta_{ak} p_{kw}^p q_w \quad \forall a \in \mathbf{A}. \tag{5.7}$$

For simplicity, define $p_{aw}^l = \sum_{k \in \mathbf{K}} \delta_{ak} p_{kw}^p$ as the link choice proportion, which represents the proportion of traffic flow in OD pair *w* passing through link *a*. Therefore, the mean value of the link flow on link *a* is a function of link choice proportions and mean OD demands going through link *a* as shown in Eq. (3.4) in Chapter 3. The covariance between the link flows on links a and a' is a function of the link choice proportions and covariance between the OD demands associated with these links as shown in Eq. (3.5) in Chapter 3.

5.3.3 Mean and covariance of travel times between node pairs, path travel times, and link travel times

The travel time observed by AVI sensor pairs may be for different paths between the nodes with AVI sensors. Considering the uncertainty in path choice, the mean travel time between nodes (t_{w_r}) in the peak hour (which is potentially captured by an AVI sensor pair) can be expressed in terms of the probability-based path travel times (t_k^p) (Xing et al., 2013):

$$t_{w_r} = \sum_{k \in \tilde{\mathbf{K}}_r} p_{kw_r}^p t_k^p \quad \forall w_r \in \mathbf{W}_r, \tag{5.8}$$

where $p_{kw_r}^p$ is the path choice proportion, i.e., the proportion of vehicular traffic flow in node pair w_r choosing path k, and t_k^p is the path travel time. t_k^p can be expressed as the sum of the link travel times (t_a^l) of the links along path k:

$$t_k^p = \sum_{a \in \mathbf{A}} \delta_{ak} t_a^l \quad \forall k \in \mathbf{K}_r, \tag{5.9}$$

The covariance of the travel times between different node pairs over the peak-hour period ($\sigma_{t_{w_r}, t_{w_{r'}}}$) can be decomposed into the covariances of the path travel times ($\sigma_{t_k, t_{k'}}^p$) and link travel times ($\sigma_{t_a, t_{a'}}^l$), as:

$$\sigma_{t_{w_r}, t_{w_{r'}}} = \sum_{k \in \tilde{\mathbf{K}}_r} \sum_{k' \in \tilde{\mathbf{K}}_r} p_{kw_r}^p p_{k'w_{r'}}^p \sigma_{t_k, t_{k'}}^p \quad \forall w_r, w_{r'} \in \mathbf{W}_r, \tag{5.10}$$

and

$$\sigma_{t_k, t_{k'}}^p = \sum_{a \in \mathbf{A}} \sum_{a' \in \mathbf{A}} \delta_{ak} \delta_{a'k'} \sigma_{t_a, t_{a'}}^l \quad \forall k, k' \in \mathbf{K}_r. \tag{5.11}$$

For convenience, the order of the links can be rearranged such that the observed links are placed first. The network-wide link travel times and corresponding var–cov matrix can be partitioned based on the links with and without point sensors:

$$\mathbf{t}^l = [\mathbf{t}_o^{l\,T}, \mathbf{t}_u^{l\,T}]^T, \tag{5.12}$$

and

$$\mathbf{\Sigma}_t^l = \begin{bmatrix} \mathbf{\Sigma}_{t_o}^l & \mathbf{\Sigma}_{t_o, t_u}^l \\ \mathbf{\Sigma}_{t_u, t_o}^l & \mathbf{\Sigma}_{t_u}^l \end{bmatrix}, \tag{5.13}$$

where $\mathbf{t}^l$ is the vector of the travel times on all links in the road network; $\mathbf{t}_o^l$ and $\mathbf{t}_u^l$ represent vectors of the travel times on observed and unobserved links, respectively; $\mathbf{\Sigma}_{t_o}^l$ and $\mathbf{\Sigma}_{t_u}^l$ denote the var–cov matrices of the travel times between the observed links and between unobserved links, respectively; and $\mathbf{\Sigma}_{t_u, t_o}^l$ and $\mathbf{\Sigma}_{t_o, t_u}^l$ are the matrices (transpose of each other) whose elements are the covariances of the travel times between observed and unobserved links.

5.3.4 Bi-level model for the estimation of stochastic OD demands and link travel times

5.3.4.1 Upper-level model: simultaneous estimation of stochastic OD demands and link travel times

To fully exploit the various types of traffic information available from multi-type sensors under different traffic conditions, as discussed in contribution **C3**, a KL divergence-based method is developed to estimate the stochastic OD demands and link travel times. The KL divergence indicates the difference between two distributions described by probability density functions (pdfs). The standard KL divergence between two pdfs, $D_{KL}(.||.)$, is defined as:

$$D_{KL}(f_{\mathbf{X}}(\mathbf{x}) \| g_{\mathbf{Y}}(\mathbf{y})) = \int_{\mathbb{R}^M} f_{\mathbf{X}}(\mathbf{x}) \log \frac{f_{\mathbf{X}}(\mathbf{x})}{g_{\mathbf{Y}}(\mathbf{x})} d\mathbf{x}, \tag{5.14}$$

where $\mathbf{X}, \mathbf{Y} \in \mathbb{R}^M$ are two random vectors with pdfs $f_{\mathbf{X}}(\mathbf{x})$ and $g_{\mathbf{Y}}(\mathbf{y})$, respectively, which have the same support.

Eq. (5.14) can be rewritten in the following entropy form:

$$D_{KL}(f_{\mathbf{X}}(\mathbf{x}) \| g_{\mathbf{Y}}(\mathbf{y})) = \int_{\mathbb{R}^M} f_{\mathbf{X}}(\mathbf{x}) \log f_{\mathbf{X}}(\mathbf{x}) d\mathbf{x} - \int_{\mathbb{R}^M} f_{\mathbf{X}}(\mathbf{x}) \log g_{\mathbf{Y}}(\mathbf{x}) d\mathbf{x}, \tag{5.15}$$

In information theory, the terms $\int_{\mathbb{R}^M} g_{\mathbf{Y}}(\mathbf{y}) \log g_{\mathbf{Y}}(\mathbf{y})\, d\mathbf{y}$ and $-\int_{\mathbb{R}^M} g_{\mathbf{Y}}(\mathbf{y}) \log f_{\mathbf{X}}(\mathbf{y}) d\mathbf{y}$ in Eq. (5.15) represent the negative (Shannon) entropy and cross-entropy, respectively. A smaller KL divergence corresponds to a higher similarity between two pdfs.

Property 5.1. The KL divergence is always non-negative because of Gibbs' inequality, that is, $D_{KL}(g(y)||f(x)) \geq 0$. The KL divergence equals zero if and only if $g(y) = f(x)$ (Kullback and Leibler, 1951).

Assume that $g(y)$ is the "true" distribution of data and that $f(x)$ is the approximate distribution of data. $D_{KL}(g(y)||f(x))$ and $D_{KL}(f(x)||g(y))$ are termed forward KL divergence and reverse KL divergence, respectively.

Property 5.2. The KL divergence is not symmetric, which means that the forward KL divergence does not equal the reverse KL divergence, i.e., $D_{KL}(g(y)||f(x)) \neq D_{KL}(f(x)||g(y))$. Hence, the solutions differ with the direction of the KL divergence (Abbas et al., 2017).

Forward KL divergence is commonly used in applications such as MLE, expectation propagation, and supervised learning (Wu and Zhang, 2021). Reverse KL divergence is useful in domains such as variational inference and reinforcement learning (Kobayashi, 2021). In this chapter, forward KL divergence is used to simultaneously estimate stochastic OD demands and link travel times.

In the considered case, the difference in the minimized KL divergence values for two different directions is not expected to be large because the traffic flow and travel time usually follow unimodal distributions (Abbas et al., 2017). However, the results of optimizing the KL divergence values in different directions may differ significantly when the target distributions are multimodal. Specifically, minimization of the forward KL divergence yields the distribution pertaining to the overall mean of different modes, whereas minimization of the reverse KL divergence corresponds to results approaching a specific mode while ignoring the other modes (Olsson et al., 2000). Due to the novelty of the developed model, the difference between the minimized values is examined by using numerical examples. These afford insights into the determination of KL divergence values in different directions in related problems.

Without loss of generality, the pdfs of observations of link flow, link travel time, and path travel time can be determined through multi-variate kernel density estimation in a following non-parametric manner (Kharoufeh and Goulias, 2002):

$$g_{1\mathbf{H}_1}\left(\tilde{\mathbf{V}}^l\right)=\frac{1}{D}\sum_{i=1}^{D}K_{\mathbf{H}_1}\left(\tilde{\mathbf{V}}^l-\tilde{\mathbf{v}}_{(d)}^l\right), \tag{5.16a}$$

$$g_{2\mathbf{H}_2}\left(\tilde{\mathbf{T}}^l\right)=\frac{1}{D}\sum_{i=1}^{D}K_{\mathbf{H}_2}\left(\tilde{\mathbf{T}}^l-\tilde{\mathbf{t}}_{(d)}^l\right), \tag{5.16b}$$

$$g_{3\mathbf{H}_3}\left(\tilde{\mathbf{T}}_{w_r}\right)=\frac{1}{D}\sum_{i=1}^{D}K_{\mathbf{H}_3}\left(\tilde{\mathbf{T}}_{w_r}-\tilde{\mathbf{t}}_{w_r(d)}\right), \tag{5.16c}$$

where $\tilde{\mathbf{V}}^l$ is a vector of the random link flow on observed links, and $\tilde{\mathbf{v}}_{(d)}^l$ is the observed average hourly traffic flow on links during the morning peak hour on day d ($d = 1,2,3,\ldots,D$). Similarly, $\tilde{\mathbf{T}}^l$ and $\tilde{\mathbf{T}}_{w_r}$ are vectors of the random link travel time on the observed links and travel time between node pairs with AVI sensors, respectively. $\tilde{\mathbf{t}}_{(d)}^l$ and $\tilde{\mathbf{t}}_{w_r(d)}$ are samples of random vectors $\tilde{\mathbf{T}}^l$ and $\tilde{\mathbf{T}}_{w_r}$, respectively. $K_{\boldsymbol{H}_1}$, $K_{\boldsymbol{H}_2}$, and $K_{\boldsymbol{H}_3}$ are kernel functions such as a standard multi-variate normal kernel (i.e., $K_{\boldsymbol{H}_i}(\mathbf{X}) = (2\pi)^{-|\mathbf{X}|/2}\mathbf{H}_i^{-1/2}e^{-\frac{1}{2}\mathbf{X}^T\mathbf{H}_i^{-1}\mathbf{X}}$ for $i = 1, 2, or\ 3$). $\mathbf{H}_1$, $\mathbf{H}_2$, and $\mathbf{H}_3$ are the symmetric and positive definite bandwidth matrices that function as covariance matrices.

The objective is to estimate the multi-variate density functions of OD demands and link travel times with a specific focus on their mean and covariance, based on the observations from point and AVI sensors. Because of the non-negative property of KL divergence (Property 5.1), the following objective function can be formulated to minimize the KL divergence between the estimated and observed pdfs of the link flow, link travel time, and path travel time:

$$\min_{\mathbf{q},\boldsymbol{\Sigma}_q,\mathbf{t}^l,\boldsymbol{\Sigma}_t^l} \omega_q D_{KL}\left(f_1\left(\mathbf{v}^l,\boldsymbol{\Sigma}_v^l\right)\|\, g_1\left(\tilde{\mathbf{v}}^l,\tilde{\boldsymbol{\Sigma}}_v^l\right)\right)$$
$$+(1-\omega_q)\left[\omega^l D_{KL}\left(f_2\left(\mathbf{t}_o^l,\boldsymbol{\Sigma}_{t_o}^l\right)\|\, g_2\left(\tilde{\mathbf{t}}^l,\tilde{\boldsymbol{\Sigma}}_t^l\right)\right)+(1-\omega^l)D_{KL}\left(f_3\left(\mathbf{t}_{w_r},\boldsymbol{\Sigma}_t^{w_r}\right)\|\, g_3\left(\tilde{\mathbf{t}}_{w_r},\tilde{\boldsymbol{\Sigma}}_t^{w_r}\right)\right)\right],$$

(5.17a)

subject to

Eqs. (3.4), (3.5), and (5.8) – (5.11), (5.17b)

where the decision variables (vectors or matrices) include the mean OD demands $\mathbf{q}$, the covariance of OD demands $\boldsymbol{\Sigma}_{\boldsymbol{q}}$, the mean link travel times $\mathbf{t}^l$, and the covariance of link travel times $\boldsymbol{\Sigma}_t^l$. In addition, the multi-variate density function (i.e., $f_1(.)$, $f_2(.)$, and $f_3(.)$) will be estimated. $f_1(.)$, $f_2(.)$, and $f_3(.)$ are the pdfs of the estimated link flow, link travel time, and node pair travel time, respectively. $g_1(.)$, $g_2(.)$, and $g_3(.)$ are the pdfs of the observed link flow, link travel time, and node pair travel time, respectively. These pdfs can be expressed through either parametric or nonparametric approaches. In a parametric approach, various distributions (such as multivariate normal or log-normal) can be assumed in accordance with the traffic conditions. In a nonparametric approach, the pdf of a variable can be estimated from historical knowledge by using (for example) kernel density estimation or the method of moments.

The first term in Eq. (5.17a) is to minimize the difference between the distributions of the observed and estimated link flows for the OD demand estimation, whereas the second and third terms intend to estimate the stochastic link travel times. Specifically, the second term is incorporated to minimize the difference between the distributions of the observed and estimated link travel times from point sensors, and the third term is incorporated to minimize the difference between the distributions of the observed and estimated travel times from AVI sensors.

In Eq. (5.17a), ω_q ($0 \le \omega_q \le 1$) is a weighting parameter that indicates the

importance of the OD demand estimates; $(1-\omega_q)$ is a weighting parameter that indicates the importance of the link travel time estimates; ω^l $(0 \leq \omega^l \leq 1)$ is a weighting parameter that indicates the significance of the point sensor observations; and $(1-\omega^l)$ is a weighting parameter that indicates the significance of the AVI sensor observations. Practically, ω_q can be set by considering the purpose of installing traffic sensors: if traffic engineers wish to obtain more accurate OD demand estimates, ω_q can be assigned a large value; in contrast, if the focus is on travel time estimates, ω_q can be assigned a small value. In addition, the value of ω^l can be set based on the sample size of observations from point or AVI sensors (Shao et al., 2018).

Property 5.3. A unique optimal value of the minimization problem displayed in Eqs. (5.17a) and (5.17b) always exists for fixed target pdfs $g_1(.)$, $g_2(.)$, and $g_3(.)$.

To prove the uniqueness of this minimization problem, its convexity and non-negativity must be proved. The non-negative property is covered in the discussion of Property 1. By expanding Eq. (5.17a) based on Eq. (5.15), it can be observed that the former entropy term is a convex function, and the latter cross-entropy term is an affine function. Therefore, the convexity is preserved under sum.

Remark 1. The covariance matrices $\boldsymbol{\Sigma_q}$ and $\boldsymbol{\Sigma}_t^l$ must be symmetric and positive semi-definite. Therefore, only half of the elements, including the diagonal elements in $\boldsymbol{\Sigma_q}$ and $\boldsymbol{\Sigma}_t^l$, must be estimated. Specifically, if $|\mathbf{W}|$ OD pairs are considered in a road network, the number of elements in $\boldsymbol{\Sigma_q}$ to be estimated is $[|\mathbf{W}|(|\mathbf{W}|+1)]/2$. To ensure that the estimated covariance matrices are positive semi-definite, the objective function must be subject to the following mathematical constraints:

$$\boldsymbol{\Sigma}_q \succeq 0 \quad \text{and} \quad \boldsymbol{\Sigma}_t^l \succeq 0, \tag{5.18}$$

Remark 2. The OD demand estimation problem is underdetermined, despite

additional information (e.g., the second-order statistical property and information from AVI sensors) being used. This is because the number of estimates pertaining to $\mathbf{q}$ and $\boldsymbol{\Sigma}_{\boldsymbol{q}}$ in the model is much larger than the dimensionality of the observations, especially in the case of a large road network. In addition, owing to mobility constraints and budget limitations, AVI and/or point sensors may not cover several links or paths in a real network. Thus, to restrict the mean OD demand estimates to a reasonable interval, prior OD demands are considered in the following constraint (Shao et al., 2014):

$$\mathbf{q}^{-} \leq \mathbf{q} \leq \mathbf{q}^{+}, \tag{5.19}$$

where $\mathbf{q}^{-}$ and $\mathbf{q}^{+}$ are the lower and upper bounds of the mean OD demand estimates, respectively, which are non-negative and can be determined from the prior mean OD demands. This constraint ensures that the estimated mean OD demands are non-negative.

Similarly, the mean link travel time estimates should be restricted by the prior information, as set in the following constraint:

$$\mathbf{t}^{l-} \leq \mathbf{t}^{l} \leq \mathbf{t}^{l+}, \tag{5.20}$$

where $\mathbf{t}^{l-}$ and $\mathbf{t}^{l+}$ are the lower and upper bounds of the mean link travel time estimates, respectively, which are non-negative and can be determined from the prior information.

Remark 3. If the covariance of link travel times is known, the travel time on links without point sensors can be calculated by (Shao et al., 2018):

$$\boldsymbol{t}_{u}^{l} = \boldsymbol{t}_{uprior}^{l} + \boldsymbol{\Sigma}_{t_u,t_o}^{l}(\boldsymbol{\Sigma}_{t_o}^{l})^{-1}(\tilde{\boldsymbol{t}}^{l} - \boldsymbol{t}_{oprior}^{l}). \tag{5.21}$$

where $\mathbf{t}_{uprior}^{l}$ and $\mathbf{t}_{oprior}^{l}$ are the prior link travel times on unobserved and observed links, respectively. This constraint means that the mean unobserved link travel times can be estimated based on the prior and observed link travel times, and the covariance

of link travel times. Eq. (5.21) is thus considered a constraint of the estimation problem. An estimated link travel time should correspond with the traffic flow on this link based on the BPR link performance function (which considers the speed–flow relationship). By considering the variability in travel time and traffic flow, a stochastic BPR link performance function can be developed as a constraint or condition for estimating OD demands and link travel times. If the link travel time and traffic flow are considered to be stochastic variables, their relationships with both the mean and covariance should be derived based on statistics. The mean link travel time can be expressed by the mean link flow as below:

$$\mathbf{t}^l = H_m(\mathbf{v}^l), \tag{5.22}$$

where $H_m(.)$ is a function used for deducing the mean link travel times from the mean and covariance of link flows. Additionally, the covariance relationship between the link travel times and link flows can be derived by (Ma and Qian, 2017):

$$\mathbf{\Sigma}_t^l = H_{\text{cov}}(\mathbf{v}^l, \mathbf{\Sigma}_v^l), \tag{5.23}$$

where $H_{cov}(.)$ is a function used for deducing the covariance between the link travel times from the mean and covariance of link flows. The explanations and derivations of functions $H_m(.)$ and $H_{cov}(.)$ are presented in Appendix D. The KL divergence of link travel times between their estimates from the proposed model and those inferred from the link performance functions in Eqs. (5.22) and (5.23) is used as an additional constraint to realize the simultaneous estimation and increase the estimation accuracy. This KL divergence is expressed as:

$$D_{KL}\left(\left(\mathbf{t}^l, \mathbf{\Sigma}_t^l\right) \| \left(H_m(\mathbf{v}^l), H_{\text{cov}}(\mathbf{v}^l, \mathbf{\Sigma}_v^l)\right)\right) \le \psi, \tag{5.24}$$

where ψ is a predetermined upper bound of the KL divergence constraint. The travel times and traffic flows on several links with point sensors can be directly observed or approximated. To avoid the generation of inconsistencies between the observations and the BPR link performance function, the BPR link performance function is only used for the links that cannot be directly observed by traffic sensors in a road network

(i.e., $\forall a \in \{\mathbf{A} \backslash \widetilde{\mathbf{A}}\}$).

Therefore, the objective of the upper-level problem (Eq. (5.17a)) is constrained by Eqs. (3.4), (3.5), (5.8)–(5.11), (5.18)–(5.21), and (5.24). To establish a more generalized model, other traffic information—such as path travel time—can be considered in the objective function for different applications. For instance, if traffic planners intend to install traffic sensors to provide information for route guidance, obtaining an accurate path travel time can be set as an alternative objective in the SLP.

5.3.4.2 Lower-level model: an adapted traffic flow simulator

To ensure consistency between the path choice patterns and estimated stochastic OD demands, an adapted traffic flow simulator (Lam and Xu, 1999; Fu et al., 2019) based on a logit-based SUE traffic assignment model is used in the lower-level model. In the logit-based SUE model, the classical BPR link performance function – which is continuous, differentiable, strictly monotone increasing, and separable (Yao et al., 2014) – is adopted. The design capacity of each link is adopted and assumed to be fixed in this chapter for strategic planning purposes, as the sensor locations will not be changed frequently in practice. Thus, with the logit-based model and classical BPR link performance function, the uniqueness of the SUE model used in this chapter can be ensured (Cantarella, 1997; Yao et al., 2014).

Although a physical capacity constraint can be easily incorporated into the adapted traffic flow simulator, it is not considered in this chapter in order to present the essential insights regarding the covariance effects on the model results.

Property 5.4. The solutions obtained from the adapted traffic-flow simulator are unique with respect to the link flows, path flows, and link choice proportions.

In the adapted traffic flow simulator, a set of OD demand matrices will be generated

based on the multi-variate density functions of peak-hour OD demand estimated in the upper level of the second-stage model. Each of these OD matrices will be assigned by a logit-based SUE model to get the link and path flows. Thus, for a fixed set of OD demand matrices, the uniqueness of the adapted traffic flow simulator could be ensured with the adopted logit-based SUE model.

5.3.5 Multi-type sensor location problem

In strategic planning, traffic sensors play primary roles in providing updated and adequate observations. Therefore, in the planning stage of the SLP, the number, locations, and types of traffic sensors should be simultaneously optimized to estimate the stochastic OD demands and network-wide link travel times.

As discussed in Section 5.1, in addition to the mean OD demands and link travel times, variance and covariance information can provide additional information that enhances the accuracy of estimation. For instance, the relationship between different travel behaviors can be inferred from the covariance of the OD demands. Moreover, the traffic condition propagation mechanism in a road network can be estimated from the covariance of the link travel times. Specifically, if two links exhibit a large travel time covariance, the travel times of these two links are expected to be strongly linearly correlated. Therefore, the links with larger travel time covariance values should be assigned greater importance when estimating link travel times. The covariance of the OD demands is controlled by a similar mechanism to that of the link travel time.

Therefore, the covariance information must be considered in the SLP to obtain accurate estimations of the mean and covariance of traffic parameters. To assign higher mathematical importance to links with larger travel time covariances in the SLP, the sum of travel time covariances between link a and other links is used as the weight on link a. Similarly, the sum of the OD demand covariances between OD pair w and other

OD pairs is used as the weight on OD pair *w*.

To incorporate the stochastic OD demand and link travel time information in the SLP, the values must be normalized by considering the coefficients of correlation and variation. The coefficients of correlation and variation for the OD demand estimates are $cc_{w,w'} = \sigma_{w,w'}/(\sigma_w \cdot \sigma_{w'})$ and $cv_w = \sigma_w/q_w$, respectively, where σ_w is the standard deviation of the OD demand of OD pair *w*. The coefficients of correlation and variation for the link travel time estimates are $cc^l_{t_a,t_{a'}} = \sigma^l_{t_a,t_{a'}}/(\sigma^l_{t_a} \cdot \sigma^l_{t_{a'}})$ and $cv^l_{t_a} = \sigma^l_{t_a}/t^l_a$, respectively, where $\sigma^l_{t_a}$ is the standard deviation of the travel time on link a.

Inspired by the researches that have been conducted by Zhou and List (2010), Simonelli et al. (2012), and Xing et al. (2013), the model in this chapter is to optimize the number and locations of point and AVI sensors by minimizing the normalized uncertainties of the stochastic OD demand and link travel time estimates. The uncertainties are weighted by the coefficients of correlation. The objective for the multi-type SLP is

$$\min_{\mathbf{z},\mathbf{z}'}\left\{\frac{\omega_z}{|\mathbf{W}|}\sum_{w\in\mathbf{W}}\left(\sum_{w'\in\mathbf{W}}|cc_{w,w'}|\right)cv_w + \frac{1-\omega_z}{|\mathbf{A}|}\sum_{a\in\mathbf{A}}\left(\sum_{a'\in\mathbf{A}}|cc^l_{t_a,t_{a'}}|\right)cv^l_{t_a}\right\}, \tag{5.25a}$$

subject to

$$\beta\sum z_a + \beta'\sum z_n' \le B, \tag{5.25b}$$

where $0 \le \omega_z \le 1$ is the weighting parameter of the OD demand estimation; β and β' denote the installation and maintenance costs of point and AVI sensors, respectively; and *B* is the total budget. According to assumption **A3**, the cost of an AVI sensor installed on a node (β') depends on the number of directions covered by this node. The decision variables of the SLP are $\mathbf{z} = [\dots, z_a, \dots]^T$ and $\mathbf{z}' = [\dots, z_n', \dots]^T$, which are vectors of binary variables. $z_a = 1$ if a point sensor is installed on link *a*; $z_a = 0$

otherwise. $z_n' = 1$ if an AVI sensor is installed on node n; $z_n' = 0$ otherwise.

5.4 Solution algorithm

The multi-type SLP model developed for OD demand and link travel time estimation is a non-convex mixed-integer programming problem that is NP-hard, especially for a real-life road network. To efficiently solve the developed optimization problems, the search strategy of the FA is enhanced by considering the mean and covariance of both the OD demands and link travel times (as mentioned in contribution **C4**).

To conveniently solve the traffic SLP, the abovementioned formulation is vectorized. First, define a mapping function $\Gamma(A)$, which outputs a new matrix whose elements are the absolute values of all of the elements in matrix A. In addition, define $1 \times |\mathbf{W}|$ row vector $\mathbf{I}_w$ and $1 \times |\mathbf{A}|$ row vector $\mathbf{I}_t$, the elements of which are all ones. Denote $\mathbf{CV}_w$ and $\mathbf{CV}_t$ as column vectors (i.e., $\mathbf{CV}_w = [\dots, cv_w, \dots]^T$ and $\mathbf{CV}_t = [\dots, cv_{t_a}^l, \dots]^T$) that represent the coefficients of variation for the OD demand and link travel time estimates, respectively, and $\mathbf{CC}_w$ and $\mathbf{CC}_t$ as symmetric matrices consisting of the coefficients of correlation for the OD demands and link travel times, respectively.

Therefore, the multi-type traffic SLP formulated in Eq. (5.25a) can be expressed in a matrix form:

$$\min_{\mathbf{z},\mathbf{z}'} \left[\frac{\omega_z}{|\mathbf{W}|} \mathbf{I}_w \cdot \Gamma(\mathbf{CC}_w) \cdot \mathbf{CV}_w + \frac{1-\omega_z}{|\mathbf{A}|} \mathbf{I}_t \cdot \Gamma(\mathbf{CC}_t) \cdot \mathbf{CV}_t \right]. \tag{5.26}$$

The multi-type SLP described in Eq. (5.26) is formulated as an integer programming model with binary decision variables to indicate the optimal locations of point and AVI sensors. This problem is NP-hard, and hence the global optimum cannot be ensured,

especially for large-scale road networks. Meta-heuristic algorithms, such as the GA (Chootinan and Chen, 2006), the sequential heuristic algorithm (SHA), or the FA can be used to solve this SLP. Referring to Section 3.5.2 and Section 4.5.1, the FA is further improved and/or extended to efficiently solve the multi-type SLP in this chapter. The numerical examples described in Section 5 demonstrate the efficiency of the improved FA in comparison with several commonly used algorithms.

In the framework of the FA, point and AVI sensor location schemes ($\mathbf{z}$ and $\mathbf{z}'$, respectively) can be conveniently represented by analogy with fireflies. Thus, $\mathbf{z}$ and $\mathbf{z}'$ are vectors with allowable values of 0 and 1, and the goal of the improved FA is to determine the values of $\mathbf{z}$ and $\mathbf{z}'$**.** One firefly represents one traffic sensor location scheme for point and AVI sensors, and each binary variable indicates the existence of a point sensor on a link or an AVI sensor on a node. Suppose that there exist *m* fireflies.

The objective of the traffic sensor location model pertains to the light intensity of the fireflies (i.e., $In(\mathbf{z}, \mathbf{z}') = (\omega_z/|\mathbf{W}|)\mathbf{I}_{\boldsymbol{w}} \cdot \Gamma(\mathbf{CC}_{\mathrm{w}}) \cdot \mathbf{CV}_{\mathrm{w}} + ((1-\omega_z)/|\mathbf{A}|)\mathbf{I}_{\mathrm{t}} \cdot \Gamma(\mathbf{CC}_{\mathrm{t}}) \cdot \mathbf{CV}_{\mathrm{t}}$). $In(\mathbf{z}, \mathbf{z}')$ is thus a fitness function that determines the attractiveness of a firefly, which is proportional to its brightness. Both attractiveness and brightness decrease as the distance increases. As an extension of the original FA (Yang, 2008), the distance between two fireflies, r_{xy}, can be calculated to assess the difference between the represented sensor location schemes.

To comprehensively consider the covariance effects of OD demands and link travel times, the search strategy of the original FA is enhanced by taking into account the light absorption coefficients $\boldsymbol{\alpha}_1^q$, $\boldsymbol{\alpha}_2^q$, $\boldsymbol{\alpha}_1^t$, and $\boldsymbol{\alpha}_2^t$. In the numerical examples of this chapter, the four light absorption coefficients are negative and with -1 as their initial value (Miguel et al., 2013). In general, the light absorption coefficients are recommended to be set in the range (-10, -0.1) (Pal et al., 2012). To ensure that the

improved FA can yield a solution as close to the global optimum as possible with rapid convergence, the light absorption coefficients $\boldsymbol{\alpha}_1^q$, $\boldsymbol{\alpha}_2^q$, $\boldsymbol{\alpha}_1^t$, and $\boldsymbol{\alpha}_2^t$ are iteratively updated according to the estimation accuracy of the mean OD demand, the covariance of OD demand, the mean link travel time, and the covariance of link travel time, respectively. The updating process of these coefficients and their relationships can be explained as below:

After each iteration i, the estimation accuracy of the mean OD demand, the covariance of OD demand, the mean link travel time, and the covariance of link travel time are evaluated by MPRE and defined as $MPRE_1^{q(i)}$, $MPRE_2^{q(i)}$, $MPRE_1^{t(i)}$, and $MPRE_2^{t(i)}$, respectively. The MPRE is defined in Section 3, and detailed formulation can be found in the studies of Yang et al. (1991) and Fu et al. (2019). For example, with the MRPEs in iteration *i*, the light absorption coefficient corresponding to the mean OD demand estimate ($\boldsymbol{\alpha}_1^q$) is updated by:

$$\boldsymbol{\alpha}_1^{q(i+1)} = \boldsymbol{\alpha}_1^{q(i)} \cdot 4MPRE_1^{q(i)}/(MPRE_1^{q(i)} + MPRE_2^{q(i)} + MPRE_1^{t(i)} + MPRE_2^{t(i)}). \tag{5.27}$$

The coefficients corresponding to covariance of OD demand ($\boldsymbol{\alpha}_2^q$), mean link travel time ($\boldsymbol{\alpha}_1^t$), and covariance of link travel time ($\boldsymbol{\alpha}_2^t$) are updated in the same manner. It can be seen from Eq. (5.27) that a smaller $MPRE_1^{q(i)}$ leads to a larger corresponding light absorption coefficient $\boldsymbol{\alpha}_1^q$ in the next iteration. In contrast, a smaller $MPRE_1^{q(i)}$, with fixed MAPEs for other characteristics (i.e., $MPRE_2^{q(i)}$, $MPRE_1^{t(i)}$, and $MPRE_2^{t(i)}$), will lead to smaller values of the other light absorption coefficients (i.e., $\boldsymbol{\alpha}_2^q$, $\boldsymbol{\alpha}_1^t$, and $\boldsymbol{\alpha}_2^t$) in the next iteration. In general, smaller light absorption coefficients correspond to a higher probability of achieving the global optimum but slower

convergence, and vice versa (Miguel et al., 2013). The upper bound and a lower bound of these light absorption coefficients are set to be -0.1 and -10, respectively.

In terms of the variation function of attractiveness (i.e., $exp[(\boldsymbol{\alpha}_1^q + \boldsymbol{\alpha}_2^q + \boldsymbol{\alpha}_1^t + \boldsymbol{\alpha}_2^t)r_{xy}]$), negative light absorption coefficients imply that a larger distance between two fireflies corresponds to a smaller attractiveness between them (Miguel et al., 2013). If the coefficients approach zero, the fireflies do not move, and their attractiveness becomes a constant. In contrast, if the coefficients approach negative infinity, the fireflies move randomly. Such random movement of fireflies helps to avoid solutions being trapped into local optimums.

The stopping criterion of the two-stage model is based on the maximum number of iterations (i.e., *i* > *MaxGeneration*) and the stopping criterion of the second-stage bi-level model based on the link travel time estimation (i.e., $\varepsilon = max\left[\left|\frac{\tilde{t}_a^l}{t_{o,a}^l} - 1\right|, \forall a \in \widetilde{\mathbf{A}}\right] \leq MaxError$) (Lam and Xu, 1999). By modeling the attractiveness with consideration of the light absorption coefficients and distance, the algorithm can determine the sensor location scheme that results in more accurate estimations of the stochastic OD demands and link travel times than other schemes. The pseudo-code of the improved FA is presented in Figure 5.2.

Input: network topology, prior OD demand, and prior link travel time
Objective function $In(\mathbf{z}_x, \mathbf{z'}_x)$
Generate initial populations of fireflies $\mathbf{z}_x$ and $\mathbf{z'}_x$ (x = 1,2,…m)
Estimate the pdfs, mean and covariance of OD demand and link travel time, and determine light intensity In_x of each firefly
Determine light absorption coefficients $\boldsymbol{\alpha_1^q}$, $\boldsymbol{\alpha_2^q}$,$\boldsymbol{\alpha_1^t}$, **and** $\boldsymbol{\alpha_2^t}$ (initialized to be -1) corresponding to the estimation accuracy of mean OD demand, **covariance of OD demand**, mean link travel time, and **covariance of link travel time**, respectively
while (i < *MaxGeneration*)
  for x = 1: m fireflies
    for y = 1: m fireflies (inner loop)
      if (In_x < In_y), move firefly x towards y; end if
      Vary attractiveness with distance r_{xy} by $\boldsymbol{exp}[(\boldsymbol{\alpha_1^q} + \boldsymbol{\alpha_2^q} + \boldsymbol{\alpha_1^t} + \boldsymbol{\alpha_2^t})\boldsymbol{r_{xy}}]$
      while ($\varepsilon > MaxError$)
        Estimate pdfs, mean and covariance of OD demand/link travel time
        Operate the adapted traffic flow simulator
        Calculate the error based on the link travel time estimation (ε)
      end while
      Evaluate new solutions and update light intensity
    end for
  end for
  Rank the fireflies and find the optimal sensor locations, set $i = i + 1$
end while
Output: the optimal multi-type sensor locations $\mathbf{z}_x^*, \mathbf{z'}_x^*$, and estimation results of mean and covariance of both OD demand and link travel time

Figure 5.2 Pseudo-code of the improved FA

5.5 Numerical examples

Two numerical examples are used to illustrate the merits of the proposed model and solution algorithm for solving the multi-type SLP for simultaneously estimating the OD demands and link travel times while also considering covariance effects. Experiments are performed on two different road networks to examine the various aspects detailed below.

Example 1: Synthetic small road network

(1) Covariance effects of OD demands and link travel times on the SLP and estimation accuracy

The effects of the OD demand and link travel time covariance on the optimal deployment of traffic sensors and estimation accuracy are examined in accordance

with contribution **C1**. Hypothetically, the estimation accuracy can be increased because the mean and covariance of the observations are incorporated into the problem, especially in congested conditions in peak-hour periods.

(2) Comparison of the SLPs for simultaneously and separately estimating the OD demands and link travel times

To achieve contribution **C2**, the estimation accuracies are investigated to demonstrate the superiority of simultaneous estimation over separate estimation (i.e., the estimation of either OD demands or link travel times) in the SLPs. Because both the traffic flow and travel time information are considered, the optimal sensor locations determined from simultaneous estimation are expected to yield more accurate results than those determined from separate estimation.

(3) Comparison between the KL divergence-based model and the GLS model

Variation in traffic conditions leads to different probability distributions of traffic flow and travel time. As mentioned in contribution C3, a KL divergence-based method is used to estimate the stochastic OD demands and link travel times to decrease the estimation bias related to variations in traffic conditions.

(4) Sensitivity analysis of the weighting parameters used in the simultaneous estimation of the OD demands and link travel times

The KL divergence-based method is used to integrate stochastic OD demands and link travel times. The weighing parameters must be adapted to various estimation schemes in the weighted-sum method.

Owing to the limited number of links and nodes in the small road network, it is difficult to clarify the tradeoff using multi-source data from different traffic sensors. Thus, it is necessary to conduct realistic experiments in a larger road network to examine the

tradeoff related to using data from different types of traffic sensors (in terms of the type of data collected and the cost of sensors) and the effect of network topology on the optimal number and locations of multi-type sensors.

Example 2: Real-life case study in Hong Kong

(5) Effects of different estimation schemes on the optimal number and locations of sensors

According to the data detected by different traffic sensors, the estimation of OD demands is primarily based on the flow data from point sensors, whereas the estimation of link travel times is based mainly on the path travel time information from AVI sensors, especially for paths that consist of many links with few point sensors.

(6) Influence of different types of sensor data on simultaneous estimation results

Each type of sensor data exhibits unique advantages. Because AVI sensors can provide only path travel time information, these sensors are used mainly to estimate link travel times. Data from point sensors, which are inexpensive, are the main type of data used to estimate OD demand and link travel times.

(7) Effects of the cost ratio between different types of sensors on the optimal number of sensors

In practice, the cost ratio between point and AVI sensors affects the budget allocation to purchase different types of sensors.

(8) Convergence and stability of the solution

The convergence and stability of the solution for the realistic road network are evaluated to demonstrate the superior efficiency of the improved FA compared to that of several commonly used algorithms, as indicated in contribution **C4**.

5.5.1 Example 1

This example is based on a small road network consisting of 7 nodes, 16 links, and 12 OD pairs, as shown in Figure 3.3 in Chapter 3. Multi-type traffic sensors are to be installed for estimating the stochastic OD demands and network-wide link travel times in the morning peak-hour period (e.g., 8:00–9:00 a.m.). Table 5.1 lists the link free-flow travel times, the design capacities, and the lengths for this network.

Table 5.1 Link free-flow travel times, design capacities, and lengths for the network in Example 1

Link nos.	Free-flow travel time (h)	Design capacity (veh/h)	Length (km)
1, 4	0.0031	425	0.22
2, 6	0.0040	610	0.28
3, 8	0.0043	380	0.30
5, 11	0.0031	520	0.22
7, 9	0.0040	300	0.28
10, 12	0.0043	580	0.30
13, 15	0.0050	850	0.25
14, 16	0.0050	690	0.25

For the sake of illustration, the “true” mean and var–cov of the hourly OD demands in the morning peak, obtained using the sampling method (Cascetta and Nguyen, 1988), are assumed to be known and are summarized in Table 5.2 and Table 5.3, respectively. The path set for each OD pair can be referred to Table 3.2 in Chapter 3. The true link flows and link and path travel times in the peak-hour period can be simulated based on the true OD demands by using an adapted traffic flow simulator (Lam and Xu, 1999), in which a Monte Carlo algorithm is implemented. To ensure that the feasible paths of the OD pairs in the numerical examples can be identified with non-excessive computational effort, the set of paths for each OD pair is assumed to be known and fixed. The other parameters in the BPR link performance function are the same as those set by Fu et al. (2019). It is assumed that the length of each link is less than the

detection zone of microwave radar point sensors (i.e., 0.3 km). Only one such point sensor is to be installed on each selected link. The influence of the link length and the number of point sensors installed on each link in the SLP should be examined in future work.

It was reported that the travel times in a road network follow log-normal and normal distributions in congested and uncongested conditions, respectively (Li et al., 2006b). The exact form of the KL divergence is obtained for multivariate normal or multivariate log-normal distributions, as presented in Eq. (5.28) (Gil, 2011). Thus, the following KL divergence formulation can be used to represent both congested and uncongested conditions in the numerical examples:

$$D_{KL}(\mathbf{X} \| \mathbf{X}^{obs}) = \frac{1}{2}\left(\log \frac{\left|\Sigma_x^{obs}\right|}{\left|\Sigma_x\right|} - d + tr\left(\left(\Sigma_x^{obs}\right)^{-1}\Sigma_x\right) + \left(\mathbf{x}^{obs} - \mathbf{x}\right)^T \left(\Sigma_x^{obs}\right)^{-1}\left(\mathbf{x}^{obs} - \mathbf{x}\right) \right), \tag{5.28}$$

where $\mathbf{X}$ and $\mathbf{X}^{obs}$ are d-dimensional random vectors that follow multivariate normal or log-normal distributions with means $\boldsymbol{x}$ and $\boldsymbol{x}^{obs}$ and covariance matrices Σ_x and Σ_x^{obs}, respectively. $\mathbf{X}^{obs}$ represents the link flows and link travel times observed at the point sensors or the travel times between a node pair observed at the AVI sensors, as indicated in Eq. (5.17a).

With reference to the studies of Yang et al. (1992) and Fu et al. (2022), the prior OD demands are set to have the following relationship with true values (Table 5.2): $q_w^{prior} = (1 - \mu \cdot cv_w^*) \cdot q_w^*$ and $\sigma_{w,w'}^{prior} = (1 - \mu \cdot cv_w^*)(1 - \mu \cdot cv_{w'}^*) \cdot \sigma_{w,w'}^*$. q_w^* and $\sigma_{w,w'}^*$ are the simulated true mean OD demand of OD pair w and covariance of the OD demand between OD pairs w and w', respectively. μ is an independent random variable that follows a normal distribution $N(0,1)$, and cv_w^* represents the coefficient of variation of the true traffic flows for OD pair w. The prior mean OD demands are input to the logit-based SUE model (with dispersion parameter $\theta = 0.2$)

to evaluate the mean link flows and path flows for the entire network. Therefore, referring to the definitions of the path choice proportion and the link-path incidence, the prior link choice proportions can be obtained based on the equilibrium results (i.e., $p_{aw}^{l} = \sum_{k \in \mathbf{K}} \delta_{ak} p_{kw}^{p}$).

Table 5.2 Network parameters and true mean of OD demands

OD number	1	**2**	3	**4**	5	6	7	8	9	10	11	12
Origin-Destination	C-B	**C-F**	C-G	**B-C**	B-F	B-G	F-C	F-B	F-G	G-C	G-B	G-F
"True" mean OD demands (veh/h)	262	**370**	135	**307**	358	384	251	272	286	185	214	308

Table 5.3 True var-cov matrix of OD demands

OD	Var-cov matrix $(\text{veh/h})^2$											
No.	1	2	3	4	5	6	7	8	9	10	11	12
1	4492.6											
2	826.1	13835.0										
3	-11.9	304.8	734.0									
4	-296.4	**4545.7**	459.2	4582.4								
5	-723.8	-2205.5	1479.6	716.2	13827.9							
6	3393.3	2138.7	-1347.6	-948.7	-3733.1	20811.0						
7	718.0	-1184.2	-707.3	-2458.7	-2400.2	2301.1	6337.7					
8	115.5	230.4	-588.0	-1557.6	971.8	159.7	947.8	5996.6				
9	2553.1	-2814.7	240.9	297.7	981.1	-1061.4	218.6	963.4	11383.4			
10	-80.8	-1488.1	180.0	133.7	1274.1	634.9	-163.6	517.7	235.1	2445.8		
11	1394.5	1018.8	103.4	898.5	-1434.9	1305.5	-1262.8	-729.2	1105.1	284.1	2884.0	
12	634.1	945.0	700.4	396.5	2214.9	-456.2	919.5	328.3	2756.3	417.2	317.6	5184.0

5.5.1.1 Covariance effects of OD demands and link travel times on the SLP and estimation accuracy

To examine the effects of the covariance of the OD demands and link travel times on the optimal solution of the multi-type SLP, various combinations of the covariance values of the OD demand and link travel time are compared, as described in the following four scenarios:

- Scenario I: The covariance of both the OD demands and link travel times is ignored.
- Scenario II: The covariance of the OD demands is considered, but that of the link travel times is ignored.
- Scenario III: The covariance of the link travel times is considered, but that of the OD demands is ignored.
- Scenario IV: The covariance of both entities is considered.

The mean absolute percentage errors (MAPEs) of the estimates of the OD demand and link travel time are used to evaluate the estimation accuracy in the four scenarios. Two AVI sensors and four point sensors are assumed to be installed in the network.

Table 5.4 indicates that the MAPEs of the OD demand and link travel time and the average MAPE for Scenarios II and III are less than those of Scenario I. This finding implies that considering the effects of covariance of the OD demands or link travel times can increase the accuracy of estimates of OD demands and link travel times for a given number of sensors. When the covariances of both the OD demands and link travel times are considered (Scenario IV), the most accurate estimates for the two traffic characteristics have the lowest average MAPE (8.83%). This finding highlights the necessity of systematically considering the effects of covariance of both the OD demands and link travel times on the SLP.

Table 5.4 Effects of the OD demand and link travel time covariances on the SLP results

Scenario	Considering OD demand covariance	Considering link travel time covariance	Optimal sensor locations	MAPE of OD demands	MAPE of link travel times	Average MAPE
I	×	×	Point: [1, 6, 7, 11] AVI: [C, D]	28.36%	32.03%	30.20%
II	✓	×	Point: [1, 3, 7, 12] AVI: [B, F]	13.92%	22.55%	18.24%
III	×	✓	Point: [2, 3, 8, 10] AVI: [B, G]	20.37%	14.92%	17.65%
IV	✓	✓	Point: [1, 3, 5, 10] AVI: [B, F]	8.47%	9.19%	**8.83%**

Moreover, Table 5.4 indicates that the optimal sensor location scheme varies according to the consideration of the covariances. The traffic sensors installed at different locations in the road network provide different types of valuable information that can be used for estimating the mean and covariance of the OD demands and link travel times. The strategies of sensor installation are examined in the real case study with empirical data.

Owing to the budget constraint in practice, only a limited number of traffic sensors can be installed in the study network. In Scenario IV in which the covariances of the OD demand and link travel time are considered, the overall estimation results can be enhanced by using the optimal sensor location scheme. In this scenario, point sensors are installed on links 1, 3, 5, and 10, and AVI sensors are installed on nodes B, and F.

The estimation results of the OD demands and link travel times in Scenario IV are presented in Figure 5.3(a) and (b), respectively. As shown in Figure 5.3(a), the largest MAPE (17.63%) of an estimated OD demand corresponds to OD pair G–F (i.e., OD pair ID 12). Moreover, the estimated OD demands are mainly based on the link flow

data observed from point sensors. In Scenario IV, the observations on links 1, 3, 5, and 10 with point sensors do not significantly contribute to the estimation of vehicular demand for OD pair G–F (with one path passing through links 16 and 13). Figure 5.3(b) shows that the estimation accuracy of the link travel time on link 14 is the lowest (16.03%) of all links. In the optimal sensor location scheme for Scenario IV, link 14 has not been observed, or covered, by either the installed point sensors or AVI sensors. Thus, the MAPE of link travel time estimates on this link is the largest, but the absolute estimation error is still less than 0.05 min.

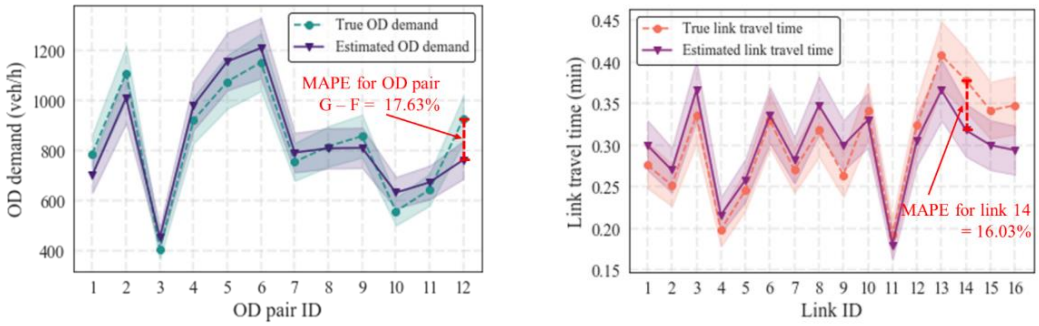

(a) OD demand estimates (b) link travel time estimates

Figure 5.3 Results of simultaneous estimation of the (a) OD demands and (b) link travel times in Scenario IV

5.5.1.2 Comparison of the SLP with simultaneous and separate estimation of the OD demands and link travel times

As described in Section 5.1, most previous studies have focused on installing traffic sensors in a road network for the estimation of either OD demands or link (or path) travel times. In contrast, in this research, various types of traffic sensors should be installed to estimate both the stochastic OD demands and link travel times in a peak-hour period based on the yearly data collected from the sensors.

Three models with different settings are compared to examine the effects of the simultaneous estimation of the OD demands and link travel times. In Model I, the

weighting parameter $\omega_z = 1$ in Eq. (5.25a) is used, indicating that sensors are installed only to estimate OD demands. In Model II, the weighting parameter $\omega_z = 0$, indicating that sensors are installed only to estimate link travel times. In Model III, the weighting parameter $\omega_z = 0.5$, indicating that sensors are installed to estimate OD demands and link travel times. Table 5.5 presents the estimated OD demands and link travel times for the three models for the given numbers of installed point and AVI sensors.

Table 5.5 indicates that the different models yield different optimal traffic sensor location schemes, corresponding to different estimation performances. For instance, when only OD demands are considered (Model I), it is preferable to install point sensors on links 1, 6, 9, and 10 and AVI sensors at nodes C and F. This difference in the schemes is attributable to the fact that traffic sensors installed at different sites exhibit different abilities for capturing the flows from different OD pairs. For example, for a link (e.g., link 6) traversed by more OD pairs and with highly correlated flows with other links, it is preferable to install a point sensor to estimate stochastic OD demand.

Based on observations from the traffic sensors, the MAPE of the estimates of stochastic OD demand from Model I is considerably less than that associated with Model II, although the accuracy of the estimation of the link travel times from Model II is higher than that from Model I.

A comparison of the results obtained using Model III with those obtained using Models I and II indicates that estimating the OD demands and link travel times in the SLPs leads to the smallest average MAPE (i.e., 10.31%). Moreover, Model III yields the most accurate estimates of the mean and covariance of both the OD demands and link travel times, as indicated by the MAPEs listed in Table 5.5. The accurate estimates

benefit from incorporating a stochastic link performance function that connects the link flow and link travel time information and can enhance the estimation of the mean and covariance. In summary, multi-type traffic sensor locations should be determined for simultaneously estimating the stochastic OD demands and link travel times, and these estimates are superior to those obtained by separately estimating each entity.

Table 5.5 Comparison of simultaneous and separate estimations

Model	Estimation scheme	Optimal traffic sensor locations	$MAPE_{\mathrm{q}}$	$MAPE_{\mathrm{t}^l}$	$MAPE_{\Sigma_q}$	$MAPE_{\Sigma_t^l}$	Average
I (ω_z=1)	OD demand	**Point: [1, 6, 9, 10] AVI: [C, F]**	8.52%	27.11%	14.17%	27.04%	19.21%
II (ω_z=0)	Link travel time	Point: [2, 4, 5, 11] AVI: [C, G]	30.56%	13.62%	25.88%	18.91%	22.24%
III (ω_z=0.5)	OD demand and link travel time	Point: [1, 3, 5, 10] AVI: [B, F]	6.63%	8.76%	12.12%	13.71%	**10.31%**

5.5.1.3 Comparison between KL divergence-based model and GLS model

The KL divergence-based model is developed to estimate the stochastic OD demands and link travel times with covariance effects. This novel model extends the existing models and is particularly suitable for simultaneous estimation in the SLP. The traditional GLS model can be regarded as a special case of the developed model that occurs when the variables are normally distributed. A comparative analysis is performed between KL divergence-based model and the traditional GLS model reported by Shao et al. (2014) in different traffic conditions to demonstrate the superiority of the proposed model.

To imitate congested and uncongested conditions, different distributions of the traffic flow and travel time are assumed. The multivariate normal and log-normal distributions represent the traffic information in uncongested and congested conditions, respectively. The true mean and variance of OD demands in congested conditions are

set to be 5 and 25 times those in uncongested conditions, respectively.

Suppose that for a random vector $\mathbf{X} \in \mathbb{R}^M$, the values of distributional parameters such as $\boldsymbol{\mu}$ and $\boldsymbol{\Sigma}$ in the multivariate normal and log-normal distributions are different. For example, the mean value in the multivariate normal and log-normal distributions is $\boldsymbol{\mu}$ and $exp(\boldsymbol{\mu} + \boldsymbol{\Sigma}/2)$, respectively. Then, based on the stochastic OD flows with different probability distributions, the parameters $\boldsymbol{\mu}_N$ and $\boldsymbol{\Sigma}_N$ in multivariate normal and $\boldsymbol{\mu}_{LN}$ and $\boldsymbol{\Sigma}_{LN}$ in multivariate log-normal distributions can be calculated. The results of the parameter estimation based on the KL divergence-based model and GLS model are compared. The MAPEs of $\boldsymbol{\mu}$ and $\boldsymbol{\Sigma}$ are calculated to evaluate the accuracy of the estimates for the two types of traffic conditions with associated distributions.

Table 5.6 Comparison of model performances with different distributions of OD demands and link travel times

	Multivariate normal		Multivariate log-normal	
	$MAPE_{\boldsymbol{\mu}_N}$	$MAPE_{\boldsymbol{\Sigma}_N}$	$MAPE_{\boldsymbol{\mu}_{LN}}$	$MAPE_{\boldsymbol{\Sigma}_{LN}}$
KL divergence-based model	8.27%	12.56%	**10.11%**	**15.24%**
GLS model	8.27%	12.56%	22.39%	27.62%

Table 5.6 exhibits that the accuracy of the estimates generated by the two models is identical when considering the multivariate normal distribution. However, for the multivariate log-normal distribution, the MAPEs of $\boldsymbol{\mu}_{LN}$ and $\boldsymbol{\Sigma}_{LN}$ from the KL divergence-based model are 10.11% and 15.24%, respectively, which are considerably less than those obtained from the GLS model. Thus, in congested conditions, the KL divergence-based model outperforms the GLS model in estimating the stochastic OD demands and link travel times. The accuracy of the estimates generated by the two models is comparable only in uncongested conditions, i.e., with a multivariate normal distribution.

Moreover, experiments are conducted to clarify the influence of the minimization of KL divergence in different directions (i.e., forward KL divergence and reverse KL divergence) on the accuracy of estimates. Another distance measurement—the Jensen–Shannon (JS) divergence, a symmetrized version of the KL divergence—is considered for comparison. The JS divergence can be calculated as:

$$JS(f(x)||g(y)) = \frac{1}{2}D_{KL}\left(f(x)||\frac{1}{2}(f(x)+g(y))\right) + \frac{1}{2}D_{KL}\left(g(y)||\frac{1}{2}(f(x)+g(y))\right). \quad (5.29)$$

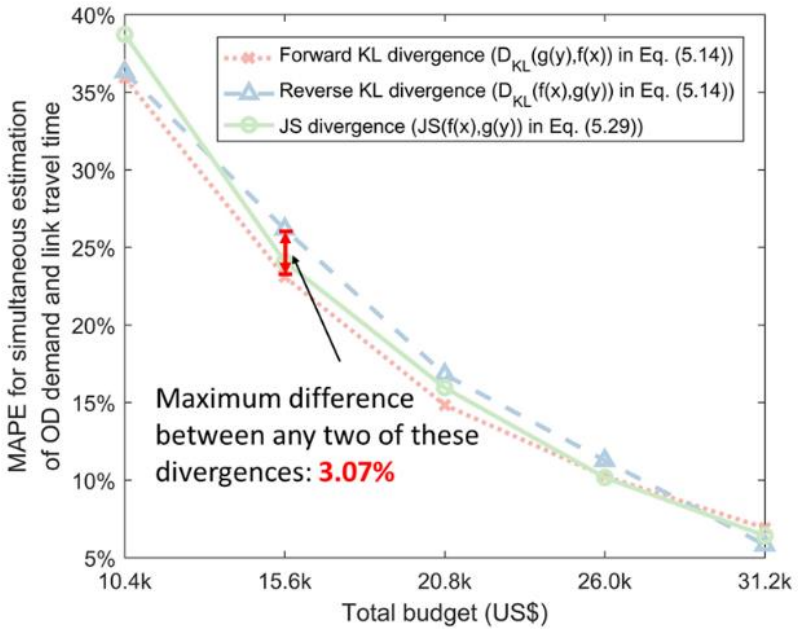

Figure 5.4 Comparison of results obtained using models based on the forward KL divergence, the reverse KL divergence, and the JS divergence

The results based on the forward KL divergence ($D_{KL}(g(y)||f(x))$ in Eq. (5.14), the reverse KL divergence ($D_{KL}(f(x)||g(y))$), and the JS divergence ($JS(f(x)||g(y))$ in Eq. (5.29) are compared under various total financial budgets. As shown in Figure 5.4, the maximum difference in the accuracy of estimates of any two of these divergences is 3.07%. This small difference is attributable to the OD demand and link travel time having unimodal distributions in general. Although this difference in the accuracy of estimates associated with the three divergences is not significant, the forward KL-divergence-based model (i.e., $D_{KL}(g(y)||f(x))$) yields more accurate estimates in

most cases. This finding supports the use of the forward KL divergence for developing the optimization model for the simultaneous estimation of stochastic OD demands and link travel times.

5.5.1.4 Sensitivity analysis of the weighting parameter used in the simultaneous estimation of the OD demands and link travel times

As discussed in Section 5.5.1.2, in the planning stage, the locations of multi-type traffic sensors should be optimized for estimating the OD demands and link travel times. Thus, the tradeoff in the significance of the estimated OD demands and link travel times in the SLP must be examined. To this end, a sensitivity analysis of the weighting parameters of the OD demand and link travel time estimates is performed. The changes in the estimates (in MAPE) of the OD demands and link travel times with the weighting parameters (ω_z in Eq. (5.25a)) are shown in Figure 5.5.

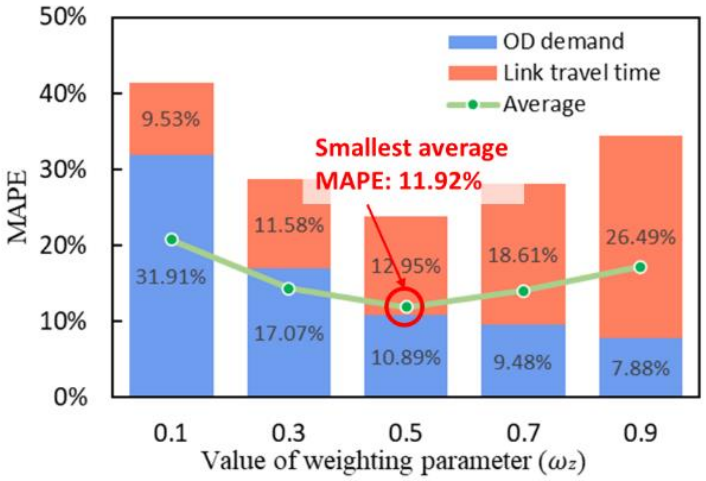

Figure 5.5 Sensitivity analysis of the weighting parameter for simultaneous estimation of OD demand and link travel time

The results in Figure 5.5 indicate that when the estimations of the OD demands and link travel times are equally weighted (i.e., $\omega_z = 0.5$), the average MAPE for the estimates of OD demand and link travel time is minimized. Moreover, the use of a larger weighting parameter for the OD demands corresponds to a lower MAPE for the

estimation of OD demand but a larger MAPE for the estimation of the link travel time. This converse is true if a smaller weighting parameter is used for the OD demands. Thus, traffic engineers who are determining sensor locations with an emphasis on the OD demands must assign a larger weighting parameter to the estimation of OD demand than to the estimation of link travel time.

5.5.2 Example 2

To demonstrate the applicability of the proposed model for solving the multi-type SLP in the real world, the Tuen Mun Road Corridor Network in Hong Kong (Figure 4.5 in Chapter 4) is used with empirical data collected for this case study. In the numerical example, with the observed feature (i.e., link flows, link travel times, and partial path travel times), the corresponding multi-variate density functions can be inferred by kernel density estimation (i.e., Eqs. (5.16a), (5.16b), and (5.16c)) without knowing their shape. By minimizing the KL divergence between the multi-variate density functions of estimated and observed features, the pdfs of the OD demand and link travel time in the study network can be estimated. As mean and covariance are the two most important characteristics of a multi-variate density function, MAPEs of these quantities are used for validation in the numerical examples.

Prior information is used to increase the estimation accuracy in this numerical example. First, historical data is collected to constrain the estimated mean OD demands and mean link travel times within a reasonable range based on the historical statistics. Apart from the means, the prior information of OD demand covariance can be inferred based on historical vehicle occupancy data (Fu et al., 2019, 2022). With the prior mean and covariance of OD demands and the assumption of a given and fixed path set (assumption **A6**), the prior stochastic travel time on each network link can be obtained using the adapted traffic flow simulator.

In this example, the design capacity of each road link will be adopted for strategic planning of sensor locations. As the design capacity of links is highly dependent on their attributes (e.g., road type, number of lanes, road width, etc.), link attributes are collected for each of all road links within the study network for defining their design capacities. True OD demands are estimated from the data obtained from all available point sensors (i.e., 18 point sensors) in the road network. The true link travel times are obtained by assigning the OD demands to the network in SUE conditions.

It is assumed that eight point sensors (four on the TMR and four on the CPR) and two AVI sensors (at the nodes connecting external zones S1 and S2) have already been installed in the network. For a given financial budget, the additional numbers and locations of traffic sensors are determined using the developed models. According to assumption **A3**, the cost of an AVI sensor is the cost of the sensor on a node covering one direction of traffic. For nodes covering more than one direction, the cost of an AVI sensor must be multiplied by the number of covered directions.

The traffic flow data obtained from the point sensors installed in Tuen Mun Road Corridor Network (Figure 3.10 in Chapter 3) show that the hourly traffic flows vary significantly and systematically by time of day and day of the year. For strategic planning, traffic planners should focus on the most congested period on typical weekdays (i.e., the morning peak hour) (Shao et al., 2014; Ma and Qian, 2018). Thus, the morning peak hour period (i.e., 7:00–8:00 a.m., as indicated in Figure 3.10 in Chapter 3) on normal weekdays over the year is chosen as the study period, and the data in this period will be used for simultaneous estimation in this chapter.

Link choice proportions on several links can be obtained based on observations from AVI sensors (Zhou and List, 2010; Fu et al., 2022). For instance, if origin node B and

destination node F in Figure 3.3 in Chapter 3 are equipped with AVI sensors, the traffic flows (v'_{BF}) with AVI tags in this OD pair w (i.e., from B to F) can be observed. It can be seen from Table 3.2 that some traffic flows of OD pair w can pass through link a (i.e., link 10), whose end nodes (D and E) are also assumed to be installed with AVI sensors. The traffic flow observed by all these four AVI sensors is represented by v'_{BDEF}. Thus, the link choice proportion of link a traversed by flows in OD pair w (i.e., origin B to destination F) can be approximately estimated as $p_{aw}^{l} = v'_{BDEF}/v'_{BF}$. Owing to the sparse distribution of AVI sensors, link choice proportions can only be inferred for a few links. It merits further studies to extend the proposed model by incorporating the additional information of link choice proportions observed from AVI sensors.

In this numerical example (Example 2), after estimating the OD demand (in the upper level of the second-stage model), the link choice proportions are iteratively updated based on the equilibrium link and path flows (in the lower level of the second-stage model) for the fixed path set. The prior link choice proportion is acquired in a similar manner from the prior OD demand information extracted from the district transport model for this road network.

5.5.2.1 Effects of different estimation schemes on the optimal numbers and locations of sensors

Empirical data is adopted to clarify the influence of the estimation scheme on the optimum number and locations of traffic sensors. For a given budget (i.e., $B =$ US\$62,400), optimal solutions are obtained for estimating (i) only the OD demands, (ii) only the link travel times, (iii) the OD demands and link travel times. The unit costs of a point sensor and an AVI sensor installed on a node covering one direction are $\beta =$ US\$2,600 and $\beta' =$ US\$5,200, respectively. According to assumption **A3**, the cost

of AVI sensors on nodes depends on the number of directions covered by the nodes.

The results shown in Table 5.7 indicate that if traffic managers intend to install traffic sensors to estimate only OD demands, only additional point sensors are required. This is because the estimation of OD demands is based on the link flow observed by point sensors; the path travel time information provided by AVI sensors does not contribute significantly to the estimation of OD demands. Thus, it is not cost-effective to install AVI sensors.

Both types of sensors must be installed in the other two estimation schemes. To estimate link travel times, there should be more AVI sensors than point sensors. In particular, given prior link travel times, the path travel time information provided by a pair of AVI sensors can help to estimate the travel time on all of the links along that path. In comparison, the data from point sensors can only be used to estimate the travel time on the links equipped with these point sensors. Thus, the installation of AVI sensors is more cost-effective than the installation of point sensors for estimating the link travel times on paths with numerous links (e.g., paths along the CPR in the study network).

More point sensors should be installed on the CPR than on the TMR for all estimation schemes. Compared to the TMR (41 links), the CPR (164 links) involves more at-grade junctions, including signalized intersections. Thus, it is more difficult to estimate the stochastic link travel times and OD demands for the CPR, and more information should be acquired from point sensors to accurately estimate the link travel times and OD demands in this road network. This is also why more AVI sensors are installed on the CPR than on the TMR.

Table 5.7 Effects of estimation schemes on optimal number and locations of additional sensors

Estimation scheme	Optimal number of additional sensors*	
	Total number of additional point sensors (on TMR + on CPR)	Total number of additional AVI sensors (on TMR + on CPR)
(i) OD demand only	**24** (8 + 16)	0
(ii) Link travel time only	4 (1 + 3)	5 (1 + 4)
(iii) Simultaneous estimation	8 (2 + 6)	4 (1 + 3)

*The additional sensors for three purposes cost the same US$62,400

For the simultaneous estimation scheme (iii), the accuracies of the OD demands and link travel times estimated simultaneously using data from eight additional point sensors and four additional AVI sensors are shown in Figure 5.6, for comparison with the results of the other two estimation schemes. The 50 percentile MAPEs of the estimated OD demands for 306 OD pairs and the estimated link travel times for 487 links are 9.01% and 9.65%, respectively.

Furthermore, the accuracies of the estimates from the scheme (iii) are mostly higher than those for the other two schemes (i.e., the schemes estimating only OD demands or link travel times). This higher accuracy of the scheme (iii) results from its more efficient use of data than the other schemes. Specifically, the link travel time estimated from AVI sensors data can be used to infer the link traffic on the unobserved links (i.e., the links not covered by point or AVI sensors) by using the link performance function, which can enhance the OD demand estimation. Similarly, the estimated link travel times of the unobserved links can be enhanced by considering the link flows obtained by assigning OD demand estimates to the study network. To clarify the contributions of different sensor types, a sensitivity test is performed to investigate the influence of multi-type sensors on the accuracy of estimated OD demands and link travel times.

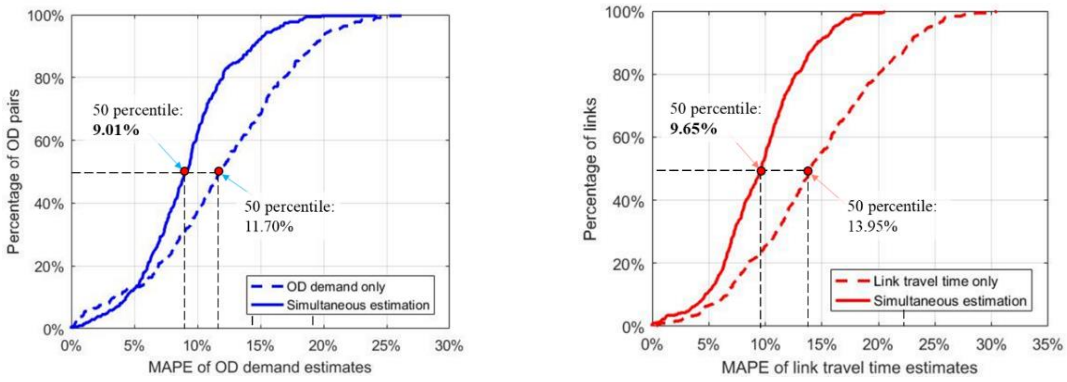

(a) Accuracy of OD demand estimates (b) Accuracy of link travel time estimates

Figure 5.6 Accuracy of estimates from different estimation schemes

5.5.2.2 Influence of different sensor data on the simultaneous estimation of OD demands and link travel times

Point and AVI sensors provide different types of traffic information for different estimation schemes, and thus this information is used in different ways for the estimation of OD demands and link travel times. It is important to clarify the influence of data from different traffic sensors on such estimations in a realistic road network. As in the experiment described in Section 5.5.2.1 for a given total budget, additional point or AVI sensors are to be installed for the simultaneous estimation of OD demands and link travel times. The weighting parameters ω_q, ω^l, and ω_z are set as 0.5.

As indicated in Table 5.8, the point sensors outperform the AVI sensors in terms of the average MAPEs of the estimates of OD demand and link travel time (10.57%). This is because point sensors can provide information on link travel times and flows, whereas AVI sensors can only provide information on path travel times.

The accuracy of estimates of link travel times obtained from six additional AVI sensors (9.04%) is higher than that obtained with 24 additional point sensors. This is because the 24 additional point sensors can observe the travel time on only 24 links, whereas

the six additional AVI sensors in cooperation with the two existing AVI sensors can provide travel time information on up to 54 (i.e., $\binom{8}{2} - \binom{2}{2}$) (sub)paths. Therefore, AVI sensors can provide sufficient data of path travel times in a cost-effective manner for enhancing estimates of link travel time, particularly for paths with many links. This finding is also related to the cost ratio of point sensors to AVI sensors. As if AVI sensors are expensive, traffic managers can afford fewer AVI sensors than point sensors for the given budget. In this situation, the amount of path travel time information obtained by an AVI sensor system and its contribution to link travel times decrease.

Table 5.8 Influence of different sensor data on the accuracy of simultaneous estimates of OD demands and link travel times

Scenario	MAPE of OD demand	MAPE of link travel time	Average MAPE
(i) Existing sensor scheme	27.15%	29.79%	28.47%
(ii) Existing sensor scheme with 24 additional point sensors	8.31%	12.82%	**10.57%**
(iii) Existing sensor scheme with six additional AVI sensors	25.53%	**9.04%**	17.29%

5.5.2.3 Influence of the cost ratio of different types of sensors on the optimal number of sensors

The cost ratio of point sensors to AVI sensors significantly affects the budget allocation for each sensor type because of budget constraints. Therefore, a sensitivity analysis of the cost ratio of point sensors to AVI sensors is performed to rationalize the budget allocation for different sensor types. In general, AVI sensors are more expensive than point sensors. Suppose that the total budget is given (i.e., $B = \text{US\$62,400}$) and the unit cost of a point sensor is fixed (i.e., $\beta = \text{US\$2,600}$). In addition, the unit cost of an AVI sensor (β') on a node covering one direction varies from $\text{US\$5,200}$ to $\text{US\$20,800}$. The cost ratio of point sensors to AVI sensors ranges from 1/2 to 1/8. As mentioned, the cost of AVI sensors depends on the number of directions covered by

the nodes of interest. Based on the model for the simultaneous estimation of OD demands and link travel times (described in Section 5.5.2.1), the optimal number of sensors and cost allocation for different sensor types are determined by solving the model for different cost ratios (Table 5.9).

As expected, Table 5.9 indicates that for a given total budget ($B = \text{US\$62,400}$), more point sensors are needed to be installed in the study network if the cost of AVI sensors increases. When the increase in the cost of AVI sensors causes the cost ratio of point sensors to AVI sensors to decrease to less than 1/8, only 24 point sensors (and no AVI sensor) are required for simultaneously estimating the OD demands and link travel times. Overall, AVI sensors cannot provide traffic information comparable to that achieved using an equivalent number of point sensors due to their high cost.

Table 5.9 Influence of cost ratio of point sensors to AVI sensors on the optimal number of sensors

Cost ratio (point/AVI)	Optimal number of sensors*	
	Total number of point sensors (cost)	Total number of AVI sensors (cost)
½	8 (US$20,800)	4 (US$41,600)
¼	12 (US$31,200)	3 (US$31,200)
1/6	16 (US$41,600)	2 (US$20,800)
1/8	**24** (US$62,400)	0 (US$0)

*Total budget $B = \text{US\$62,400}$

5.5.2.4 Convergence and stability of the solution

Considering the non-convex two-stage model and meta-heuristic solution algorithm (Zhou and List, 2010; Hu et al., 2015; Fu et al., 2019), it is extremely challenging to guarantee global optimality and stability of the model solution. To demonstrate the superiority of the improved FA in searching for the near-to-global optimal solutions, this experiment compares the performance of the improved FA with those of three commonly used algorithms: original FA, the GA (Salari et al., 2021), and the SHA

(Zhou and List, 2010; Xing et al., 2013) for solving the non-convex SLPs. The brute force algorithm is used as the baseline method for benchmarking different meta-heuristic algorithms, as it can enumerate candidate sensor location solutions and select the global optimum. However, it requires an extremely long computation time to do so. The OD demands are doubled to demonstrate the capability of the solution algorithms for solving the SLPs in a congested network. The maximum number of iterations (*MaxGeneration* in Figure 5.2) for each of these algorithms is set to 250. The stopping criterion parameter (*MaxError* in Figure 5.2) of the second-stage bi-level model is set to 0.005. The tests are performed on a laptop computer with an Intel Core i7-2600 CPU running at 3.40 GHz and 8 GB RAM.

Figure 5.7 shows that the improved FA achieves the best result with the smallest objective function value compared to the other algorithms. Furthermore, the improved FA converges faster than the other algorithms. Specifically, the improved FA requires 3.1 hours only to converge to the near-to-global optimum solution, while the original FA spends almost three times of that (i.e., 8.7 hours) to reach a similar solution. Using the brute-force method, it needs 51.8 hours to search the global optimum, which is only slightly better than the near-to-global optimum solution obtained from the improved FA. The smallest value of objective function achieved by improved FA (6.179) among meta-heuristic algorithms demonstrates its efficacy to search the near-to-global optimal solution as compared to the global optimum (6.177). Specifically, the optimal solution obtained from improved FA has the value of objective function smaller than 99.9% of feasible solutions, while the other three algorithms could only obtain optimum solutions that are better than at most 98% of feasible solutions. Besides, the shortest computation time of improved FA shows the efficient convergence of the proposed solution algorithm. With such efficient convergence, the improved FA can yield a better solution (i.e., closer to the global optimum) if stringent convergence stopping criteria are adopted for the sensor location and simultaneous

estimation problems.

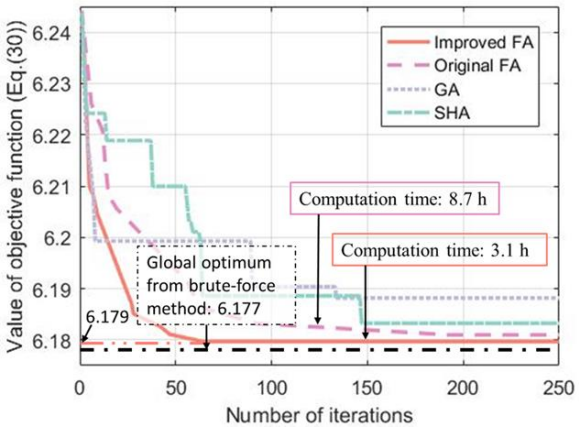

Figure 5.7 Convergence of the solution algorithms

Further to the convergence of solution, a numerical test, which takes into account different initial feasible solutions of the sensor locations, is performed to illustrate that the improved FA can yield a stable solution. Table 5.10 lists the nine scenarios with randomly selected initial feasible sensor locations that are used to evaluate the stability of the solution. Using the improved FA, it is found that all these scenarios converge to the same optimal solution (last column of Table 5.10). The above result indicates the improved FA is capable of yielding a stable optimal solution for the multi-type SLP considered in this chapter.

Table 5.10 Scenarios with various initial feasible solutions used to test the stability of the solution for multi-type SLPs

Scenario	Initial feasible solution of multi-type sensor locations with total budget $B = US\$62{,}400$		Optimal solution
	Number and locations of point sensors	Number and locations of AVI sensors	
I	four on TMR	five on TMR	two point sensors and one AVI sensor on the **same links or nodes** on TMR; six point sensors and three AVI sensors on the **same links or nodes** on CPR
II	four on CPR	five on CPR	
III	two on TMR and two on CPR	two on TMR and three on CPR	
IV	24 on TMR	0	
V	24 on CPR	0	
VI	12 on TMR and 12 on CPR	0	
VII	0	six on TMR	
VIII	0	six on CPR	
IX	0	three on TMR and three on CPR	

5.6 Summary

This chapter is to optimize the number and locations of multi-type sensors (point and AVI sensors) while also explicitly considering the spatial covariance relationships associated with OD demands and link travel times. The multi-type traffic sensors are deployed for simultaneously estimating the stochastic OD demands and network-wide link travel times over a typical hourly period on a daily scale.

To overcome the inconsistency between different data sources, a new KL divergence-based model is innovatively proposed to solve the simultaneous estimation problem in this chapter. Such a proposed model can flexibly deal with the skewed data for different probability distributions under various traffic conditions. Based on the estimation results of both link travel times and OD demands, the number and locations of point and AVI sensors can be determined by minimizing the normalized uncertainties of both stochastic OD demand and link travel time estimates. The corresponding coefficients of correlation weigh their uncertainties.

In Section 5.5 of this chapter, it has been demonstrated that the optimal sensor locations for simultaneous estimation could lead to more accurate estimates compared with those for separate estimation (i.e., for estimation of OD demands or link travel times only) studied in previous Chapters 3 and 4. This finding mainly results from the utilization of more available data from multi-type sensors and the inherent interrelationship between vehicular link flow and link travel time.

6. Conclusions

This research has addressed the timely and important SLPs for estimation of stochastic OD traffic demands and/or link travel time in a road network with uncertainty. With multi-type traffic sensing systems developed for smart transportation in smart cities, this research has proposed new models to efficiently and accurately estimate stochastic traffic states in terms of hourly OD demands and link/path travel times with taking into account the traffic demand variation and/or travel time uncertainty. In this chapter, the major contributions and key findings of this research are summarized in Section 6.1. Recommendations for further studies are given in Section 6.2.

6.1 Summary of research findings

The research presented in this thesis contributes to current literature related to SLPs, by considering the variations of travel patterns by time of day and day of the year. Specifically, the covariance effects of vehicular traffic demands between various OD pairs and the inter-relationships of travel time between different links during multiple time periods have been explicitly modeled to determine the optimal traffic sensor locations. The three research objectives outlined in Section 1.2 of Chapter 1 have been achieved in this thesis.

The first contribution of this research corresponds to Objective 1. A traffic sensor (i.e., traffic count) location model is proposed to estimate the mean and covariance of OD demand under uncertainty, as presented in Chapter 3. A new criterion named WMPRE is introduced to explicitly measure the stochasticity of OD demand estimates. The following research findings from Chapter 3 are summarized:

- It is found in numerical examples of Chapter 3 that the weighted-sum approach,

WMPRE ($(1-\alpha)$WMPREM + αWMPREC) is a generalized criterion for optimizing traffic sensor location schemes in practice, in contrast to the use of the MPREM only as a criterion. For a given traffic sensor location scheme and weighting parameter α, the values of WMPREM and WMPREC could not both reach the optimum at the same time. When the total number of traffic sensors increases, the variances of WMPREM and WMPREC would both change with different impacts on the SLP solutions.

- To get the Pareto optimal solutions of sensor locations, a Pareto front approach may be used to solve the bi-objective problem concerned. However, no unique optimal solutions could be obtained from the Pareto front approach, as demonstrated in Section 3.6. In contrast, the weighted-sum approach is more practical to determine a unique sensor location scheme when the weighting parameter can be specified based on traffic planners' preference in the mean or covariance of OD demand.

- The estimation of mean OD demands is less accurate under congested conditions compared to that under uncongested conditions. However, the estimation of OD demand covariances would be more accurate when the traffic network becomes congested. The data observed under congested conditions could provide more information about the covariance of OD demands as more travelers may choose joint travel and trip chaining strategies for their daily trips.

- The performance and convergence of the proposed model and solution algorithm have also been testified using the Sioux Falls network. To solve the bi-objective optimization problem, the FA has been adapted and improved for the weighted-sum approach and the Pareto front approach, respectively. To better understand the efficiency of the improved FA, the widely used classical

GA is also applied for comparison. It can be concluded from the numerical example in Section 6.2 that the improved FA can dramatically reduce the computation time for convergence.

The second contribution of the research relates to Objective 2. Both the spatial and temporal covariance of traffic demand between different OD pairs during different hourly periods are incorporated in the multi-type traffic sensor location model proposed in Chapter 4. The following research findings from Chapter 4 are summarized:

- The consideration of multi-period OD demand covariance can efficiently reduce the uncertainty of OD estimates and increase the average estimation accuracy regardless of traffic congestion conditions. During congestion periods in the daytime, the multi-period OD demands are highly correlated with one another. As such, the multi-period SLP model outperforms the single-period model even for the OD demand estimates in its own period under congested conditions. Therefore, it is recommended to design a multi-type traffic sensor network for multi-period OD demand estimation and to incorporate the multi-period covariance relationship of OD demand, particularly in peak hour periods on weekdays and weekends.

- For multi-period OD demand estimation, both the number and locations of multi-type traffic sensors, including point sensors and AVI sensors, can be optimized using the proposed model. It has been proved mathematically and numerically that a combination of information from both types outperforms the utilization of single-type sensors for multi-period OD demand estimation. This finding is true particularly when the measurement errors of AVI sensors and point sensors do not differ remarkably. Having established that additional data

can be provided by multi-period OD demands, a PCA-based Kalman filter method is adopted to extract the essential features of the OD demands and enhance the estimation efficiency. It has been demonstrated that the adoption of PCA can significantly reduce the computation time while guaranteeing the optimal location scheme of multi-type traffic sensors.

The third contribution corresponding to Objective 3 is achieved in Chapter 5. An integrated sensor location model is proposed for simultaneous estimation of OD demands and link travel times in a road network under uncertainty. The following research findings from Chapter 5 are summarized:

- The accuracy of stochastic OD demand and link travel time estimates can be increased by considering their spatial covariance effects. Numerical results highlight that the integration of link flow and travel time information can increase the accuracy of estimates of the stochastic OD demands and link travel times for the entire road network. The estimated OD demands can be used to determine the hourly link flows for the study road network, thereby facilitating automatic and large-scale traffic count surveys (e.g., the ATC in Hong Kong (Traffic and Transport Survey Division, 2018)). Moreover, the estimated link travel times and corresponding link speeds could be used to support various transport planning studies and traffic monitoring purposes.

- To obtain more comprehensive information for the simultaneous estimation problem, different types of stationary sensor data should be used in a coordinated manner, especially in a big data environment for smart city development. According to the real-world case study shown in Chapter 5 with empirical data, under the budget constraint, more point sensors should be used for simultaneous estimation as they are less expensive than AVI sensors. AVI

sensors that provide path travel time information are normally more cost-effective than point sensors for improving the accuracy of estimates of link travel time, especially for paths with many links but few point sensors. In practical scenarios, more point sensors should be installed on paths with many interruptions from traffic lights and at-grade junctions, as these traffic interruptions would make it difficult to estimate the stochastic link travel times and OD demands accurately.

6.2 Recommendations for further studies

It should be acknowledged that even though the research presented in this thesis covers a broad horizon of SLPs for estimation of vehicular travel demand and link/path travel time with uncertainty, several interesting and pivotal extensions merit further studies. Some of these potential directions are outlined below:

1. The efficiency of the improved firefly algorithm has been demonstrated in Chapters 3, 4, and 5 with numerical examples in a real-world road network in Hong Kong. A more advanced metaheuristic algorithm could be further investigated to improve the computational efficiency for larger-size realistic road networks (Zhu et al., 2014; Xiang et al., 2015; Yu et al., 2019).

2. It would be worth exploring to extend the proposed models to consider the effects of multi-user classes and their covariances in SLPs for a multi-modal traffic network (Sumalee et al., 2011; Munizaga and Palma, 2012; Zangui et al., 2015; Fu and Lam, 2018). This extension can be supported by additional available information on vehicle composition and occupancy, such as from ATC data in Hong Kong (Transport Department, 2021b).

3. The use of the reliability-based stochastic user equilibrium model or AVI data can be further investigated for assessing the impacts of the updated stochastic link choice proportions on the SLP.

4. It is important to assess the cost-effectiveness of various traffic-sensor locations. This could be achieved by measuring whether a given location leads to a reduction in the error of estimates of link speed and link flow per unit of additional budget (Matute and Chester, 2015). Such examinations of cost-effectiveness should be carried out in future studies.

5. The quality and reliability of the information provided by sensors highly depend on various sources of uncertainties such as sensor measurement error and systematic error from sensor failure (Vanajakshi and Rilett, 2006**,** Turner et al., 1999). Even though under normal conditions, the data obtained from traffic sensors can still be adulterated with measurement errors (Payne et al., 1976, Xu et al., 2016). To establish a more reliable sensor network, heterogeneous SLPs should be studied considering multiple-source uncertainties of sensors (Hu et al., 2015; Gu et al., 2020). In addition to demand variation, supply variation caused by extreme weather conditions or traffic accidents should be considered when determining network vulnerability in sensor location problems.

6. A limitation of the proposed models is that the link flow obtained by assigning OD demands onto the study road network may exceed the link capacity, especially under congested conditions. However, from empirical data collected from traffic sensors, the traffic flow under congestion will not be larger than the link capacity in accordance with the link-based fundamental diagrams. To address this issue, a novel reliability-based dynamic traffic assignment model merits further studies for solving SLPs in congested road networks (Li et al., 2015).

Appendix A Proofs of mathematical properties in Chapter 3

The matrix $\mathbf{M}^{\boldsymbol{\lambda}}$ in Eq. (3.41) in Chapter 3 could be obtained as follows:

$$\mathbf{M}^{\lambda}\mathrm{vec}(\boldsymbol{\lambda}^{\mathrm{cov}}) = \mathbf{0} \tag{A.1}$$

$$\tilde{\mathrm{P}}\Sigma^{\mathrm{q}}\boldsymbol{\lambda}^{\mathrm{cov}}\tilde{\mathrm{P}}^{T} = \mathbf{0} \tag{A.2}$$

Set $\boldsymbol{A} = \tilde{\mathrm{P}}\Sigma^{\boldsymbol{q}}$,

$$\tilde{\mathrm{P}}\Sigma^{\mathrm{q}}\boldsymbol{\lambda}^{\mathrm{cov}}\tilde{\mathrm{P}}^{T} = \mathbf{A}\boldsymbol{\lambda}^{\mathrm{cov}}\tilde{\mathrm{P}}^{T} \tag{A.3}$$

$$\mathbf{M}^{\lambda} = [a_1 \otimes p_1 \;\; a_2 \otimes p_1 \;\; \ldots \;\; a_{\tilde{m}} \otimes p_1 \;\; a_2 \otimes p_2 \;\; \ldots \;\; a_{\tilde{m}} \otimes p_2 \;\; \ldots \;\; a_{\tilde{m}} \otimes p_{\tilde{m}}]^{T} \tag{A.4}$$

Proofs of mathematical properties in Chapter 3 are given below:

Proof of property 3.1.

Define $Y = \Sigma^{\mathrm{q}}\tilde{\mathrm{P}}^{\mathrm{T}}$, the Eq. (3.7) can be rewritten as:

$$\Sigma^{\mathrm{v}} = \tilde{\mathrm{P}}Y \tag{A.5}$$

For convenience, matrices $\Sigma^{\boldsymbol{v}}$ and Y is partitioned by column vectors as follows.

$$\Sigma^{\mathrm{v}} = [\sigma_1, \sigma_2, ..., \sigma_m] \tag{A.6}$$

$$Y = [y_1, y_2, ...y_m] \tag{A.7}$$

According to Eqs. (A.6) and (A.7), Eq. (A.5) can be rewritten as:

$$[\sigma_1, \sigma_2, ..., \sigma_m] = \tilde{\mathrm{P}}[y_1, y_2, ...y_m] \tag{A.8}$$

If $\tilde{\mathrm{P}}$ is a matrix with full column rank, the system of linear equations $\sigma_i = \tilde{P}y_i$ ($i = 1, 2, ..., m$) has a unique solution. In other words, the matrix $Y = [y_1, y_2, \ldots y_m]$ would also have a unique solution.

Transpose both sides of the equation $Y = \Sigma^{\mathrm{q}}\tilde{\mathrm{P}}^{\mathrm{T}}$, it follows that

$$Y^{T} = \tilde{\mathrm{P}}\Sigma^{\mathrm{q}T} \tag{A.9}$$

Using the similar matrix partition method, it can be proved that when $\tilde{\mathrm{P}}$ is a matrix with full column rank, $\Sigma^{\mathrm{q}T}$ can be uniquely identified according to Eq. (A.9)

provided Y is unique. Then, the OD demand covariance Σ^{q} can be uniquely identified if $\widetilde{P}$ is a matrix with full column rank. This is the end of the proof.

Proof of property 3.2.

Yang et al. (1991) proved that the WMPREM ($G(\boldsymbol{\lambda}^{mean})$) is finite if and only if the traffic flows between any OD pair are observed by at least one traffic sensor location. Thus, it only needs to prove the case where finite WMPREC ($H(\boldsymbol{\lambda}^{cov})$) is the necessary condition of OD Covering Rule to complete the proof of Property 3.2.

According to condition (ii) in the text, the relationship between covariance and mean OD demands can be obtained as follow

$$\sigma_{w,w'} = r_{w,w'}(c_w q_w)(c_{w'} q_{w'}) = r_{w,w'}(c_w c_{w'})(q_w q_{w'}) \tag{A.10}$$

According to the definitions of λ_w^{mean}, $\lambda_{w,w'}^{cov}$ and Eq. (A.10), the following relationships can be obtained,

$$\lambda_w^{mean} = (q_w^* - q_w)/q_w = q_w^*/q_w - 1 \tag{A.11}$$

$$\lambda_{w'}^{mean} = (q_{w'}^* - q_w)/q_{w'} = q_{w'}^*/q_{w'} - 1 \tag{A.12}$$

$$\lambda_{w,w'}^{\mathrm{cov}} = (\sigma_{w,w'}^* - \sigma_{w,w'})/\sigma_{w,w'}$$

$$= (r_{w,w'} c_w c_{w'} q_w^* q_{w'}^* - r_{w,w'} c_w c_{w'} q_w q_{w'})/r_{w,w'} c_w c_{w'} q_w q_{w'}$$

$$= q_w^* q_{w'}^*/q_w q_{w'} - 1 \tag{A.13}$$

For convenience, denote $x = q_w^*/q_w$ and $y = q_{w'}^*/q_{w'}$, then it follows

$\lambda_w^{mean} = x-1$, $\lambda_{w'}^{mean} = y-1$, and $\lambda_{w,w'}^{\mathrm{cov}} = xy-1$

According to the identity relation $xy-1=(x-1)+(y-1)+(x-1)(y-1)$, it follows that

$$\lambda_{w,w'}^{\mathrm{cov}} = \lambda_w^{mean} + \lambda_{w'}^{mean} + \lambda_w^{mean}\lambda_{w'}^{mean} \tag{A.14}$$

Thus, $\lambda_{w,w'}^{cov}$ is finite because λ_w^{mean} is finite. Then, it can be seen that WMPREM ($G(\boldsymbol{\lambda}^{mean})$) and WMPREC ($H(\boldsymbol{\lambda}^{cov})$) are both finite according to Eqs. (3.13) and

(3.24), This is the end of the proof.

Proof of property 3.3.

Similar to the proof of Property 3.2, it only needs to prove the WMPREC ($H(\boldsymbol{\lambda}^{cov})$) is finite if the OD Covering Rule is satisfied. The method of reduction to absurdity is used. It is assumed that WMPREC ($H(\boldsymbol{\lambda}^{cov})$) is infinite, and the OD Covering Rule is satisfied. On the one hand, it follows from the infinity $H(\boldsymbol{\lambda}^{cov})$ that there exists at least one $\lambda^{cov}_{w_0,w'_0}$ ($w_0, w'_0 \in \mathbf{W}$), which is infinite (say take any real value greater than -1). On the other hand, as the OD Covering Rule is satisfied, for OD pairs $w_0, w'_0 \in \mathbf{W}$, there exist at least two (not necessarily different) traffic sensor locations to collect the traffic flows of these two OD pairs. Mathematically, there exist $a, b \in \widetilde{\mathbf{A}}$ such that $p_{a,w_0} \neq 0$ and $p_{b,w'_0} \neq 0$. It then follows that $p_{a,w_0} p_{b,w'_0} \neq 0$. According to Eq. (3.27b), it follows that

$$\lambda^{\text{cov}}_{w_0,w'_0} = \frac{-\sum_{w\in\mathbf{W},w\neq w_0}\sum_{w'\in\mathbf{W},w'\neq w'_0} p_{a,w}p_{b,w'}\sigma^{q}_{w,w'}\lambda^{\text{cov}}_{w,w'}}{p_{a,w_0}p_{b,w'_0}\sigma^{q}_{w_0,w'_0}} \tag{A.15}$$

$\Rightarrow$

$$\lambda^{\text{cov}}_{w_0,w'_0} = \frac{\sum_{w\in\mathbf{W},w\neq w_0}\sum_{w'\in\mathbf{W},w'\neq w'_0} p_{a,w}p_{b,w'} - (\sigma^{q}_{w,w'}\lambda^{\text{cov}}_{w,w'})}{p_{a,w_0}p_{b,w'_0}\sigma^{q}_{w_0,w'_0}} \tag{A.16}$$

$$\lambda^{\text{cov}}_{w,w'} \geq -1 \Rightarrow -\lambda^{\text{cov}}_{w,w'} \leq 1 \tag{A.17}$$

According to condition (ii), it follows that

$$\sigma^{q}_{w,w'} > 0 \quad \forall w, w' \in \mathbf{W} \tag{A.18}$$

Then, it follows from Ineqs. (A.17) and (A.18) that

$$-\sigma^{q}_{w,w'}\lambda^{\text{cov}}_{w,w'} \leq \sigma^{q}_{w,w'} \quad \forall w, w' \in \mathbf{W} \tag{A.19}$$

It follows from Eq. (A.16) and Ineq. (A.19) that

$$\lambda^{\text{cov}}_{w_0,w'_0} \leq \frac{\sum_{w\in\mathbf{W},w\neq w_0}\sum_{w'\in\mathbf{W},w'\neq w'_0} p_{a,w}p_{b,w'}\sigma^{q}_{w,w'}}{p_{a,w_0}p_{b,w'_0}\sigma^{q}_{w_0,w'_0}} \overset{define}{=} c^{\text{cov}}_{w_0,w'_0} \tag{A.20}$$

where $c^{cov}_{w_0,w'_0}$ is a positive constant, which is the upper bound of $\lambda^{cov}_{w_0,w'_0}$. Thus,

$\lambda^{cov}_{w_0,w'_0}$ is bounded, which contradicts the infinity assumption of $\lambda^{cov}_{w_0,w'_0}$. Therefore, $H(\boldsymbol{\lambda}^{cov})$ is bounded if the OD Covering Rule is satisfied. The proof of necessary condition is completed.

Appendix B Proofs of mathematical properties in Chapter 4

The matrix calculated from the equation $\Theta_0\boldsymbol{\Sigma}_{c0}\Theta_0^T + \boldsymbol{\Sigma}_e$ in Eq. (4.20a) is always invertible, with the assumption that the measurement errors on different links are independent and their variances are not equal to zero.

Proof: Note that $\Theta_0\boldsymbol{\Sigma}_{c0}\Theta_0^T = \boldsymbol{\Sigma}_{v0}$ is the covariance of the prior link flows. According to linear algebra, the covariance matrix $\boldsymbol{\Sigma}_{v0}$ is always positive semi-definite and thus invertible. In addition, the covariance matrix of measurement error $\boldsymbol{\Sigma}_e$ is positive definite if the measurement errors of different links are independent and their variances are not equal to zero. Therefore, the summation of these two matrices is positive definite and thus invertible. The proof has been completed.

Proofs of mathematical properties in Chapter 4 are given below:

Proof of Proposition 4.1

The mathematical expression of Proposition 4.1 is equivalent to the following.

Given z^*, then $tr(\boldsymbol{\Sigma}_c - \boldsymbol{\Sigma}_{c0})_{m\text{cov}} \geq tr(\boldsymbol{\Sigma}_c - \boldsymbol{\Sigma}_{c0})_{b\text{cov}} \geq tr(\boldsymbol{\Sigma}_c - \boldsymbol{\Sigma}_{c0})_{no\text{cov}}$, where $tr(\boldsymbol{\Sigma}_c - \boldsymbol{\Sigma}_{c0})_{m\text{cov}}$, $tr(\boldsymbol{\Sigma}_c - \boldsymbol{\Sigma}_{c0})_{b\text{cov}}$, and $tr(\boldsymbol{\Sigma}_c - \boldsymbol{\Sigma}_{c0})_{no\text{cov}}$ are the uncertainty reductions considering the covariance of OD demand in multiple periods, the covariance in one period, and no covariance, respectively.

First, let us define three mapping functions $\Gamma(A), Diag(A), \text{and } BDiag(A,t)$ for matrix A as follows:

$$A = \begin{bmatrix} a_{11} & a_{12} & \cdots & a_{1n} \\ a_{21} & a_{22} & \cdots & a_{2n} \\ \vdots & \vdots & \ddots & \vdots \\ a_{n1} & a_{n2} & \cdots & a_{nn} \end{bmatrix}. \tag{B.1}$$

A is an $n \times n$ matrix.

$$\Gamma(A)=\begin{bmatrix} |a_{11}| & |a_{12}| & \cdots & |a_{1n}| \\ |a_{21}| & |a_{22}| & \cdots & |a_{2n}| \\ \vdots & \vdots & \ddots & \vdots \\ |a_{n1}| & |a_{n2}| & \cdots & |a_{nn}| \end{bmatrix} \tag{B.2}$$

The function $\Gamma(A)$ obtains the absolute values of all elements for matrix A.

$$Diag(A)=\begin{bmatrix} a_{11} & & & \\ & a_{22} & & \\ & & \ddots & \\ & & & a_{nn} \end{bmatrix} \tag{B.3}$$

The function $Diag(A)$ extracts the diagonal elements for matrix A and forms a new diagonal matrix.

$$BDiag(A,t)=\begin{bmatrix} a_{11} & \cdots & a_{1t} & & & & \\ \vdots & \ddots & \vdots & & & & \\ a_{t1} & \cdots & a_{tt} & & & & \\ & & & \ddots & & & \\ & & & & a_{n-t+1,n-t+1} & \cdots & a_{n-t+1,n} \\ & & & & \vdots & \ddots & \vdots \\ & & & & a_{n,n-t+1} & \cdots & a_{nn} \end{bmatrix} \tag{B.4}$$

The function $BDiag(A,t)$ extracts the block diagonal elements for matrix A and forms a new block diagonal matrix. The size of each block is t by t.

To prove Proposition 4.1, recall the matrix inversion lemma, which states that $(A-B)^{-1}=B^{-1}(B^{-1}-A^{-1})^{-1}A^{-1}$.

The following equations are deduced:

$$\begin{aligned} (\boldsymbol{\Sigma}_c-\boldsymbol{\Sigma}_{c0})^{-1} &= \boldsymbol{\Sigma}_{c0}{}^{-1}(\boldsymbol{\Sigma}_{c0}{}^{-1}-\boldsymbol{\Sigma}_c{}^{-1})^{-1}\boldsymbol{\Sigma}_c{}^{-1} \\ &= -\boldsymbol{\Sigma}_{c0}{}^{-1}(\Theta_0^T\boldsymbol{\Sigma}_e^{-1}\Theta_0+\Theta'^T_0\,\boldsymbol{\Sigma}'^{-1}_e\,\Theta'_0)^{-1}\boldsymbol{\Sigma}_c{}^{-1} \\ &= -\boldsymbol{\Sigma}_{c0}{}^{-1}(\Theta_0^T\boldsymbol{\Sigma}_e^{-1}\Theta_0+\Theta'^T_0\,\boldsymbol{\Sigma}'^{-1}_e\,\Theta'_0)^{-1}(\boldsymbol{\Sigma}_{c0}{}^{-1}+\Theta_0^T\boldsymbol{\Sigma}_e^{-1}\Theta_0+\Theta'^T_0\,\boldsymbol{\Sigma}'^{-1}_e\,\Theta'_0) \\ &= -\boldsymbol{\Sigma}_{c0}{}^{-1}(\Theta_0^T\boldsymbol{\Sigma}_e^{-1}\Theta_0+\Theta'^T_0\,\boldsymbol{\Sigma}'^{-1}_e\,\Theta'_0)^{-1}\boldsymbol{\Sigma}_{c0}{}^{-1}-\boldsymbol{\Sigma}_{c0}{}^{-1}. \end{aligned} \tag{B.5}$$

Performing the inversion operation on both sides of the above equation, then

$$\boldsymbol{\Sigma}_c-\boldsymbol{\Sigma}_{c0}=-\left(\boldsymbol{\Sigma}_{c0}{}^{-1}(\Theta_0^T\boldsymbol{\Sigma}_e^{-1}\Theta_0+\Theta'^T_0\,\boldsymbol{\Sigma}'^{-1}_e\,\Theta'_0)^{-1}\boldsymbol{\Sigma}_{c0}{}^{-1}+\boldsymbol{\Sigma}_{c0}{}^{-1}\right)^{-1}. \tag{B.6}$$

If the covariance of OD demand is not considered, it implies that all of the OD pairs

are considered as independent, thus $\boldsymbol{\Sigma}_{c0} = Diag(\boldsymbol{\Sigma}_{c0})$ and $\boldsymbol{\Sigma}_c = Diag(\boldsymbol{\Sigma}_c)$.

Then,

$$tr(\boldsymbol{\Sigma}_c - \boldsymbol{\Sigma}_{c0}) = -\Big(Diag({\boldsymbol{\Sigma}_{c0}}^{-1})\left(\Theta_0^T\boldsymbol{\Sigma}_e^{-1}\Theta_0 + \Theta'^T_0{\boldsymbol{\Sigma}'_e}^{-1}\Theta'_0\right)^{-1}Diag({\boldsymbol{\Sigma}_{c0}}^{-1}) + Diag({\boldsymbol{\Sigma}_{c0}}^{-1})\Big)^{-1}.$$

If only the covariance of OD demand in a single period is incorporated, then the OD demands in period h_1 should be independent of those in period h_2. Given that there are *k* periods of interest, thus $\boldsymbol{\Sigma}_{c0} = BDiag(\boldsymbol{\Sigma}_{c0}, k)$ and $\boldsymbol{\Sigma}_c = BDiag(\boldsymbol{\Sigma}_c, k)$. Then,

$$tr(\boldsymbol{\Sigma}_c - \boldsymbol{\Sigma}_{c0}) = -\Big(BDiag({\boldsymbol{\Sigma}_{c0}}^{-1}, k)(\Theta_0^T\boldsymbol{\Sigma}_e^{-1}\Theta_0 + \Theta'^T_0\boldsymbol{\Sigma}'^{-1}_e\Theta'_0)^{-1}BDiag({\boldsymbol{\Sigma}_{c0}}^{-1}, k) + BDiag({\boldsymbol{\Sigma}_{c0}}^{-1}, k)\Big)^{-1}.$$

As $\boldsymbol{\Sigma}_e$ and $\boldsymbol{\Sigma}'_e$ are both positive definite, the inversion of these two matrices gives ${\boldsymbol{\Sigma}_e}^{-1}$ and ${\boldsymbol{\Sigma}'_e}^{-1}$, which are also positive definite, so that all of the elements in the matrix $\Theta_0^T\boldsymbol{\Sigma}_e^{-1}\Theta_0 + \Theta'^T_0\boldsymbol{\Sigma}'^{-1}_e\Theta'_0$ are positive.

Therefore,

$$\begin{aligned}
&{\boldsymbol{\Sigma}_{c0}}^{-1}(\Theta_0^T\boldsymbol{\Sigma}_e^{-1}\Theta_0 + \Theta'^T_0\boldsymbol{\Sigma}'^{-1}_e\Theta'_0)^{-1}{\boldsymbol{\Sigma}_{c0}}^{-1} \\
&\geq BDiag({\boldsymbol{\Sigma}_{c0}}^{-1}, k)(\Theta_0^T\boldsymbol{\Sigma}_e^{-1}\Theta_0 + \Theta'^T_0\boldsymbol{\Sigma}'^{-1}_e\Theta'_0)^{-1}BDiag({\boldsymbol{\Sigma}_{c0}}^{-1}, k) \\
&\geq Diag({\boldsymbol{\Sigma}_{c0}}^{-1})(\Theta_0^T\boldsymbol{\Sigma}_e^{-1}\Theta_0 + \Theta'^T_0\boldsymbol{\Sigma}'^{-1}_e\Theta'_0)^{-1}Diag({\boldsymbol{\Sigma}_{c0}}^{-1}). \qquad \text{(B.7)}
\end{aligned}$$

Thus, if the traffic sensor locations are given, then

$$tr(\boldsymbol{\Sigma}_c - \boldsymbol{\Sigma}_{c0})_{m\,\mathrm{cov}} \geq tr(\boldsymbol{\Sigma}_c - \boldsymbol{\Sigma}_{c0})_{b\,\mathrm{cov}} \geq tr(\boldsymbol{\Sigma}_c - \boldsymbol{\Sigma}_{c0})_{no\,\mathrm{cov}}. \qquad \text{(B.8)}$$

The proof is completed.

Proof of Proposition 4.2

Mathematically, assume that the unit costs of AVI sensors and point sensors have the following relationship: $\beta' = \alpha \cdot \beta$. Denote $[\alpha]$ as a floor function that gives the greatest integer less than or equal to α.

Case 1: If $\left(\Theta'_{rw(h)}\right)^2\left(\varepsilon'_{r(h)}\right)^{-1} > \max\sum_{a=1}^{[\alpha]}\left(\left(\Theta_{aw(h)}\right)^2\left(\varepsilon_{a(h)}\right)^{-1}\right)$ for $\forall r \in \mathbf{R}, a \in \mathbf{A}$, only AVI sensors should be chosen for the multi-period OD demand estimation.

Case 2: Conversely, if $\left(\Theta'_{rw(h)}\right)^2\left(\varepsilon'_{r(h)}\right)^{-1} < \min\sum_{a=1}^{[\alpha]}\left(\left(\Theta_{aw(h)}\right)^2\left(\varepsilon_{a(h)}\right)^{-1}\right)$ for $\forall r \in \mathbf{R}, a \in \mathbf{A}$, only point sensors should be chosen.

Case 3: However, if $\exists r \in \mathbf{R}, a \in \mathbf{A}$ so that $\min\sum_{a=1}^{[\alpha]}\left(\left(\Theta_{aw(h)}\right)^2\left(\varepsilon_{a(h)}\right)^{-1}\right) \le \left(\Theta'_{rw(h)}\right)^2\left(\varepsilon'_{r(h)}\right)^{-1} \le \max\sum_{a=1}^{[\alpha]}\left(\left(\Theta_{aw(h)}\right)^2\left(\varepsilon_{a(h)}\right)^{-1}\right)$, both AVI and point sensors are needed.

First, Case 1 is proved. As shown in Eq. (4.22a), the objective of the multi-type traffic SLP is restated as:

$$\min_{z,z'}\sum_{w\in\mathbf{W},h\in\mathbf{H}}\left(\sum_{w'\in\mathbf{W},h'\in\mathbf{H}}|\sigma_{w(h),w'(h')}|\right)\sigma_{w(h)} \quad . \tag{B.9}$$

For a clear presentation, denote $\kappa_{w(h)} = \sum_{w'\in\mathbf{W},h'\in\mathbf{H}}|\sigma_{w(h),w'(h')}|$, so that the above equation then becomes

$$\min_{z,z'}\sum_{w\in\mathbf{W},h\in\mathbf{H}}\kappa_{w(h)}\sigma_{w(h)}$$

$$\Rightarrow \min_{z,z'}\sum_{w\in\mathbf{W},h\in\mathbf{H}}\kappa_{w(h)}\left(\sigma_{w(h)0}{}^{-1}+\sum_{a\in\mathbf{A}}(\Theta_{aw0(h)})^2(\varepsilon_{a(h)})^{-1}+\sum_{r\in\mathbf{R}}(\Theta'_{rw0(h)})^2(\varepsilon'_{r(h)})^{-1}\right)^{-1}. \tag{B.10}$$

For Case 1, if $\left(\Theta'_{rw(h)}\right)^2\left(\varepsilon'_{r(h)}\right)^{-1} > \max\sum_{a=1}^{[\alpha]}\left(\left(\Theta_{aw0(h)}\right)^2\left(\varepsilon_{a(h)}\right)^{-1}\right)$ for $\forall r \in \mathbf{R}, a \in \mathbf{A}$, given the fixed budget constraint $\beta\sum z + \beta'\sum z' \le B$ and $\beta' = \alpha\cdot\beta$, it is always satisfied that

$$\left(\Theta'_{rw(h)}\right)^2\left(\varepsilon'_{r(h)}\right)^{-1} < \left(\max\sum_{a=1}^{[\alpha]}\left(\left(\Theta_{aw0(h)}\right)^2\left(\varepsilon_{a0(h)}\right)^{-1}\right)\right)^{-1} \text{ for } \forall r \in \mathbf{R}, a \in \mathbf{A}.$$

As $\kappa_{w(h)} \ge 0$, the above equation implies that

$$\min_{z,z'}\sum_{w\in\mathbf{W},h\in\mathbf{H}}\kappa_{w(h)}\left(\sigma_{w(h)0}{}^{-1}+\sum_{r\in\mathbf{R}}(\Theta'_{rw0(h)})^2(\varepsilon'_{r(h)})^{-1}\right)^{-1}$$

$$\leq \min_{z,z'} \sum_{w\in\mathbf{W},h\in\mathbf{H}} \kappa_{w(h)} \left({\sigma_{w(h)0}}^{-1} + \sum_{a\in\mathbf{A}} (\Theta_{aw0(h)})^2 (\varepsilon_{a(h)})^{-1} + \sum_{r\in\mathbf{R}} (\Theta'_{rw0(h)})^2 (\varepsilon'_{r(h)})^{-1} \right)^{-1}, \tag{B.11}$$

s. t.

$$\beta \sum z + \beta' \sum z' \leq B \quad . \tag{B.12}$$

The proof of Case 1 is completed. Cases 2 and 3 can be easily proved in a similar way.

Appendix C KL divergence between two multivariate normal distributions

In Chapter 5, to derive the KL divergence between two OD demand vectors following multivariate normal distributions, recall the pdf of an OD demand vector following a multivariate normal distribution $\mathbf{X}\sim N_M(\boldsymbol{\mu},\boldsymbol{\Sigma})$:

$$f_{\mathbf{X}}(\mathbf{X})=\frac{1}{(2\pi)^{d/2}\left|\boldsymbol{\Sigma}\right|^{1/2}}\exp\left(-\frac{1}{2}(\mathbf{X}-\boldsymbol{\mu})^{T}\boldsymbol{\Sigma}^{-1}(\mathbf{X}-\boldsymbol{\mu})\right). \tag{C.1}$$

Let us focus on two M-dimensional OD demand vectors $\mathbf{X}\sim N_M(\boldsymbol{\mu_x},\boldsymbol{\Sigma_x})$ and $\mathbf{Y}\sim N_M(\boldsymbol{\mu_y},\boldsymbol{\Sigma_y})$, the KL divergence between these two OD demand vectors is

$$D_{KL}(\mathbf{X}\,\|\,\mathbf{Y})=\int_{\mathbb{R}^M} f_{\mathbf{X}}(\mathbf{x})\log\frac{f_{\mathbf{X}}(\mathbf{x})}{g_{\mathbf{Y}}(\mathbf{x})}d\mathbf{x} \tag{C.2}$$

$$=\int_{\mathbb{R}^M} f_{\mathbf{X}}(\mathbf{x})\log f_{\mathbf{X}}(\mathbf{x})d\mathbf{x}-\int_{\mathbb{R}^M} f_{\mathbf{X}}(\mathbf{x})\log g_{\mathbf{Y}}(\mathbf{x})d\mathbf{x} \tag{C.3}$$

$$=\int_{\mathbb{R}^M} f_{\mathbf{X}}(\mathbf{x})\left[\frac{1}{2}\log\frac{\left|\boldsymbol{\Sigma}_y\right|}{\left|\boldsymbol{\Sigma}_x\right|}-\frac{1}{2}(\mathbf{X}-\boldsymbol{\mu}_x)^{T}\boldsymbol{\Sigma}_x^{-1}(\mathbf{X}-\boldsymbol{\mu}_x)+\frac{1}{2}(\mathbf{X}-\boldsymbol{\mu}_y)^{T}\boldsymbol{\Sigma}_y^{-1}(\mathbf{X}-\boldsymbol{\mu}_y)\right]d\mathbf{x} \tag{C.4}$$

$$=\frac{1}{2}\log\frac{\left|\boldsymbol{\Sigma}_y\right|}{\left|\boldsymbol{\Sigma}_x\right|}-\frac{1}{2}\int_{\mathbb{R}^M} f_{\mathbf{X}}(\mathbf{x})\left[(\mathbf{X}-\boldsymbol{\mu}_x)^{T}\boldsymbol{\Sigma}_x^{-1}(\mathbf{X}-\boldsymbol{\mu}_x)\right]d\mathbf{x}+\frac{1}{2}\int_{\mathbb{R}^M} f_{\mathbf{X}}(\mathbf{x})\left[(\mathbf{X}-\boldsymbol{\mu}_y)^{T}\boldsymbol{\Sigma}_y^{-1}(\mathbf{X}-\boldsymbol{\mu}_y)\right]d\mathbf{x}. \tag{C.5}$$

According to the Matrix Cookbook (Petersen and Pedersen, 2012), the second term can be rewritten as follow:

$$\frac{1}{2}\int_{\mathbb{R}^M} f_{\mathbf{X}}(\mathbf{x})\left[(\mathbf{X}-\boldsymbol{\mu}_x)^{T}\boldsymbol{\Sigma}_x^{-1}(\mathbf{X}-\boldsymbol{\mu}_x)\right]d\mathbf{x} \tag{C.6}$$

$$=\frac{1}{2}\mathrm{E}\left[tr\left\{(\mathbf{X}-\boldsymbol{\mu}_x)^{T}\boldsymbol{\Sigma}_x^{-1}(\mathbf{X}-\boldsymbol{\mu}_x)\right\}\right] \tag{C.7}$$

$$=\frac{1}{2}\mathrm{E}\left[tr\left\{(\mathbf{X}-\boldsymbol{\mu}_x)(\mathbf{X}-\boldsymbol{\mu}_x)^{T}\boldsymbol{\Sigma}_x^{-1}\right\}\right] \tag{C.8}$$

$$=\frac{1}{2}tr\left\{\boldsymbol{\Sigma}_x\boldsymbol{\Sigma}_x^{-1}\right\} \tag{C.9}$$

$$=\frac{M}{2}. \tag{C.10}$$

The third term can also be simplified as:

$$\frac{1}{2}\int_{\mathbb{R}^M} f_{\mathbf{X}}(\mathbf{x})\left[(\mathbf{X}-\boldsymbol{\mu}_y)^{T}\boldsymbol{\Sigma}_y^{-1}(\mathbf{X}-\boldsymbol{\mu}_y)\right]d\mathbf{x} \tag{C.11}$$

$$= \frac{1}{2}\mathrm{E}\left[tr\left\{ (\mathbf{X}-\boldsymbol{\mu}_y)^T \boldsymbol{\Sigma}_y^{-1} (\mathbf{X}-\boldsymbol{\mu}_y) \right\} \right] \tag{C.12}$$

$$= \frac{1}{2}(\boldsymbol{\mu}_x-\boldsymbol{\mu}_y)^T \boldsymbol{\Sigma}_y^{-1} (\boldsymbol{\mu}_x-\boldsymbol{\mu}_y) + \frac{1}{2} tr\left\{ \boldsymbol{\Sigma}_y^{-1}\boldsymbol{\Sigma}_x \right\}. \tag{C.13}$$

Combining Eqs. (C.5), (C.10), and (C.13), the following equation can be obtained:

$$D_{KL}(\mathbf{X} \| \mathbf{Y}) = \frac{1}{2}\left(\log\frac{|\boldsymbol{\Sigma}_y|}{|\boldsymbol{\Sigma}_x|} - M + tr\left(\left(\boldsymbol{\Sigma}_y\right)^{-1} \boldsymbol{\Sigma}_x \right) + (\boldsymbol{\mu}_x-\boldsymbol{\mu}_y)^T \boldsymbol{\Sigma}_y^{-1} (\boldsymbol{\mu}_x-\boldsymbol{\mu}_y) \right). \tag{C.14}$$

Appendix D Mean and covariance relationship between link flows and between link travel times

To derive the mean and covariance relationship between link flows and between link travel times in Eqs. (5.22) and (5.23), respectively in Chapter 5, recall the standard BPR link travel time function:

$$T_a = T_{a0}(1+\alpha(\frac{V_a}{c_a})^{\beta}) \quad \forall a \in \mathbf{A}, \tag{D.1}$$

where V_a represents the random variable of traffic flow on link a with mean v_a and variance σ_a^2. By taking an example of $\alpha = 0.15$ and $\beta = 4$, then

$$E\begin{pmatrix} V_{a_1}^4 \\ V_{a_2}^4 \\ \vdots \\ V_{a_m}^4 \end{pmatrix} = \begin{pmatrix} E(V_{a_1}^4) \\ E(V_{a_2}^4) \\ \vdots \\ E(V_{a_m}^4) \end{pmatrix}, \text{ and} \tag{D.2}$$

$$Var\begin{pmatrix} V_{a_1}^4 \\ V_{a_2}^4 \\ \vdots \\ V_{a_m}^4 \end{pmatrix} == \begin{pmatrix} E(V_{a_1}^8)-\left(E(V_{a_1}^4)\right)^2 & E(V_{a_1}^4V_{a_2}^4)-E(V_{a_1}^4)E(V_{a_2}^4) & \dots & E(V_{a_1}^4V_{a_m}^4)-E(V_{a_1}^4)E(V_{a_m}^4) \\ E(V_{a_2}^4V_{a_1}^4)-E(V_{a_2}^4)E(V_{a_1}^4) & E(V_{a_2}^8)-\left(E(V_{a_2}^4)\right)^2 & \dots & E(V_{a_2}^4V_{a_m}^4)-E(V_{a_2}^4)E(V_{a_m}^4) \\ \vdots & \vdots & \ddots & \vdots \\ E(V_{a_m}^4V_{a_1}^4)-E(V_{a_m}^4)E(V_{a_1}^4) & E(V_{a_m}^4V_{a_2}^4)-E(V_{a_m}^4)E(V_{a_2}^4) & \dots & E(V_{a_m}^8)-\left(E(V_{a_m}^4)\right)^2 \end{pmatrix}. \tag{D.3}$$

Based on probability theory and statistics (Isserlis, 1918), the moment generating function corresponding to the link flow $N(V_a; v_a, \sigma_a^2)$ as an example can be expressed as

$$M_{V_a}(t) = exp(v_a t + \frac{1}{2}{\sigma_a}^2 t^2). \tag{D.4}$$

The *n*th moment can be calculated by the *n*th derivative of the moment generating function, evaluated at $t = 0$:

$$E(V_a^n) = M_{V_a}^{(n)}(0) = \left.\frac{d^n M_{V_a}}{dt^n}\right|_{t=0}. \tag{D.5}$$

Taking the $E(V_a^4)$ and $E(V_a^8)$ as an example, the 4th and 8th moments are deduced as follow:

$$E(V_a^4) = M_{V_a}^{(4)}(0) = \left.\frac{d^4 M_{V_a}}{dt^4}\right|_{t=0} = v_a^4 + 6v_a^2\sigma_a^2 + 3\sigma_a^4, \tag{D.6}$$

$$E(V_a^8) = M_{V_a}^{(8)}(0) = \left.\frac{d^8 M_{V_a}}{dt^8}\right|_{t=0} = v_a^8 + 28v_a^6\sigma_a^2 + 210v_a^4\sigma_a^4 + 420v_a^2\sigma_a^6 + 105\sigma_a^8. \tag{D.7}$$

The functions $H_m(.)$ and $H_{cov}(.)$ for all links in a road network can then be derived.

References

Abbas, A., H. Cadenbach, A., Salimi, E., 2017. A Kullback–Leibler view of maximum entropy and maximum log-probability methods. Entropy 19, 232.

Akamatsu, T., 1996. Cyclic flows, Markov process and stochastic traffic assignment. Transportation Research Part B: Methodological 30, 369–386.

Altshuler, T., Altshuler, Y., Katoshevski, R., Shiftan, Y., 2019. Modeling and prediction of ride-sharing utilization dynamics. Journal of Advanced Transportation 2019.

Antoniou, C., Barceló, J., Breen, M., Bullejos, M., Casas, J., Cipriani, E., Ciuffo, B., Djukic, T., Hoogendoorn, S., Marzano, V., Montero, L., Nigro, M., Perarnau, J., Punzo, V., Toledo, T., van Lint, H., 2016. Towards a generic benchmarking platform for origin-destination flows estimation/updating algorithms: Design, demonstration and validation. Transportation Research Part C: Emerging Technologies 66, 79–98.

Antoniou, C., Ben-Akiva, M., Koutsopoulos, H.N., 2004. Incorporating automated vehicle identification data into origin-destination estimation. Transportation Research Record: Journal of the Transportation Research 1882, 37–44.

Ashok, K., Ben-Akiva, M.E., 1993. Dynamic origin-destination matrix estimation and prediction for real-time traffic management systems, in: Daganzo, C. (Ed.), Proceedings of the 12th International Symposium on Transportation. Elsevier, pp. 465–484.

Ballis, H., Dimitriou, L., 2020. Revealing personal activities schedules from synthesizing multi-period origin-destination matrices. Transportation Research Part B: Methodological 139, 224–258.

Ban, X. (Jeff), Chu, L., Herring, R., Margulici, J.D., 2011. Sequential modeling framework for optimal sensor placement for multiple intelligent transportation system applications. Journal of Transportation Engineering 137, 112–120.

Bhat, C.R., Goulias, K.G., Pendyala, R.M., Paleti, R., Sidharthan, R., Schmitt, L., Hu,

H.H., 2013. A household-level activity pattern generation model with an application for Southern California. Transportation 40, 1063–1086.

Bian, B., Zhu, N., Ling, S., Ma, S., 2015. Bus service time estimation model for a curbside bus stop. Transportation Research Part C: Emerging Technologies 57, 103–121.

Bianco, L., Confessore, G., Reverberi, P., 2001. A network based model for traffic sensor location with implications on O/D matrix estimates. Transportation Science 35, 50–60.

Bielli, M., Caramia, M., Carotenuto, P., 2002. Genetic algorithms in bus network optimization. Transportation Research Part C: Emerging Technologies 10, 19–34.

Bierlaire, M., 2002. The total demand scale: A new measure of quality for static and dynamic origin–destination trip tables. Transportation Research Part B: Methodological 36, 837–850.

Caggiani, L., Ottomanelli, M., Sassanelli, D., 2013. A fixed point approach to origin-destination matrices estimation using uncertain data and fuzzy programming on congested networks. Transportation Research Part C: Emerging Technologies 28, 130–141.

Cantarella, G.E., 1997. A general fixed-point approach to multimode multi-user equilibrium assignment with elastic demand. Transportation Science 31, 107–128.

Cantelmo, G., Qurashi, M., Prakash, A.A., Antoniou, C., Viti, F., 2020. Incorporating trip chaining within online demand estimation. Transportation Research Part B: Methodological 132, 171–187.

Carlin, B., Louis, T., Louis, T.A., 2000. Bayes and empirical bayes methods for data analysis, second edition, Chapman & Hall/CRC Texts in Statistical Science. Chapman and Hall/CRC.

Cascetta, E., 1984. Estimation of trip matrices from traffic counts and survey data: A generalized least squares estimator. Transportation Research Part B 18, 289–299.

Cascetta, E., 2009. Transportation systems analysis: models and applications, Springer

Science & Business Media.

Cascetta, E., Nguyen, S., 1988. A unified framework for estimating or updating origin/destination matrices from traffic counts. Transportation Research Part B: Methodological 22, 437–455.

Castillo, E., Grande, Z., Calviño, A., Szeto, W.Y., Lo, H.K., 2015. A state-of-the-art review of the sensor location, flow observability, estimation, and prediction problems in traffic networks. Journal of Sensors 2015.

Castillo, E., Menéndez, J.M., Sánchez-Cambronero, S., 2008a. Predicting traffic flow using Bayesian networks. Transportation Research Part B: Methodological 42, 482–509.

Castillo, E., Menéndez, J.M., Sánchez-Cambronero, S., 2008b. Traffic estimation and optimal counting location without path enumeration using Bayesian networks. Computer-Aided Civil and Infrastructure Engineering 23, 189–207.

Castillo, E., Rivas, A., Jiménez, P., Menéndez, J.M., 2012. Observability in traffic networks. Plate scanning added by counting information. Transportation 39, 1301–1333.

Chen, A., Ji, Z., Recker, W., 2002. Travel time reliability with risk-sensitive travelers. Transportation Research Record: Journal of the Transportation Research Board 1783, 27–33.

Chootinan, P., Chen, A., 2006. Constraint handling in genetic algorithms using a gradient-based repair method. Computers and Operations Research 33, 2263–2281.

Chootinan, P., Chen, A., 2011. Confidence interval estimation for path flow estimator. Transportation Research Part B: Methodological 45, 1680–1698.

Cipriani, E., Fusco, G., Gori, S., Petrelli, M., 2006. Heuristic methods for the optimal location of road traffic monitoring. IEEE Conference on Intelligent Transportation Systems, Proceedings, ITSC 1072–1077.

Clark, S., Watling, D., 2005. Modelling network travel time reliability under stochastic

demand. Transportation Research Part B: Methodological 39, 119–140.

Coifman, B., 2004. An assessment of loop detector and RTMS performance, California Path Program, Institute of Trasnportation Studies, University of California, Berkeley.

Danczyk, A., Liu, H.X., 2011. A mixed-integer linear program for optimizing sensor locations along freeway corridors. Transportation Research Part B: Methodological 45, 208–217.

Djukic, T., Flötteröd, G., Van Lint, H., Hoogendoorn, S., 2012. Efficient real time OD matrix estimation based on principal component analysis, in: IEEE Conference on Intelligent Transportation Systems, Proceedings, ITSC. pp. 115–121.

Duthie, J.C., Unnikrishnan, A., Waller, S.T., 2011. Influence of demand uncertainty and correlations on traffic predictions and decisions. Computer-Aided Civil and Infrastructure Engineering 26, 16–29.

Fei, X., Mahmassani, H.S., Murray-Tuite, P., 2013. Vehicular network sensor placement optimization under uncertainty. Transportation Research Part C: Emerging Technologies 29, 14–31.

Fu, H., Lam, W.H.K., Shao, H., Kattan, L., Salari, M., 2022. Optimization of multi-type traffic sensor locations for estimation of multi-period origin-destination demands with covariance effects. Transportation Research Part E: Logistics and Transportation Review 157, 102555.

Fu, H., Lam, W.H.K., Shao, H., Xu, X.P., Lo, H.P., Chen, B.Y., Sze, N.N., Sumalee, A., 2019. Optimization of traffic count locations for estimation of travel demands with covariance between origin-destination flows. Transportation Research Part C: Emerging Technologies 108, 49–73.

Fu, X., Lam, W.H.K., 2018. Modelling joint activity-travel pattern scheduling problem in multi-modal transit networks. Transportation 45, 23–49.

Gentili, M., Mirchandani, P.B., 2012. Locating sensors on traffic networks: models, challenges and research opportunities. Transportation Research Part C: Emerging

Technologies 24, 227–255.

Gentili, M., Mirchandani, P.B., 2018. Review of optimal sensor location models for travel time estimation. Transportation Research Part C: Emerging Technologies 90, 74–96.

Gil, M., 2011. On Rényi divergence measures for continuous alphabet sources. Doctoral disseration,PhD thesis, Queen's University.

Giuliano, G., Levine, D.W., Teal, R.F., 1990. Impact of high occupancy vehicle lanes on carpooling behavior. Transportation 17, 159–177.

Goel, P., Kulik, L., Ramamohanarao, K., 2016. Optimal pick up point selection for effective ride sharing. IEEE Transactions on Big Data 3, 154–168.

Gu, Y., Fu, X., Liu, Z., Xu, X., Chen, A., 2020. Performance of transportation network under perturbations: Reliability, vulnerability, and resilience. Transportation Research Part E: Logistics and Transportation Review 133, 101809.

Guo, F., Gu, X., Guo, Z., Dong, Y., Wallace, S.W., 2020. Understanding the marginal distributions and correlations of link travel speeds in road networks. Scientific Reports 2020 10:1 10, 1–8.

Guo, J., Liu, Y., Li, X., Huang, W., Cao, J., Wei, Y., 2019. Enhanced least square based dynamic OD matrix estimation using radio frequency identification data. Mathematics and Computers in Simulation 155, 27–40.

How Uber Works: Insights into the Business and Revenue Model, 2018. <https://jungleworks.com/uber-business-model-revenue-insights/> (accessed 01/14/2019).

Hu, S.R., Peeta, S., Liou, H.T., 2015. Integrated determination of network origin-destination trip matrix and heterogeneous sensor selection and location strategy. IEEE Transactions on Intelligent Transportation Systems 17, 195–205.

Isserlis, L., 1918. On a formula for the product-moment coefficient of any order of a normal frequency distribution in any number of variables. Biometrika 12, 134–139.

Jati, G.K., Suyanto, 2011. Evolutionary discrete firefly algorithm for travelling salesman problem. Adaptive and Intelligent Systems. ICAIS 2011. 393–403.

Jolliffe, I.T., 2002. Principal component analysis. Springer, New York, US.

Jones, L.K., Gartner, N.H., Shubov, M., Stamatiadis, C., Einstein, D., 2018. Modeling origin-destination uncertainty using network sensor and survey data and new approaches to robust control. Transportation Research Part C: Emerging Technologies 94, 121–132.

Kharoufeh, J.P., Goulias, K.G., 2002. Nonparametric identification of daily activity durations using kernel density estimators. Transportation Research Part B: Methodological 36, 59–82.

Kobayashi, T., 2021. Optimistic reinforcement learning by forward Kullback-Leibler divergence optimization. arXiv preprint arXiv 2105, 12991.

Krishnakumari, P., van Lint, H., Djukic, T., Cats, O., 2020. A data driven method for OD matrix estimation. Transportation Research Part C: Emerging Technologies 113, 38–56.

Kullback, S., Leibler, R.A., 1951. On information and sufficiency. The Annals of Mathematical Statistics 22, 79–86.

Lam, W.H.K., Xu, G., 1999. A traffic flow simulator for network reliability assessment. Journal of Advanced Transportation 33, 159–182.

Larsson, T., Lundgren, J.T., Peterson, A., 2010. Allocation of link flow detectors for Origin-Destination matrix estimation-a comparative study. Computer-Aided Civil and Infrastructure Engineering 25, 116–131.

Li, R., Rose, G., Sarvi, M., 2006a. Evaluation of speed-based travel time estimation models. Journal of Transportation Engineering 132, 540–547.

Li, R., Rose, G., Sarvi, M., 2006b. Using automatic vehicle identification data to gain insight into travel time variability and its causes. Transportation Research Record: Journal of the Transportation Research Board 1945, 24–32.

Li, X., Lam, W.H.K., Shao, H., Gao, Z., 2015. Dynamic modelling of traffic incident

impacts on network reliability. Transportmetrica A: Transport Science 11, 856–872.

Li, X., Ouyang, Y., 2011. Reliable sensor deployment for network traffic surveillance. Transportation Research Part B: Methodological 45, 218–231.

Li, Y., Liu, Y., Xie, J., 2020. A path-based equilibrium model for ridesharing matching. Transportation Research Part B: Methodological 138, 373–405.

Lo, H.P., Zhang, N., Lam, W.H.K., 1996. Estimation of an origin-destination matrix with random link choice proportions: a statistical approach. Transportation Research Part B: Methodological 30, 309–324.

Ma, W., Qian, Z. (Sean), 2017. On the variance of recurrent traffic flow for statistical traffic assignment. Transportation Research Part C: Emerging Technologies 81, 57–82.

Ma, W., Qian, Z. (Sean), 2018. Statistical inference of probabilistic origin-destination demand using day-to-day traffic data. Transportation Research Part C: Emerging Technologies 88, 227–256.

Ma, Y., 2016. The use of advanced transportation monitoring data for official statistics. PhD thesis, Erasmus University Rotterdam.

Maher, M.J., 1983. Inferences on trip matrices from observations on link volumes: a Bayesian statistical approach. Transportation Research Part B: Methodological 17, 435–447.

Marzano, V., Papola, A., Simonelli, F., Papageorgiou, M., 2018. A Kalman filter for quasi-dynamic o-d flow estimation/updating. IEEE Transactions on Intelligent Transportation Systems 19, 3604–3612.

Matute, J.M., Chester, M. V., 2015. Cost-effectiveness of reductions in greenhouse gas emissions from High-Speed Rail and urban transportation projects in California. Transportation Research Part D: Transport and Environment 40, 104–113.

Meng, Q., Wang, T., 2011. A scenario-based dynamic programming model for multi-period liner ship fleet planning. Transportation Research Part E: Logistics and

Transportation Review 47, 401–413.

Meng, Q., Wang, T., Wang, S., 2015. Multi-period liner ship fleet planning with dependent uncertain container shipment demand. Maritime Policy & Management 42, 43–67.

Menon, A.K., Cai, C., Wang, W., Wen, T., Chen, F., 2015. Fine-grained OD estimation with automated zoning and sparsity regularisation. Transportation Research Part B: Methodological 80, 150–172.

Miguel, Leandro Fleck Fadel, Lopez, R.H., Miguel, Letícia Fleck Fadel, 2013. Multimodal size, shape, and topology optimisation of truss structures using the Firefly algorithm. Advances in Engineering Software 56, 23–37.

Mirchandani, P.B., Gentili, M., He, Y., 2009. Location of vehicle identification sensors to monitor travel-time performance. IET Intelligent Transport Systems 3, 289–303.

Munizaga, M., Palma, C., 2012. Estimation of a disaggregate multimodal public transport origin-destination matrix from passive smartcard data from Santiago, Chile. Transportation Research Part C: Emerging Technologies 24, 9–18.

Nayeem, M.A., Rahman, M.K., Rahman, M.S., 2014. Transit network design by genetic algorithm with elitism. Transportation Research Part C: Emerging Technologies 46, 30–45.

Ohazulike, A.E., Still, G., Kern, W., van Berkum, E.C., 2013. An origin-destination based road pricing model for static and multi-period traffic assignment problems. Transportation Research Part E: Logistics and Transportation Review 58, 1–27.

Olsson, U.H., Foss, T., Troye, S. V., Howell, R.D., 2000. The performance of ML, GLS, and WLS estimation in structural equation modeling under conditions of misspecification and nonnormality. Structural Equation Modeling 7, 557–595.

Owais, M., Moussa, G.S., Hussain, K.F., 2019. Sensor location model for O/D estimation: Multi-criteria meta-heuristics approach. Operations Research Perspectives 6, 100100.

Pal, S.K., Rai, C.S., Singh, A.P., 2012. Comparative study of firefly algorithm and particle swarm optimization for noisy non-linear optimization problems. Intelligent Systems and Applications 10, 50–57.

Park, H., Haghani, A., 2015. Optimal number and location of Bluetooth sensors considering stochastic travel time prediction. Transportation Research Part C: Emerging Technologies 55, 203–216.

Parry, K., Hazelton, M.L., 2012. Estimation of origin-destination matrices from link counts and sporadic routing data. Transportation Research Part B: Methodological 46, 175–188.

Payne, H.J., Helfenbein, E.D., Knobel, H.C., 1976. Development and testing of incident detection algorithms. Vol. 2, research methodology and detailed results.

Petersen, K.B., Pedersen, M.S., 2012. The matrix cookbook (version: November 15, 2012). Technical Manual, Technical university of denmark.

Ride Hailing - United States | Statista Market Forecast, 2018. <https://www.statista.com/outlook/368/109/ride-hailing/united-states#> (accessed 01/14/2019).

Rinaldi, M., Viti, F., 2017. Exact and approximate route set generation for resilient partial observability in sensor location problems. Transportation Research Part B: Methodological 105, 86–119.

Salari, M., Kattan, L., Lam, W.H.K., Esfeh, M.A., Fu, H., 2021. Modeling the effect of sensor failure on the location of counting sensors for origin-destination (OD) estimation. Transportation Research Part C: Emerging Technologies 132, 103367.

Salari, M., Kattan, L., Lam, W.H.K., Lo, H.P., Esfeh, M.A., 2019. Optimization of traffic sensor location for complete link flow observability in traffic network considering sensor failure. Transportation Research Part B: Methodological 121, 216–251.

Sayadi, M.K., Ramezanian, R., Ghaffari-Nasab, N., 2010. A discrete firefly meta-heuristic with local search for makespan minimization in permutation flow shop

scheduling problems. International Journal of Industrial Engineering Computations 1, 1–10.

Schubert, R., Heide, P., Magori, V., 1995. Microwave doppler sensors measuring vehicle speed and travelled distance: Realistic system tests in railroad environment. In Proc. of MIOP Conf. 365–369.

Shao, H., Lam, W.H.K., Sumalee, A., Chen, A., 2013. Journey time estimator for assessment of road network performance under demand uncertainty. Transportation Research Part C: Emerging Technologies 35, 244–262.

Shao, H., Lam, W.H.K., Sumalee, A., Chen, A., 2018. Network-wide on-line travel time estimation with inconsistent data from multiple sensor systems under network uncertainty. Transportmetrica A : Transport Science 14, 110–129.

Shao, H., Lam, W.H.K., Sumalee, A., Chen, A., Hazelton, M.L., 2014. Estimation of mean and covariance of peak hour origin–destination demands from day-to-day traffic counts. Transportation Research Part B: Methodological 68, 52–75.

Shao, H., Lam, W.H.K., Sumalee, A., Hazelton, M.L., 2015. Estimation of mean and covariance of stochastic multi-class OD demands from classified traffic counts. Transportation Research Part C: Emerging Technologies 7, 192–211.

Simonelli, F., Marzano, V., Papola, A., Vitiello, I., 2012. A network sensor location procedure accounting for O–D matrix estimate variability. Transportation Research Part B: Methodological 46, 1624–1638.

Smartmicro, 2020. The most advanced radar technology. https://www.smartmicro.com/traffic-radar (accessed 12.13.20).

Spiess, H., 1987. A maximum likelihood model for estimating origin-destination matrices. Transportation Research Part B 21, 395–412.

Sumalee, A., Uchida, K., Lam, W.H.K., 2011. Stochastic multi-modal transport network under demand uncertainties and adverse weather condition. Transportation Research Part C: Emerging Technologies 19, 338–350.

Tan, Z., Yang, H., Guo, R., 2014. Pareto efficiency of reliability-based traffic equilibria

and risk-taking behavior of travelers. Transportation Research Part B: Methodological 66, 16–31.

Tani, R., Kato, T., Uchida, K., 2020. A method for structuring stochastic travel time by using risk premiums of stochastic link flow. Transportmetrica A: Transport Science.

Taylor, M.A.P., 2013. Travel through time: The story of research on travel time reliability. Transportmetrica B: Transport Dynamics 1, 174–194.

Tian, J., Jia, N., Zhu, N., Jia, B., Yuan, Z., 2014. Brake light cellular automaton model with advanced randomization for traffic breakdown. Transportation Research Part C: Emerging Technologies 44, 282–298.

Toi S., 1986. A study on the disposing method of traffic counting point, in: Proceeding of the 43th Annual Conference of The Japan Society of Civil Engineering. pp. 480–481.

Transport Department, 2004. The 2004 Base District Traffic Models, Transport Planning Division, Transport Department, Government of the Hong Kong SAR.

Transport Department, 2018. The Annual Traffic Census 2017, Traffic and Transport Survey Division, Transport Department, Government of the Hong Kong SAR.

Transport Department, 2020. Traffic detectors on strategic routes. <https://www.td.gov.hk/en/transport_in_hong_kong/its/intelligent_transport_systems_strategy_review_and_/traffic_detectors/index.html> (accessed 01/09/2021).

Transport Department, 2021a. Speed Map Panels, Transport Department, Government of the Hong Kong SAR.

Transport Department, 2021b. The Annual Traffic Census 2020. Traffic and Transport Survey Division, Transport Department, Government of the Hong Kong SAR.

Turner, S.M., Eisele, W.L., Gajewski, B.J., Albert, L.P., Benz, R.J., 1999. ITS data archiving: case study analyses of San Antonio TransGuide. Texas Transportation Institute.

Van Zuylen, H.J., Willumsen, L.G., 1980. The most likely trip matrix estimated from traffic counts. Transportation Research Part B: Methodological 14, 281–293.

Vanajakshi, L., Rilett, L.R., 2006. System wide data quality control of inductance loop data using nonlinear optimization. Journal of Computing in Civil Engineering 20, 187–196.

Viti, F., Rinaldi, M., Corman, F., Tampère, C.M.J., 2014. Assessing partial observability in network sensor location problems. Transportation Research Part B: Methodological 70, 65–89.

Viti, F., Verbeke, W., Tampère, C.M.J., 2008. Sensor locations for reliable travel time prediction and dynamic management of traffic networks. Transportation Research Record: Journal of the Transportation Research Board 2049, 103–110.

Waller, S.T., Unnikrishnan, A., Duthie, J., 2006. Network evaluation with uncertain and correlated long-term demand, in: Proceedings of the 85th Transportation Research Board Annual Meeting, CD-ROM. Washington D.C.

Wu, C., Zhang, J., 2021. Robust semi-supervised spatial picture fuzzy clustering with local membership and KL-divergence for image segmentation. International Journal of Machine Learning and Cybernetics 1–25.

Wu, X., Guo, J., Xian, K., Zhou, X., 2018. Hierarchical travel demand estimation using multiple data sources: A forward and backward propagation algorithmic framework on a layered computational graph. Transportation Research Part C: Emerging Technologies 96, 321–346.

Xiang, W., Zhu, N., Ma, S., Meng, X., An, M., 2015. A dynamic shuffled differential evolution algorithm for data clustering. Neurocomputing 158, 144–154.

Xing, T., Zhou, X., Taylor, J., 2013. Designing heterogeneous sensor networks for estimating and predicting path travel time dynamics: An information-theoretic modeling approach. Transportation Research Part B: Methodological 57, 66–90.

Xiong, T., Bao, Y., Hu, Z., 2014. Multiple-output support vector regression with a firefly algorithm for interval-valued stock price index forecasting. Knowledge-

Based Systems 55, 87–100.

Xu, X., Lo, H.K., Chen, A., Castillo, E., 2016. Robust network sensor location for complete link flow observability under uncertainty. Transportation Research Part B: Methodological 88, 1–20.

Yang, H., 1995. Heuristic algorithms for the bilevel origin-destination matrix estimation problem. Transportation Research Part B: Methodological 29, 231–242.

Yang, H., Iida, Y., Sasaki, T., 1991. An analysis of the reliability of an origin-destination trip matrix estimated from traffic counts. Transportation Research Part B: Methodological 25, 351–363.

Yang, H., Meng, Q., Bell, M.G.H., 2001. Simultaneous estimation of the Origin-Destination matrices and travel-cost coefficient for congested networks in a stochastic user equilibrium. Transportation Science 35, 107–123.

Yang, H., Sasaki, T., Iida, Y., 1992. Estimation of origin-destination matrices from link traffic counts on congested networks. Transportation Research Part B: Methodological 26, 417–434.

Yang, H., Yang, C., Gan, L., 2006. Models and algorithms for the screen line-based traffic-counting location problems. Computers & Operations Research 33, 836–858.

Yang, H., Zhou, J., 1998. Optimal traffic counting locations for origin–destination matrix estimation. Transportation Research Part B: Methodological 32, 109–126.

Yang, X.-S., 2008. Firefly algorithm, in: Nature-Inspired Metaheuristic Algorithms. Luniver Press, London, UK.

Yang, X., Lu, Y., Hao, W., 2017. Origin-destination estimation using probe vehicle trajectory and link counts. Journal of Advanced Transportation 2017, 1–18.

Yang, Y., Fan, Y., Royset, J.O., 2019. Estimating probability distributions of travel demand on a congested network. Transportation Research Part B: Methodological 122, 265–286.

Yang, Y., Fan, Y., Wets, R.J.B., 2018. Stochastic travel demand estimation: Improving network identifiability using multi-day observation sets. Transportation Research Part B: Methodological 107, 192–211.

Yao, J., Chen, A., Ryu, S., Shi, F., 2014. A general unconstrained optimization formulation for the combined distribution and assignment problem. Transportation Research Part B: Methodological 59, 137–160.

Ye, P., Wen, Di., 2017. Optimal traffic sensor location for origin-destination estimation using a compressed sensing framework. IEEE Transactions on Intelligent Transportation Systems 18, 1857–1866.

Yin, B., Liu, L., Coulombel, N., Viguié, V., 2017. Evaluation of ridesharing impacts using an integrated transport land-use model: A case study for the Paris region, in: Transportation Research Procedia. Elsevier B.V., pp. 824–831.

Yin, Y., 2000. Genetic-algorithms-based approach for bilevel programming models. Journal of Transportation Engineering 126, 115–120.

Yin, Y., Madanat, S.M., Lu, X.-Y., 2009. Robust improvement schemes for road networks under demand uncertainty. European Journal of Operational Research 198, 470–479.

Yu, Q., Fang, K., Zhu, N., Ma, S., 2019. A matheuristic approach to the orienteering problem with service time dependent profits. European Journal of Operational Research 273, 488–503.

Zangui, M., Yin, Y., Lawphongpanich, S., 2015. Sensor location problems in path-differentiated congestion pricing. Transportation Research Part C: Emerging Technologies 55, 217–230.

Zhang, K., Jia, N., Zheng, L., Liu, Z., 2019. A novel generative adversarial network for estimation of trip travel time distribution with trajectory data. Transportation Research Part C: Emerging Technologies 108, 223–244.

Zhang, L., Yin, Y., Lou, Y., 2010. Robust signal timing for arterials under day-to-day demand variations. Transportation Research Record: Journal of the

Transportation Research Board 2192, 156–166.

Zheng, F., Van Zuylen, H., 2013. Urban link travel time estimation based on sparse probe vehicle data. Transportation Research Part C: Emerging Technologies 31, 145–157.

Zhou, X., List, G.F., 2010. An information-theoretic sensor location model for traffic origin-destination demand estimation applications. Transportation Science 44, 254–273.

Zhu, N., Fu, C., Ma, S., 2018. Data-driven distributionally robust optimization approach for reliable travel-time-information-gain-oriented traffic sensor location model. Transportation Research Part B: Methodological 113, 91–120.

Zhu, N., Liu, Y., Ma, S., He, Z., 2014. Mobile traffic sensor routing in dynamic transportation systems. IEEE Transactions on Intelligent Transportation Systems 15, 2273–2285.

Zhu, N., Ma, S., Zheng, L., 2017. Travel time estimation oriented freeway sensor placement problem considering sensor failure. Journal of Intelligent Transportation Systems 21, 26–40.

Zhu, S., Zheng, H., Peeta, S., Guo, Y., Cheng, L., Sun, W., 2016. Optimal heterogeneous sensor deployment strategy for dynamic Origin–Destination demand estimation. Transportation Research Record: Journal of the Transportation Research Board 2567, 18–27.

Zhu, Y., He, Z., Sun, W., 2019. Network-wide link travel time inference using trip-based data from automatic vehicle identification detectors. IEEE Transactions on Intelligent Transportation Systems 21, 1–11.

Zhu, Z., Xiong, C., Chen, X., He, X., Zhang, L., 2018. Integrating mesoscopic dynamic traffic assignment with agent-based travel behavior models for cumulative land development impact analysis. Transportation Research Part C: Emerging Technologies 93, 446–462.

Zhu, Z., Zhu, S., Zheng, Z., Yang, H., 2019. A generalized Bayesian traffic model.

Transportation Research Part C: Emerging Technologies 108, 182–206.